APPLICATIONS OF CHIRAL PERTURBATION THEORY TO LATTICE QUANTUM CHROMODYNAMICS

Nolan B. Miller

A dissertation submitted to the faculty of the University of North Carolina at Chapel Hill in partial fulfillment of the requirements for the degree of Doctor of Philosophy in the Department of Physics and Astronomy.

Chapel Hill
2022

Approved by:

Amy Nicholson

Joaquin Drut

Jon Engel

Fabian Heitsch

Reyco Henning

ABSTRACT

Nolan B. Miller: Applications of chiral perturbation theory to lattice quantum chromodynamics
(Under the direction of Amy Nicholson)

In this dissertation, we calculate hadronic observables through the application of chiral perturbation theory to lattice quantum chromodynamics. Quantum chromodynamics is the quantum field theory for the strong interaction which, in the low-energy regime, becomes non-perturbative. The lattice acts as a regulator for the theory and allows us to make predictions at low-energy even without a perturbative expansion. However, since these lattice calculations require non-zero lattice spacing and often assume light quark masses much greater than those provided by Nature, calculating observables requires us to extrapolate the results from multiple lattice ensembles to the physical, continuum limit. We perform these extrapolations using chiral perturbation theory, an effective field theory for quantum chromodynamics in which the degrees of freedom are the pseudo-Goldstone bosons emerging from the explicit, spontaneous breaking of chiral symmetry.

We concentrate particularly on determining the gradient flow scales w_0 and t_0, which allow us to set the scale of our lattice; the ratio of the pseudoscalar decay constants F_K/F_π, from which we determine the ratio of the Cabibbo-Kobayashi-Maskawa matrix elements $|V_{us}|/|V_{ud}|$; the masses of the cascades, as a precursor to a lattice determination of the hyperon transition matrix elements; and finally the nucleon sigma term, which has implications for the cross section of the neutralino in the minimal supersymmetric Standard Model.

To my parents, and my parent’s parents, too.

ACKNOWLEDGEMENTS

I'd like to open these acknowledgements by thanking my advisor, Amy Nicholson. Amy joined the department two years into my graduate degree, which would typically be well after a student had already selected an advisor. However, my graduate career was at a crossroads, as my advisor at the time had left the department, leaving me in the awkward position of having finished my quals but lacking a research project to focus on.

In retrospect my former advisor's departure proved to be a stroke of good luck for me, as I doubt I otherwise would've had the opportunity to work with Amy. While stress cannot be eliminated from graduate school, never did I feel that Amy was the source. Amy remained patient—perhaps too patient—even as she re-explained some concept to me for the thousandth time. She effused just the right amount of casualness—not so nonchalant that I felt neglected, but just enough to force my growth as an *independent* researcher.

Next I'd like to thank André Walker-Loud, my second advisor in all but formalities. Although I was thankful for having switched to a field that played to my strengths (programming) instead of testing my grit (tedious mathematical abstraction), there are a surprising number of steps required before we can quote a result, even after the lattice calculations have been run and the data has been packaged. At some point this entire process became overwhelming, and I floundered. André guided me through each step and cross-checked my work. Once I had internalized those lessons, I finally began to feel like a collaborator instead of a confused grad student.

All of my successes I attribute to them (but all of my failures are solely mine).

Of course, a lattice collaboration is more than just three people. There are at least a dozen folk in our group whom I had scant personal interactions with, but their work was nonetheless a prerequisite for my own. I appreciate their effort, even as I'm blissfully unaware of the minutiae of their research problems. I'm grateful for the students and postdocs I've worked with—specifically Grant Bradley, Zack Hall, Malcolm Lazarow, Christopher Körber, and Henry Monge-Camacho—who all helped me grow as a researcher in one way or another.

Thank you also to my committee for slogging through this thesis.

Finally, I thank my friends and family, who supported my decision to pursue a physics career even as their eyes glazed over and they struggled to remember my specialty. I love you all anyway. To my fiancée: thank you for shouldering more than your share of the chores these last few months, as well as your willingness to settle on microwavable dinners when it was my turn to cook.

And while we're here, I may as well thank my cat, Buttons. Her snuggles remain the best stress relief.

TABLE OF CONTENTS

LIST OF TABLES

LIST OF FIGURES

LIST OF ABBREVIATIONS AND SYMBOLS

χPT	chiral perturbation theory
CKM	Cabibbo-Kobayashi-Maskawa (matrix)
EFT	effective field theory
FLAG	the Flavor Lattice Averaging Group
GMOR	Gell-Mann–Oakes–Renner (relations)
LEC	low energy constant
LO	leading order
MSSM	minimal supersymmetric Standard Model
N^{x}LO	$\underbrace{\text{next-to-}\cdots\text{-next-to}}_{\text{x times}}$-leading order
PDG	Particle Data Group
QCD	quantum chromodynamics
QED	quantum electrodynamics

A_μ	a gluon field
B	a low energy constant from the chiral Lagrangian related to the quark masses
D_μ	a covariant derivative
F	a low energy constant from the chiral Lagrangian related to pseudoscalar decay
F_π	the pseudoscalar decay constant of the pion
F_K	the pseudoscalar decay constant of the kaon
G	a group
$G^a_{\mu\nu}$	a gluon field strength tensor
$\mathfrak{g}$	a Lie algebra
γ^μ, γ^5	a gamma matrix
$K_{\ell 2}$	leptonic kaon decay: $K \to l\nu_l$
$K_{\ell 3}$	semi-leptonic kaon decay: $K \to \pi l\nu_l$
$\mathcal{L}$	a Lagrangian density
L_i	a Gasser-Leutwyler low energy constant (from the chiral Lagrangian)
$\bar{l}_i$	a Gasser-Leutwyler low energy constant defined at a different renormalization scale

λ^a	a Gell-Mann matrix
Λ_χ	the chiral cutoff (~ 1 GeV)
$\hat{m}$	the average mass of the light (up and down) quarks
N	a nucleon field
ϕ	a complex scalar field
π^a	a pion field
ψ	a Dirac field
Q^a	a charge
q_f	a quark field
σ^i, τ^i	a Pauli matrix
$\sigma_{\pi N}$	the nucleon sigma term
SU(N)	the special unitary group
$\mathfrak{su}(N)$	the special unitary Lie algebra
t_0	a gradient flow scale
T^a	a generator of the SU(N) Lie algebra
$V_{ff'}$	The CKM matrix element describing the mixing between quark flavors f and f'
w_0	another gradient flow scale

Regarding lattice quantum chromodynamics

.

Quantum chromodynamics

In the same space one could write the range equation for projectile motion, we can write the Lagrangian density for quantum chromodynamics (QCD), which describes the majority of visible matter in the universe. To wit,

$$\mathcal{L} = \sum_f \overline{q}_f \left(i\gamma^\mu D_\mu - m_f \right) q_f - \frac{1}{4} G^a_{\mu\nu} G^{\mu\nu}_a \, . \tag{1.1}$$

A quantum field theory (QFT) is only as good as its symmetries; QCD imposes color SU(3) "symmetry" (manifest in Roman indices $a, b, c, \ldots$) and Lorentz symmetry (manifest in the Greeks indices $\mu, \nu, \ldots$). Of course, there is nothing surprising about including the latter symmetry: all quantum field theories have it.

We'll avoid asking *why* the degrees of freedom of the QCD Lagrangian, i.e. the gluon and quark fields, have the quantum numbers they have: that question can be (unsatisfactorily) answered with "because experiment demands so." Instead, we'll see how the particular quantum numbers demanded by the theory (e.g., gluons being spin-1 particles) require the Lagrangian written above.

A refresher on Lie groups, their algebras, and their representations

To check whether a Lagrangian respects a proposed symmetry, we verify that the Lagrangian remains invariant under a transformation of the fields by that symmetry. In practice this means that we codify a symmetry by expressing it in terms of some (matrix) Lie group. Often, rather than work directly with the Lie groups (which in general can be quite messy), we instead work with the Lie algebras (which are linear). These objects are not always carefully between in the physics literature.

Colloquially, we often talk about Lie groups as being exponentiated Lie algebras. More rigorously, if G is a Lie group, then we define the *Lie algebra* of G as [1]

$$\mathfrak{g} = \left\{ X \mid e^{itX} \in G \quad \forall t \in \mathbb{R} \right\} . \tag{1.2}$$

From this definition, the following theorem follows: if $X, Y \in \mathfrak{g}$, then also $i(XY - YX) \in \mathfrak{g}$, which perhaps explains the ubiquity of Lie brackets in QFT. Alternatively, one can endow a vector space V with a bilinear operation $[\cdot, \cdot] : V \times V \to V$ and (assuming a few other requirements are met) generate a Lie algebra that way.

As perhaps the most important example in QFT, consider the Lorentz group, which is the group of rotations and Lorentz boosts (technically we're interested in a subset of the Lorentz group, the restricted Lorentz group SO$^+(1, 3)$, which forces time and parity operations to be discrete rather than continuous). The corresponding Lie algebra $\mathfrak{so}(1, 3)$ is just the vector space $\mathbb{C}^{4\times 4}$ with the Lie bracket [2]

$$[\mathcal{J}^{\rho\sigma}, \mathcal{J}^{\tau\nu}] = i \left(\eta^{\sigma\tau} \mathcal{J}^{\rho\nu} - \eta^{\rho\tau} \mathcal{J}^{\sigma\nu} + \eta^{\rho\nu} \mathcal{J}^{\sigma\tau} - \eta^{\sigma\nu} \mathcal{J}^{\rho\tau}\right) \tag{1.3}$$

$$= i f^{\rho\sigma\tau\nu}{}_{\alpha\beta} \mathcal{J}^{\alpha\beta} \tag{1.4}$$

where $\mathcal{J}^{\mu\nu}$ is an infinitesimal generator of the Lorentz group. A generic element of the Lorentz Lie group can then be written

$$\Lambda^{\alpha}{}_{\beta} = \left[\exp\left(-i\omega_{\mu\nu}\mathcal{J}^{\mu\nu}\right)\right]^{\alpha}{}_{\beta} \tag{1.5}$$

where the antisymmetric $\omega_{\mu\nu}$ is a parameter of the transformation (one can think of $J^{\mu\nu}$ as being the basis elements and $\omega_{\mu\nu}$ as selecting a particular Λ).

Of particular interest to us are *representations* of the Lorentz group. A (matrix) representation D of the Lorentz groups is a map (technically, homomorphism) taking the Lorentz group to the set of invertible $n \times n$ matrices, i.e.

$$D : \text{SO}^+(3, 1) \to GL(n; \mathbb{C}) \tag{1.6}$$

such that $D[\Lambda_1]D[\Lambda_2] = D[\Lambda_1\Lambda_2]$ (see Chapter 4 of [3]). Further, every representation of a Lie group gives rise to a representation of its corresponding Lie algebra (see Theorem 3.18 of [1]), and often the converse holds too. In the next section, we'll see how these representations are used to characterize particles of different spins.

Lorentz symmetry

To understand how Lorentz symmetry is encoded into QCD, we must dig a little deeper into its Lagrangian. First consider the gluon fields A_μ^a, which are hidden inside $G_{\mu\nu}^a$:

$$G_{\mu\nu}^a = \partial_\mu A_\nu^a - \partial_\nu A_\mu^a + g f_{abc} A_\mu^b A_\nu^c \, . \tag{1.7}$$

For now, we are only interested in the Lorentz (Greek) indices.

In general, given a field ϕ^α, we require the field transform under a Lorentz transformation Λ as

$$\phi^\alpha(x) \to \phi'^\alpha(x) = D[\Lambda]^\alpha{}_\beta \phi^\beta(\Lambda^{-1}x) \tag{1.8}$$

where the matrices $D[\Lambda]$ form a representation of the Lorentz (Lie) group. When constructing the QCD Lagrangian, we might first consider what the correct representation is for the quark fields with respect to Lorentz symmetry. For instance, given the Klein-Gordon Lagrangian

$$\mathcal{L}_{\text{K-G}} = \frac{1}{2}\left(\partial_\mu \phi \partial^\mu \phi - m^2 \phi^2\right) \tag{1.9}$$

the scalar (spin-0) field ϕ need only transform per the trivial representation in order to preserve Lorentz symmetry: $D[\Lambda] = \mathbf{1}$. That is,

$$\phi(x) \to \phi'(x) = \phi(\Lambda^{-1}x) \, . \tag{1.10}$$

It's straightforward to check that the Klein-Gordon Lagrangian remains unchanged when we take $\phi(x) \to \phi'(x)$: just apply the chain rule and use the relation $\eta^{\sigma\tau}\Lambda^\mu{}_\sigma \Lambda^\nu{}_\tau = \eta^{\mu\nu}$ along with $\Lambda_\nu{}^\mu = (\Lambda^{-1})^\mu{}_\nu$.

Next, consider a vector (spin-1) field A_μ. The simplest example we can concoct is quantum electrodynamics (QED) without sources, i.e. QED with photons only. The corresponding Lagrangian is

$$\mathcal{L}_{\text{QED-light}} = -\frac{1}{4} F_{\mu\nu} F^{\mu\nu} \tag{1.11}$$

where $F_{\mu\nu} = \partial_\mu A_\nu - \partial_\nu A_\mu$. As a vector field, A_μ transforms per the fundamental representation: $D[\Lambda] = \Lambda$. Thus

$$A_\mu(x) \to A'_\mu(x) = \Lambda_\mu{}^\nu A_\nu(\Lambda^{-1}x)\,. \tag{1.12}$$

Again, one can check that under a Lorentz transformation of the fields, in this case $A_\mu(x) \to A'_\mu(x)$, the Lagrangian remains unchanged.

The similarity between $F_{\mu\nu}$ and $G^a_{\mu\nu}$ is obvious, especially if we suppress the color indices. One might worry about the extra term quadratic in the gluon fields, but this term is Lorentz invariant for the same reason $\partial_\mu\phi\partial^\mu\phi$ is Lorentz invariant in the scalar theory. All of this is to be expected: the gluon, like the photon, is a spin-1 particle.

So far we have considered two different representations of the Lorentz group: the trivial representation, which gives rise to spin-0 particles, and the fundamental representation, which gives rise to spin-1 particles such as the gluon. In some sense, these are the simplest representations of the Lorentz group. However, experiments require that the quarks be neither spin-0 nor spin-1 but spin-$\frac{1}{2}$ particles. To that end, we consider the Dirac equation

$$(i\gamma^\mu\partial_\mu - m)\,\phi = 0\,. \tag{1.13}$$

Historically, the Dirac equation stems from Dirac's attempt to write a Lorentz invariant wave equation *linear* in ∂_μ (contrast to the Klein-Gordon Lagrangian above). If $\gamma^\mu \to a^\mu$ is just an ordinary number, this task is evidently impossible: $a^\mu\partial_\mu$ is a directional derivative with a clearly preferred direction. But if we act on this wave equation with $(i\gamma^\mu\partial_\mu + m)$, we have that

$$\left(-\gamma^\mu\gamma^\nu\partial_\mu\partial_\nu + m^2\right)\phi = 0\,. \tag{1.14}$$

Using the fact that derivatives commute, we can write $\gamma^\mu\gamma^\nu\partial_\mu\partial_\nu = \frac{1}{2}\{\gamma^\mu, \gamma^\nu\}\partial_\mu\partial_\nu$. From this, we see that $\{\gamma^\mu, \gamma^\nu\} = 2\eta^{\mu\nu}$, which means that γ^μ and γ^ν must be an elements of the Clifford algebra $C\ell_{1,3}(\mathbb{R})$.

So far we've spoken of representations of Lie groups, but as mentioned in the previous section, one can also have representations of Lie algebras. One representation of the Lorentz Lie algebra (1.3) is

$$\tilde{D}[\mathcal{J}^{\rho\sigma}] = \mathcal{S}^{\rho\sigma} = \frac{i}{4}\left[\gamma^\rho, \gamma^\sigma\right] \tag{1.15}$$

from which we can define the adjoint representation of the Lorentz group: $D[\Lambda] = \exp\left(-i\omega_{\mu\nu}\mathcal{S}^{\mu\nu}\right)$. Like the fundamental representation, the adjoint representation is also composed of 4×4 matrices; however, it's worth keeping in mind that this representation is unique. The Dirac field therefore transforms as

$$\phi^{\alpha}(x) \to \phi'^{\alpha}(x) = \left(e^{-i\omega_{\mu\nu}\mathcal{S}^{\mu\nu}}\right)^{\alpha}{}_{\beta}\phi^{\beta}(\Lambda^{-1}x)\,. \tag{1.16}$$

Now we're equipped to understand the Dirac Lagrangian,

$$\mathcal{L} = \overline{\phi}(i\gamma^{\mu}\partial_{\mu} - m)\phi\,. \tag{1.17}$$

Here we define $\overline{\phi} = \phi^{\dagger}\gamma^{0}$, where $\gamma^{0} = I \otimes \sigma_{3}$ (the factor of γ^{0} is required for the Lagrangian to remain Lorentz invariant since $D[\Lambda]$ is not unitary for this particular representation). Following some algebra involving γ-matrices, we see that this Lagrangian is indeed Lorentz invariant under $\phi \to \phi'$.

Of course, this is all analogous to the case of QCD. With respect to Lorentz symmetry, the quark fields transform in the same way.

Color SU(3)

Even after the success of Gell-Mann's eightfold way and the advent of the quark model in the early 1960s, there was one major hurdle to the quark model remaining: it appeared to violate the Pauli exclusion principle [4]. Particles like $\Delta^{++} = (uuu)$ required the quarks to all be in the same state if flavor and spin are all there is. In 1964, Oscar Greenberg proposed a solution in which the quarks also carried another quantum number—color. With this addition, the quark model was relatively complete, baring the inclusion of yet unseen heavier quarks. (Nevertheless, it still took another ten years or so before physicists fully accepted the quark model).

Experiments show that quarks must come in three different colors (and three different anti-colors), which we label as red, blue, and green. There are also strong theoretical reasons to believe this, too: due to the triangle anomaly, the Standard Model is only internally consistent if quarks come in three colors (see Chapter 4.2 of [5]).

f_{123}		1
f_{147}	$-f_{156}$	
f_{246}	f_{257}	$\frac{1}{2}$
f_{345}	$-f_{367}$	
f_{458}	f_{678}	$\frac{\sqrt{3}}{2}$

Table 1.1: Structure constants of $\mathfrak{su}(3)$.

Much of our work in the previous section carries over to explain the color symmetry of QCD. [1] If one is willing to accept that the quarks transform according to the fundamental representation of some color group that forms a color triplet $q_f = (q_f^r \;\; q_f^b \;\; q_f^g)^T$, then that group must necessarily be SU(3). (To use technical jargon, SU(3) is the only semi-simple Lie group with complex irreducible triplets; again, see [5]). The Lie algebra $\mathfrak{su}(3)$ of the color group is described by its Lie bracket

$$[\lambda^a, \lambda^b] = 2if^{abc}\lambda_c \tag{1.18}$$

where the λ^a are the Gell-Mann matrices (i.e., the SU(3) analogs of the SU(2) Pauli matrices). For completeness, the structure constants are given in Table 1.1. As stated before, it is natural to assume (and indeed, it is the case) that the quarks transform per the fundamental representation of color SU(3):

$$q_f^a \to q_f'^a = \left(e^{-i\theta_c\lambda^c/2}\right)^a{}_b q_f^b \tag{1.19}$$

The gluons must be in the adjoint representation of SU(3). The easiest way to see this is by considering the dimensions of the irreducible representations of SU(3). If color charge is conserved, then gluons must carry away the excess charge; e.g., if $q_f(r)$ becomes $q_f(b)$, then the outgoing gluon must have quantum numbers $g(r, \bar{b})$. From this, one sees there are 9 possible combinations of color/anti-color combinations and might assume that there are 9 gluons. However, this cannot be the case: were it so, the color singlet $(r\bar{r} + b\bar{b} + g\bar{g})/\sqrt{3}$ would be ubiquitous in nature, revealing itself as a long-range force between hadrons. Evidently such particles do not exist, leaving us with 8 gluons [4]. And since there is only one irreducible representation of SU(3) with dimension 8—the adjoint representation—the gluons must transform per this representation.

[1] Technically, only *global* SU(3) color is a symmetry, as the gauge bosons play an active (dynamical) role in the theory; thus when we promote this global gauge symmetry to a local one, it is more accurate to describe the resulting local SU(3) gauge "symmetry" as a gauge redundancy [6].

The adjoint representation Γ of a Lie algebra can be defined in terms of its structure constants (see Chapter 3.3 of [7]). That is, $\Gamma[\lambda^c]^a{}_b = if^a{}_{cb}$, so the the gluon fields transform under color as

$$A^a \to A'^a = \left(e^{-i\theta_c f^c{}_{de}}\right)^a{}_b A^b \,. \tag{1.20}$$

The last piece of the QCD Lagrangian to explain is the covariant derivative.

$$D_\mu = \partial_\mu - ig\frac{\lambda_a}{2}A^a_\mu \tag{1.21}$$

The covariant derivative acts to parallel transport a field from $x^\mu \to x^\mu + \epsilon^\mu$ in a manner analogous to how the covariant derivative transports a vector in general relativity (see Chapter 4.1 of [5]). In general relativity, the derivative is corrected using the Christoffel symbols, which connects different points on the manifold; in QCD, the extra term accounts for the positional dependence of the gauge. By taking the commutator of the covariant derivatives, we get the piece of the gauge that is physical,

$$[D_\mu, D_\nu] = \frac{\lambda_a}{2}G^a_{\mu\nu}. \tag{1.22}$$

In principle, one could check that the QCD Lagrangian is invariant under the transformations $q_f \to q'_f$ and $A \to A'$ as defined above, but that would be quite unusual. I've written the transformations in this manner only to show the similarity to the Lorentz group representations. (For the conventional approach, see e.g. Chapter 2.1 of [8].)

Lattice QCD

Central to lattice QCD is the path integral formulation of QFT. Recall that the correlation function of two operators can be written

$$\langle O_2(t)O_1(0)\rangle = \frac{1}{Z_0}\int \mathcal{D}[q,\overline{q}]\mathcal{D}[A]\, e^{iS_{\mathrm{QCD}}[q,\overline{q},A]}O_2[q,\overline{q},A]O_1[q,\overline{q},A] \tag{1.23}$$

where the integral is over each of the six quark flavors

$$\mathcal{D}[q,\overline{q}] = \prod_{f\in\{u,d,s,c,b,t\}} \mathcal{D}[q_f,\overline{q}_f]\,, \tag{1.24}$$

the partition function Z_0 is just the integral without the operators

$$Z_0 = \int \mathcal{D}[q, \overline{q}]\mathcal{D}[A]\, e^{iS_{\text{QCD}}[q,\overline{q},A]}\,, \tag{1.25}$$

and the QCD action is integrated from 0 to t (and over space)

$$S_{QCD} = \int_0^t d^4x\, \mathcal{L}_{QCD}\,. \tag{1.26}$$

Unlike the path integral formulation of quantum mechanics, in QFT the degrees of freedom are no longer points in space but the fields (which themselves are positioned at some point in space). In quantum mechanics, we think of the path integral as being some sort of weighted average for a particle to get from x_A to x_B, following every conceivable path. In QFT, the fields already permeate ever point in space—rather than have the fields move, they fluctuate like springs on a mattress, with each fluctuation contributing to the likelihood that an excitation—a particle—flows from x_A to x_B.

The need for lattice QCD stems from the running of the coupling constant in QCD. At high energies, we can approximate the coupling constant as

$$\alpha_S(Q^2) = \frac{g^2(Q^2)}{4\pi} \approx \frac{4\pi}{\beta_0 \log(Q^2/\Lambda^2_{\text{QCD}})} \tag{1.27}$$

where Λ_{QCD} is the QCD scale and Q^2 is the momentum transfer. However, as $\sqrt{Q^2} \to \Lambda_{\text{QCD}} \sim 200$ MeV (i.e., for temperatures below $\Lambda_{\text{QCD}}/k_B \sim 10^{12}$ °C), the coupling constant blows up [9] (in fact, this is how we can define Λ_{QCD}). Consequently, perturbative methods fail in this regime: if we were to expand our path integral in terms of Feynman diagrams, the more complicated diagrams (those with more vertices) would actually contribute more greatly than the simpler ones; stated another way, at low energies we can no longer think of a nucleon as being composed of naught but three quarks. A nucleon is something much messier, constantly interacting with a sea of virtual quarks and gluons.

Without perturbative methods, we instead evaluate the path integral directly. Analytically, this task is almost certainly futile—with the exception of a few important cases, there is a no general schema for solving the path integral. Instead, we make a couple approximations: (1) we replace the infinite dimensional path integral with a finite dimensional integral by discretizing the location of the fields, forcing them to points on a lattice; and (2) rather than integrate over all of space, we integrate over a finite (and periodic) volume of space.

In fact, theoretically we're on better footing than we might expect: these two assumptions are regulators of the continuum field theory. The former serves as an ultraviolet cutoff (there can be no particles with momenta smaller than the lattice spacing), and the latter serves as an infrared cutoff (there can be no particles with momenta greater than twice the box length).

With these modifications of the path integral in mind, let's rewrite our path integral for the lattice. Splitting up the QCD action, the fermionic part becomes

$$S_F[q,\overline{q},A] = \int d^4x\,\overline{q}(x)\left[i\gamma^\mu\left(\partial_\mu - ig\frac{\lambda_a}{2}A^a_\mu(x)\right) + m\right]q(x) \tag{1.28}$$

$$\to a^4\sum_{n\in\Lambda}\overline{q}(n)\left(\gamma^\mu\frac{U_\mu(n)q(n+\hat{\mu}) - U_{-\mu}(n)q(n-\hat{\mu})}{2a} + mq(n)\right) = S_F[q,\overline{q},U]\,. \tag{1.29}$$

Here we have introduced the link variables U_μ, which we will explain shortly. If we temporarily turn off the gluons, the free fermionic action is obtained by taking $U_\mu \to 1$. In particular, we have that $\partial_\mu q(x) \to (q(n+\hat{n}) - q(n-\hat{n}))/2a$, i.e. the partial derivative becomes the central difference. [2] So what about the link variables?

As mentioned previously, the covariant derivative D_μ (and its lattice equivalent) serves to parallel transport a field from one location to another. In particular, under a gauge transformation $\Omega \in \mathrm{SU}(3)$, we take

$$q(n) \to q'(n) = \Omega(n)q(n)\,, \qquad \overline{q}(n) \to \overline{q}'(n) = \overline{q}(n)\Omega(n)^\dagger\,. \tag{1.30}$$

Clearly the mass term remains invariant under such a transformation. However, the kinetic term does not.

$$\overline{q}'(x)D_\mu q'(x) \to \overline{q}'(n)\left[\frac{q'(n+\hat{\mu}) - q'(n-\hat{\mu})}{2a}\right] + \text{parallel transport} \tag{1.31}$$

$$= \overline{q}(n)\Omega(n)^\dagger\left[\frac{\Omega(n+\hat{\mu})q(n+\hat{\mu}) - \Omega(n-\hat{\mu})q(n-\hat{\mu})}{2a}\right] + \text{parallel transport} \tag{1.32}$$

(The gauge terms $\Omega(n)^\dagger\Omega(n+\hat{\mu})$ need not cancel since, in general, we can have a different transformation at each point on the lattice.) To ensure that the kinetic term remains invariant under a gauge transformation, we

[2]The central difference, compared to the forward or backward difference, has the advantage of introducing errors at $\mathcal{O}(a^2)$ instead of $\mathcal{O}(a)$.

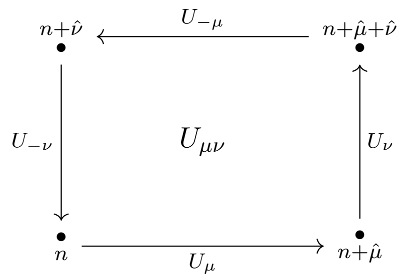

Figure 1.1: Plaquette $U_{\mu\nu}$.

introduce link variables $U_\mu(n)$ such that

$$U_\mu(n) \to U'_\mu(n) = \Omega(n) U_\mu(n) \Omega(n+\hat{\mu})^\dagger \,. \tag{1.33}$$

By including these variables (and noting that $U_{-\mu}(n) = U_\mu(n-\hat{\mu})^\dagger$), we see that the fermionic action is invariant under a transformation $\{q, \overline{q}, U_\mu\} \to \{q', \overline{q}', U'_\mu\}$.

Finally, as a point on terminology, we note that the link between adjacent lattice sites can alternatively be written in matrix notation as

$$S_F[q,\overline{q}] = a^4 \sum_{n_1,n_2\in\Lambda} \overline{q}_{n_1} D_{n_1 n_2} q_{n_2} \,. \tag{1.34}$$

In the lattice literature, such a matrix $D_{n_1 n_2}$ is referred to as a Dirac operator.

Before we consider the gluonic part of the QCD action, it's worth asking: what happened to the gauge fields A_μ? As it so happens, if we write

$$U_\mu(n) = e^{iaA_\mu(n)} = 1 + iaA_\mu(n) + \mathcal{O}(a^2) \tag{1.35}$$

and substitute this definition of U_μ into (1.29), we recover the (discretized) version of the fermionic action with the original gauge fields. But using U_μ instead of A_μ isn't merely some book-keeping trick; it amounts to a change in the degrees of freedom in our theory, effecting us to change the measure in our path integral: $\mathcal{D}[q,\overline{q}]\mathcal{D}[A] \to \mathcal{D}[q,\overline{q}]\mathcal{D}[U]$. [3]

[3]That is, we have changed from using algebra-valued fields to group-valued fields; see Chapter 2.2 of [8].

Continuing with our discussion on how to discretize the QCD action, we now write the gluonic part.

$$S_G[U] = \frac{1}{4}\int d^4x\, G^a_{\mu\nu} G^{\mu\nu}_a \tag{1.36}$$

$$\to 2 \sum_{n\in\Lambda} \sum_{\mu<\nu} \text{Re tr}\left[1 - U_{\mu\nu}(n)\right] = S_G[U] \tag{1.37}$$

Central to understanding this action is the plaquette, defined as

$$U_{\mu\nu}(n) = U_\mu(n) U_\nu(n+\hat{\mu}) U_{-\mu}(n+\hat{\mu}+\hat{\nu}) U_{-\nu}(n+\hat{\nu}) \tag{1.38}$$

$$= U_\mu(n) U_\nu(n+\hat{\mu}) U_\mu(n+\hat{\nu})^\dagger U_\nu(n)^\dagger \,. \tag{1.39}$$

(See Fig. 1.1.) Using the gauge transformation for link variables given above, it's easy to verify that the plaquette is gauge invariant.

We should check that the discretized gluonic action written in terms of the link variables U_μ reduces to the gluonic action written in terms of the gauge fields A_μ. By substituting in $U_\mu(n) = \exp(iaA_\mu(n))$, employing the Baker-Campbell-Hausdorf formula, and Taylor expanding the gauge fields (e.g., $A_\nu(n+\mu) = A_\nu(n) + a\partial_\mu(n) + \mathcal{O}(a^2)$), we eventually find that

$$U_{\mu\nu}(n) = \exp\left[ia^2 G_{\mu\nu}(n) + \mathcal{O}(a^3)\right] \tag{1.40}$$

$$\approx 1 + ia^2 G_{\mu\nu}(n) \tag{1.41}$$

and thus

$$S_G[A] \approx \frac{1}{4}\sum_{n\in\Lambda} \text{Re}\left\{1 - \left(1 + ia^2 G_{\mu\nu}(n)\right)^a \left(1 + ia^2 G^{\mu\nu}(n)\right)_a\right\} \tag{1.42}$$

$$= \frac{a^4}{4}\sum_{n\in\Lambda} G^a_{\mu\nu}(n) G^{\mu\nu}_a(n) \tag{1.43}$$

as expected.

At this point, one might think we're finished. We have managed to discretize the path integral, reducing the number of integrals from infinity to some finite number. However, a typical lattice has something like $32^4 \approx 10^6$ lattice sites—far too many for us to perform directly. Instead we can only estimate the path integral using Monte Carlo techniques.

There is a snag, however; the exponential in (1.23) is imaginary, meaning that the phase will also matter when sampling, leading to the emergence of a *sign problem*. To get around this issue, we perform a *Wick rotation*, taking $t \to it$. The exponential therefore becomes real, with such a path integral known as a *Euclidean* path integral. Now the expectation value of observables (as well as correlator of observables) can be calculated.

$$\langle O \rangle = \frac{1}{N} \sum_{\{q,\overline{q},U\}} O[q,\overline{q},U] \qquad \text{where } \{q,\overline{q},U\} \sim e^{-S[q,\overline{q},U]} \tag{1.44}$$

That is, we generate a particular field configuration with probability proportional to $e^{-S[q,\overline{q},U]}$. We can ensure that a field configuration is generated per the correct distribution by using the Metropolis algorithm, e.g. Further details are available in Chapter 4 of [8].

Effective theories applied to quantum fields

Although one could, given near infinite resources, calculate the motion of a Frisbee from the Standard Model Lagrangian, one does not need to understand quantum field theory to understand Newtonian mechanics. Indeed we often have a clear separation of scales, which allows one to be a veterinarian, for example, without being a nuclear physicist.

In physics vernacular, we can *integrate out* the *irrelevant* degrees of freedom that are inaccessible at a particular scale. The resulting description of physics is known as an *effective theory*. When this concept is applied to quantum field theory, the resulting theory is known as an *effective field theory*.

Lattice practitioners typically employ effective field theories in their work. By definition, the lattice can never produce data at the physical point, as that would require calculations at zero lattice spacing and infinite volume—clearly an oxymoron. At a minimum we must extrapolate to the infinite volume and continuum limit. Moreover, despite the fact that we could spend all of our computational resources generating data near the physical u- and d-quark masses, it is significantly cheaper to generate lattice data with the u- and d-quark masses tuned to larger values. Thus we typically extrapolate in the quark masses, too. Effective field theory, particularly chiral perturbation theory, serves as the tool for guiding these extrapolations.

Effective theories

Before defining an effective field theory, we first give some examples of effective theories. Although there is no standard definition for effective theories, effective theories share some common features.[1] First, the effective theory is necessarily incomplete—it is only valid in some regime. Consequently the effective theory may obfuscate the details of the complete, underlying theory. Second, there should be a clear separation of scales (e.g., an expansion parameter), so that we may estimate when the effective theory stops being a robust approximation of the full theory. Finally the effective theory should remain valid for its domain even if we do not understand the full theory.

[1] See [10] for alternate sets of *desiderata*.

The harmonic oscillator

The harmonic oscillator serves as the most ubiquitous example of an effective theory in physics [11], with applications ranging from quantum field theory to cosmology. In the 17th century, Robert Hooke used this law to describe linear-elastic bodies such as springs. Of course, when formulated in a more modern language, we see that Hooke's law has much broader applicability. Consider a generic potential $V(x)$ and expand around the minimum at x_0.

$$V(x) = V(x_0) + \left.\frac{dV}{dx}\right|_{x_0} x + \frac{1}{2}\left.\frac{d^2V}{dx^2}\right|_{x_0} x^2 + \frac{1}{6}\left.\frac{d^3V}{dx^3}\right|_{x_0} x^3 + \cdots \tag{2.1}$$

Since we are only interested in potential differences, we can ignore the constant term; moreover since we have expanded about a minimum, the linear term is necessarily 0. Therefore to next-to-leading (NLO) order, the expanded potential is

$$V(x_0) = \frac{1}{2}\left.\frac{d^2V}{dx^2}\right|_{x_0} x^2 + \frac{1}{6}\left.\frac{d^3V}{dx^3}\right|_{x_0} x^3 + \cdots \tag{2.2}$$

and so long as

$$x < x_{\text{crit}} = 3\frac{\left.\frac{d^2V}{dx^2}\right|_{x_0}}{\left.\frac{d^3V}{dx^3}\right|_{x_0}} \tag{2.3}$$

the leading order (LO) term will dominate. For convenience, let us write $\frac{1}{2}\left.\frac{d^2V}{dx^2}\right|_{x_0} = k_1$, and so forth, and $w_1^2 = k_1/m$, and so forth. Then

$$m\ddot{x} = -k_1 x - k_2 x^2\,, \tag{2.4}$$

or perhaps more suggestively,

$$\ddot{x} = -\omega_1^2 x\,(1 + \Lambda x)\;. \tag{2.5}$$

In the limit where $\Lambda x \to 0$, it is straightforward to calculate the period ($T \to 2\pi/\omega_1$). Thus given some measurements of the period, we could determine the parameter w_1 in our effective theory. But how do we know whether this single parameter sufficiently describes our theory at the scale at which we're working? With a little bit of thought, we realize that although the LO term is restoring, the NLO term has a preferred direction. Therefore if the NLO term cannot be neglected, there will be an asymmetry in the amount of time for the system to pass between the turning points t_1 and t_2, depending on whether the system is evolving from $t_1 \to t_2$ or $t_2 \to t_1$.

If these half-periods are the same, we have good reason to suspect that this single-parameter effective theory is sufficient. Of course, it could be the case that there exist symmetries in the system (e.g., parity) that preclude the NLO term while leaving higher order terms in tact.

Newtonian gravity from the weak field approximation

Let us now consider Newtonian gravity as an effective theory of general relativity via *linearized gravity* [12]. Let us work in the regime where:

1. test particles are slow compared to the speed of light ($v \ll c$),
2. the gravitational field is weak, and
3. the bodies are rigid.

Because the gravitational field is assumed to be weak, we perturbatively expand around the Minkowski metric,

$$g_{\mu\nu} = \eta_{\mu\nu} + h_{\mu\nu} \, , \tag{2.6}$$

with signature $\eta_{\mu\nu} = \text{diag}(-1, 1, 1, 1)$. Let us suggestively write

$$\begin{bmatrix} h_{00} & h_{01} & h_{02} & h_{03} \\ h_{10} & h_{11} & h_{12} & h_{13} \\ h_{20} & h_{21} & h_{22} & h_{23} \\ h_{30} & h_{31} & h_{32} & h_{33} \end{bmatrix} = \begin{bmatrix} -2\phi & A_1 & A_2 & A_3 \\ A_1 & 0 & 0 & 0 \\ A_2 & 0 & 0 & 0 \\ A_3 & 0 & 0 & 0 \end{bmatrix} . \tag{2.7}$$

Here we have used the rigid body assumption to set the h_{ij} components equal to zero, as these components would ultimately correspond to shear forces in the body.

Next we solve the geodesic equation,

$$\frac{d^2 x^\lambda}{d\tau^2} + \Gamma^\lambda_{\mu\nu} \frac{dx^\mu}{d\tau} \frac{dx^\nu}{d\tau} = 0 \, , \tag{2.8}$$

for this metric. In the slow-moving limit, the timelike part of the derivative dominates: $\frac{dx^0}{d\tau} \approx e^i$, so $\frac{d^2 x^0}{d\tau^2} \approx 0$. We concentrate on the derivative with respect to the spacial indices, $\frac{d^2 x^i}{d\tau^2} \equiv \ddot{x}^i$.

Solving the geodesic equation requires us to evaluate the Christoffel symbols, which parameterize the parallel transport of vectors.

$$\Gamma^{\lambda}_{\mu\nu} = \frac{1}{2} g^{\lambda\sigma} \left(\partial_\nu g_{\sigma\mu} + \partial_\mu g_{\sigma\nu} - \partial_\sigma g_{\mu\nu}\right) \tag{2.9}$$

$$\approx \frac{1}{2} \eta^{\lambda\sigma} \left(\partial_\nu h_{\sigma\mu} + \partial_\mu h_{\sigma\nu} - \partial_\sigma h_{\mu\nu}\right) \tag{2.10}$$

In particular,

$$\Gamma^{i}_{00} \frac{d\,x^0}{d\,\tau} \frac{d\,x^0}{d\,\tau} = \left(\partial_0 A_i + \partial_i \phi\right) e^i \qquad \rightarrow \partial_t \boldsymbol{A} + \boldsymbol{\nabla}\phi \,,$$

$$2\Gamma^{i}_{j0} \frac{d\,x^j}{d\,\tau} \frac{d\,x^0}{d\,\tau} = \left(\partial_j A_i - \partial_i A_j\right) \dot{x}^j e^i \qquad \rightarrow -\dot{\boldsymbol{x}} \times \left(\boldsymbol{\nabla} \times \boldsymbol{A}\right) \,.$$

We ignore the terms associated with the Γ^k_{ij} Christoffel symbols as these will be suppressed by factors of $(v/c)^2$. Combining everything gives us

$$\ddot{\boldsymbol{x}} = -\left(\partial_t \boldsymbol{A} + \boldsymbol{\nabla}\phi\right) + \dot{\boldsymbol{x}} \times \left(\boldsymbol{\nabla} \times \boldsymbol{A}\right) \,. \tag{2.11}$$

The first term is the familiar Newtonian potential for the correct choice of gauge ($\partial_t \boldsymbol{A} = 0$). When $\nabla^2 \phi \sim \rho$ (the matter density), we recover Newton's law of universal gravitation. This is the *gravitoelectric* field, to make an analogy to electromagnetism.

More curious is the second term, corresponding to the *gravitomagnetic* field. Here we see that the effective theory provides an insight lacking in Newton's formulation of gravity. Like the magnetic field, the gravitomagnetic field is velocity-dependent, but it is suppressed compared to the gravitoelectric field by a factor of v/c. More generally there exists a gravitational analog to Maxwell's equations, which was first recognized by Heaviside in the 19th century even before the advent of relativity [13].

An estimate for the gravitomagnetic field of the earth can be found by analogy to the magnetic field generated by a rotating ball of uniform volume charge density; the only difference between the two expressions will be the constant prefactors. Taking the electromagnetic solution [14] and replacing the constants by dimensional analysis, we expect the gravitomagnetic field above Earth to be

$$\boldsymbol{B}_g(r,\theta) \sim \frac{GMR^2\omega}{c^2 r^3} \left(2\cos\theta\,\hat{r} + \sin\theta\,\hat{\theta}\right) \tag{2.12}$$

with θ the latitude, and so the strength of the gravitomagnetic acceleration on the surface should be roughly $GM\omega^2/c^2 \sim 10^{-12}g$. Gravity Probe B verified the presence of the gravitomagnetic field by measuring the Lense-Thirring precession of the Earth [15].[2]

Effective field theories

In an effective *field* theory, one posits that the ultraviolet physics of the full theory are suppressed below a scale Λ, where often $\Lambda \sim M$ is the mass of the lightest particle excluded by the theory. By the uncertainty principle, these particles will not be able to propagate far, so their interactions will appear point-like. One then constructs the most general Lagrangian compatible with the symmetries of the full theory and matches (or measures) the coefficients of the effective Lagrangian.

Unlike a quantum field theory, which is renormalizable, an effective field theory need not be. Instead the Lagrangian becomes a tower of infinitely many terms organized by an expansion in the scale. Consider the following contrived extension of ϕ^4-theory which will demonstrate the principles of effective field theories.

$$\mathcal{L}_{\text{free}} = \frac{1}{2}\left(\partial_\mu \phi\right)^2 - \frac{1}{2}m^2\phi^2 + \lambda\phi^4 \tag{2.13}$$

Since we require the action be dimensionless, it is straightforward to see that the operators have mass dimension

$$\left[(\partial_\mu \phi)^2\right] = 4 \qquad \text{and} \qquad [\phi] = 1\,. \tag{2.14}$$

Under the effective field theory philosophy, we include all *irrelevant* combinations of these operators (i.e., combinations with mass dimension greater than 4). Consequently the prefactors must have negative mass dimension (here the $c_{n,m}$ coefficients are dimensionless low energy constants).

$$\mathcal{L}_{\text{eff}} = \frac{1}{2}\left(\partial_\mu \phi\right)^2 - \frac{1}{2}m^2\phi^2 + \lambda\phi^4 + \sum_{n=5}^{\infty}\sum_{m=0}^{4m\leq n}\frac{c_{n,m}}{\Lambda^{n-4}}\left(\partial_\mu\phi\right)^{2m}\phi^{n-4m} \tag{2.15}$$

If the theory is “natural” each coefficient will be $\mathcal{O}(1)$, with the higher order terms being suppressed by additional powers of Λ. We can further reduce the number of terms in this expansion by imposing symmetry

[2]In fact, the gravitomagnetic field equals half the Lense-Thirring precession, as described in Chapter 12 of [16]. (Unfortunately for most of us, the reference is in German. However, the derivation is still surprisingly intelligible, assuming you know the starting point and conclusion.)

constraints; for instance, if we require ϕ to be parity invariant, then the terms with odd powers of ϕ would drop out.

Two scalar fields

Although the previous example shows the elements of an effective field theory, it is unclear what Λ should be. Let us now consider the simplest non-trivial effective field theory: two free scalar fields, ϕ and ρ, with an interaction term [17, 18]. Let us further assume that the ρ field is much heavier than the ϕ field, $M \gg m$. The full Lagrangian is

$$\mathcal{L} = \frac{1}{2}\left(\partial_\mu \phi\right)^2 + \frac{1}{2}\left(\partial_\mu \rho\right)^2 - m^2\phi^2 - M^2\rho^2 + \kappa\phi^2\rho\,. \tag{2.16}$$

(Note $[\kappa] = [m] = [M] = 1$.) Recall that under the path integral formulation observables are weighed by a factor of $\exp(iS[\phi,\rho])$. When $\Lambda \ll M$, we expect the heavy scalar field to have little influence in mediating interactions. We would therefore like to integrate-out the heavy field so that we have an effective field theory involving only the light field. That is,

$$e^{iS_{\text{eff}}[\phi]} \approx \int \mathcal{D}[\rho] e^{iS[\phi,\rho]}\,. \tag{2.17}$$

If we Wick rotate ($iS \to -S$), it is clear that the weight is maximal when $\delta S/\delta\rho = 0$.

$$\frac{\delta S}{\delta \rho} = \int d^4x \left[-\partial^2\phi\frac{\delta\phi}{\delta\rho} - \partial^2\rho - 2m^2\phi\frac{\delta\phi}{\delta\rho} - 2M^2\rho - \kappa\left(\phi^2 + 2\phi\rho\frac{\delta\phi}{\delta\rho}\right)\right] = 0 \tag{2.18}$$

Since $\delta\phi/\delta\rho = 0$, we require

$$\left(\frac{\partial^2}{2M^2} + 1\right)\rho_0 = -\frac{\kappa\phi^2}{2M^2}\,. \tag{2.19}$$

We expand the solution perturbatively,

$$\rho_0 = -\left[1 - \frac{\partial^2}{2M^2} + \left(\frac{\partial^2}{2M^2}\right)^2 - \cdots\right]\frac{\kappa\phi^2}{2M^2}\,, \tag{2.20}$$

and reinsert the solution into our original Lagrangian.

$$\mathcal{L}_{\text{eff}} = \frac{1}{2}\left(\partial_\mu \phi\right)^2 + \frac{1}{2}\left(\partial_\mu \left\{\left[1 - \frac{\partial^2}{2M^2} + \left(\frac{\partial^2}{2M^2}\right)^2 - \cdots\right]\frac{\kappa\phi^2}{2M^2}\right\}\right)^2 \tag{2.21}$$
$$- m^2\phi^2 - M^2\left(\left[1 - \frac{\partial^2}{2M^2} + \left(\frac{\partial^2}{2M^2}\right)^2 - \cdots\right]\frac{\kappa\phi^2}{2M^2}\right)^2$$
$$+ \kappa\phi^2\left[1 - \frac{\partial^2}{2M^2} + \left(\frac{\partial^2}{2M^2}\right)^2 - \cdots\right]\frac{\kappa\phi^2}{2M^2}$$

As written there are many redundant terms. For concreteness, let us write out the first few terms to this effective Lagrangian $\mathcal{L}_{\text{eff}} = \mathcal{L}_0 + \mathcal{L}_1 + \cdots$.

$$\mathcal{L}_0^{\text{free}} = \frac{1}{2}\left(\partial_\mu\phi\right)^2 - m^2\phi^2 \tag{2.22}$$

$$\begin{aligned}\mathcal{L}_0^{\text{int}} &= -\frac{\kappa}{4M}\phi^4 + \frac{\kappa}{2M}\phi^4 \\ &= \frac{\kappa}{4M}\phi^4\end{aligned} \tag{2.23}$$

$$M\mathcal{L}_1 = 0 \tag{2.24}$$

$$\begin{aligned}M^2\mathcal{L}_2 &= \frac{\kappa^2}{2M^2}\left(\phi^2\left(\partial_\mu\phi\right)^2\right) + \frac{\kappa^2}{2M^2}\left(\phi^2\left(\partial_\mu\phi\right)^2 + \phi^3\partial^2\phi\right) \\ &\quad - \frac{\kappa^2}{M^2}\left(\phi^2\left(\partial_\mu\phi\right)^2 + \phi^3\partial^2\phi\right) \\ &= -\frac{\kappa^2}{2M^2}\phi^3\partial^2\phi\end{aligned} \tag{2.25}$$

The second derivative is a bit awkward, but fortunately we can recast it as something more quotidian. Because $\partial_\mu(\phi^3\partial_\mu\phi) = \phi^3\partial^2\phi + 3\phi^2(\partial_\mu\phi)^2$, and because observables are insensitive to adding a gradient to the action, we can replace $\phi^3\partial^2\phi$ with $-3\phi^2(\partial_\mu\phi)^2$ in the Lagrangian. Yet even these choices aren't unique. Shifting the irrelevant operators by a term proportional to an equation of motion is equivalent to redefining the fields, which by the equivalence theorem will have no impact on scattering calculations [19]. From the

Euler-Lagrange equations, we see that

$$\partial^2\phi = -2m\phi^2 + 2\kappa\rho\phi\,, \tag{2.26}$$

with the second term contributing at a higher order than the first, thus allowing us to equivalently write $M^2\mathcal{L}_2 \sim \phi^6$.

Regardless, let us reconsider the generic scalar effective Lagrangian from before, (2.15). In that case, we took a "bottom-up" approach, in which we constructed our EFT without specifying the full theory. In this case we have taken a "top-down" approach, in which we started with a theory involving two scalar fields and integrated-out the heavy one. Indeed, we see that the bottom-up Lagrangian (2.15) could also describe the top-down Lagrangian (2.22) by matching coefficients.

The Standard Model?

Some physicists (e.g., [20, 21]) have argued that the Standard Model itself is an effective field theory. Recall that when constructing a quantum field theory, we expect the theory to be renormalizable. As a practical matter renormalizable theories are convenient, as observables can be calculated at any scale using only a finite number of parameters. Let us contrast this approach with the effective field theory approach. When constructing an effective field theory, we write down the most general Lagrangian compatible with the symmetries/gauge redundancies of the system. This Lagrangian will generally include irrelevant terms which will not be renormalizable.

The Standard Model is a renormalizable theory. Consequently we can calculate observables from this Lagrangian at any scale without encountering unphysical divergences (whether we might have other difficulties in this calculation is a separate matter). But how can we *know* whether the predictions at, for example, 10^{20} GeV are correct without an experimental check? Perhaps there are non-renormalizable terms that must be added to the Standard Model to make the correct prediction. Indeed, history teaches that the "full theory" of yesteryear becomes the effective theory of today.

Of course, if the Standard Model is better thought of as an effective field theory, we would like to know the scale Λ_{SM} at which the renormalizable part of the theory breaks down. One possible candidate for Λ_{SM} comes from neutrinos. When the Standard Model was originally formulated, experimental data suggested a neutrino mass compatible with zero, an (incorrect) assumption that was then baked into the Standard Model Lagrangian. There are a few ways to cure this deficiency, but let's focus on an EFT approach.

There is only a single dimension-5 operator that can be added to the Standard Model while preserving the SU(3)×SU(2)×U(1) gauge group [21, 22, 23]. To wit, it is the Weinberg operator

$$\mathcal{L}_5 = \frac{1}{\Lambda} \sum_{f,f'} c_{f,f'} \left(\overline{L}_f \cdot \widetilde{H} \right) \left(\widetilde{H}^\dagger \cdot L_{f'} \right)^c + \text{h.c.} \tag{2.27}$$

Here $L = (\nu_\mathrm{L},\ l_\mathrm{L})^T$ and $H = (\phi^+,\ \phi^0)^T$ are doublets of SU(2) weak isospin with sums over flavor $f, f' = e, \mu, \tau$. Expanding this term in the unitary gauge $H = (0, h + v)$, we see there is a term proportional to $(v^2/\Lambda)\nu\nu$, where $v \sim 100$ GeV is the vacuum expectation value of the Higgs. Assuming the dimensionless coupling is order $c \sim 1$ and the heaviest neutrino mass is $m_\nu \sim 0.1$ MeV, we can estimate the EFT scale to be $\Lambda_\mathrm{SM} \sim 10^{14}$ GeV—but only if such an interaction actually occurs in nature. Violation of $B - L$ conservation would be evidence for such a term, as the Weinberg operator does not preserve this number.

Chiral Perturbation Theory

We previously constructed an effective field theory from two scalar fields by integrating out the heavy scalar. In that approach, we assumed that the heavy scalar varied slowly compared to the light scalar, which allowed us to remove the heavy scalar by assuming the action remained stationary under variations of this field. Unfortunately, this procedure is untenable in low-energy QCD: we do not know how to integrate out the quarks and gluons in the theory since the theory is non-perturbative in this regime.

However, that is only one technique for constructing an effective field theory. One can alternatively begin with the observed degrees of freedom and subject them to the symmetry restraints (or in our case, the approximate restraints) of the full theory. This is the approach we will take to construct chiral perturbation theory, a low-energy effective field theory for QCD in which the degrees of freedom of the full theory (the quarks) are replaced with the degrees of freedom at low energy (light hadrons). [1]

The meaning of chirality

Let us revisit the QCD Lagrangian.

$$\mathcal{L} = \sum_f \overline{q}_f \left(i\gamma^\mu D_\mu - m_f\right) q_f - \frac{1}{4} G^a_{\mu\nu} G^{\mu\nu}_a \tag{3.1}$$

The spin-$\frac{1}{2}$ field q_f is a complex bispinor built from two Weyl spinors. We can get an intuition for each of these spinors by considering how they behave under rotations and boosts. Recall from Chapter 1 that spin-$\frac{1}{2}$ fields transform as

$$\psi^\alpha(x) \to \psi'^\alpha(x) = \left(e^{-i\omega_{\mu\nu}\mathcal{S}^{\mu\nu}}\right)^\alpha{}_\beta \psi^\beta(\Lambda^{-1}x)\,. \tag{3.2}$$

[1] The author found the following references useful for understanding the topics covered in this chapter: [24, 25, 26, 27, 28, 29, 30, 31].

where $\mathcal{S}^{\mu\nu} = \frac{i}{4}\left[\gamma^\mu, \gamma^\nu\right]$. Let us explicitly write the γ-matrices in the Weyl/chiral basis. [2]

$$\gamma^0 \overset{\text{Weyl}}{=} \begin{bmatrix} 0 & \mathbb{1} \\ \mathbb{1} & 0 \end{bmatrix} \qquad \gamma^k \overset{\text{Weyl}}{=} \begin{bmatrix} 0 & \sigma_k \\ -\sigma_k & 0 \end{bmatrix} \tag{3.3}$$

Here σ_k denotes the familiar Pauli matrices. Rotations occur when $\mu, \nu \in \{1, 2, 3\}$; boosts occur when either $\mu = 0$ or $\nu = 0$. For example, we can explicitly write a rotation by $\omega_{12} = \omega$ in the xy-plane as

$$\left(e^{-i\omega_{12}\mathcal{S}^{12}}\right)^{\alpha}_{\ \beta} \overset{\text{Weyl}}{=} \begin{bmatrix} e^{-i\omega\sigma_3/2} & 0 \\ 0 & e^{-i\omega\sigma_3/2} \end{bmatrix} . \tag{3.4}$$

We observe the two Weyl spinors behave identically under rotations. (However, it is worth noting that the factor of $1/2$ means that a spinor must be rotated by 4π to return to its original state; this is one manner in which spinors can be distinguished from vectors.)

The situation with boosts is slightly different. Boosting in the x-direction by $\omega_{01} = \chi$, we have

$$\left(e^{-i\omega_{01}\mathcal{S}^{01}}\right)^{\alpha}_{\ \beta} \overset{\text{Weyl}}{=} \begin{bmatrix} e^{-i\chi\sigma_1/2} & 0 \\ 0 & e^{+i\chi\sigma_1/2} \end{bmatrix} . \tag{3.5}$$

Here we see that the two Weyl spinors can be distinguished under boosts. Formally, we say that the representation for Dirac bispinors is reducible. Which representation a spinor belongs to can be thought of as just another quantum number; we call this quantum number *chirality*.[3]

We can project out the chiral components of a Dirac bispinor through the "fifth" γ-matrix, defined as

$$\gamma^5 = i\gamma^0\gamma^1\gamma^2\gamma^3 \overset{\text{Weyl}}{=} \begin{bmatrix} -\mathbb{1} & 0 \\ 0 & \mathbb{1} \end{bmatrix} . \tag{3.6}$$

[2] Identities involving the gamma matrices and projection operators (defined later in this section) are available in Appendix A.

[3] Although chirality can be related to helicity, they are conceptually different; helicity is frame-dependent for massive particles, whereas chirality is Lorentz-invariant.

Writing $\psi = (\psi^{(L)},\ \psi^{(R)})^T$, we define the projection operators $P_{L/R} = \frac{1}{2}(\mathbb{1} \mp \gamma^5)$. Thus

$$\psi = \underbrace{\frac{1}{2}(\mathbb{1} - \gamma^5)\psi}_{\psi_L = P_L\psi} + \underbrace{\frac{1}{2}(\mathbb{1} + \gamma^5)\psi}_{\psi_R = P_R\psi} \tag{3.7}$$

where $\psi_L = (\psi^{(L)},\ 0)^T$ and $\psi_R = (0,\ \psi^{(R)})^T$.

To understand why this quantum number is known as chirality, let us consider how $\psi = \psi_L + \psi_R$ transforms under the parity operator $\mathcal{P}$. Recall that $\mathcal{P}$ reverses momentum while leaving spin intact. From Eqs. 3.4 and 3.5, we see that both ψ_L and ψ_R transform identically under rotations (spin) but oppositely under boosts (momentum). Thus, we require

$$\mathcal{P} : \begin{bmatrix} \psi^{(L)}(\mathbf{x}, t) \\ \psi^{(R)}(\mathbf{x}, t) \end{bmatrix} \to \begin{bmatrix} \psi^{(R)}(-\mathbf{x}, t) \\ \psi^{(L)}(-\mathbf{x}, t) \end{bmatrix} \tag{3.8}$$

This is, under $\mathcal{P}$, the components of the Dirac bispinor are swapped. A spinor that once transformed under a left-handed coordinate system now transforms under a right-handed one.

Global symmetries in QCD beyond color

Additional symmetries arise in QCD through acting on the quarks in *flavor* space, rather than acting in *color* space. Let us rearrange the quark fields into a vector $q = (q_1, \ldots, q_N)^T$ and the mass terms into a diagonal matrix $M = \text{diag}(m_{q_1}, \ldots, m_{q_N})$ while generalizing the 6 flavors of QCD to N flavors. The QCD Lagrangian now becomes

$$\mathcal{L}_{\text{QCD}} = \overline{q}\left(i\gamma^\mu D_\mu - M\right) q - \frac{1}{4} G^a_{\mu\nu} G^{\mu\nu}_a \tag{3.9}$$

We will see that certain global transformations can mix flavors, depending on our assumptions about M.

U(1) vector symmetry

The simplest global flavor symmetry comes from a U(1) transformation, which is trivially seen to leave the vectorized QCD Lagrangian invariant.

$$\begin{aligned} q \to q' &= e^{i\alpha} q \\ \overline{q} \to \overline{q}' &= e^{-i\alpha} \overline{q} \end{aligned} \tag{3.10}$$

The significance of this symmetry can be gleaned by analyzing the associated Noether current.

$$\begin{aligned} \alpha V^{\mu} &= -\left(\frac{\partial \mathcal{L}}{\partial \partial_{\mu} q} \delta q + \frac{\partial \mathcal{L}}{\partial \partial_{\mu} \overline{q}} \delta \overline{q} \right) \\ &= -\left(\overline{q} i \gamma^{\mu} \right) (i\alpha) + 0 \\ \implies V^{\mu} &= \overline{q} \gamma^{\mu} q \end{aligned} \tag{3.11}$$

We see that this current transforms as a vector, hence the name. When we calculate the charge,

$$Q^V = \int d^3x \, V^0 = \int d^3x \, \overline{q} \gamma^0 q = \int d^3x \, q^{\dagger} q \,, \tag{3.12}$$

we find that we have a volume integral of a number density. This number counts the total number of quark minus antiquarks, from which we conclude that the vector current is associated with baryon number conservation.

U(1) axial symmetry

The axial U(1) transformation is defined similarly as the vector transformation except with the inclusion of the γ^5 matrix.

$$\begin{aligned} q \to q' &= e^{i\alpha\gamma^5} q \\ \overline{q} \to \overline{q}' &= e^{-i\alpha\gamma^5} \overline{q} \end{aligned} \tag{3.13}$$

Although the kinetic term preserves the symmetry in the Lagrangian, the mass term does not.

$$\begin{aligned}\overline{q}\gamma^\mu D_\mu q \to \overline{q}'\gamma^\mu D_\mu q' = \overline{q}e^{i\alpha\gamma^5}\gamma^\mu e^{i\alpha\gamma^5} D_\mu q &= \overline{q}\gamma^\mu D_\mu q \\ \overline{q}Mq \to \overline{q}'Mq' = \overline{q}e^{i\alpha\gamma^5} M e^{i\alpha\gamma^5} q &= \overline{q}e^{2i\alpha\gamma^5} Mq\end{aligned}$$

Thus except when $M = 0$, the U(1) axial transformation is not a global symmetry. Regardless, we can calculate the current anyway.

$$A^\mu = \overline{q}\gamma^\mu\gamma^5 q \tag{3.14}$$

We observe that this current transforms as an axial vector, hence the name. Unsurprisingly, the axial current is not conserved; in fact, an additional term must be included in the divergence due to a quantum anomaly.

SU(N) vector symmetry

Unlike the other global transformations defined so far, the SU(N) vector symmetry mixes the flavor of the quarks.

$$\begin{aligned} q^a \to q'^a &= \left(e^{i\theta_c T^c}\right)^a_{\ b} q^b \\ \overline{q}^a \to \overline{q}'^a &= \left(e^{-i\theta_c T^c}\right)^a_{\ b} \overline{q}^b \end{aligned} \tag{3.15}$$

That is, the quark fields transform under the fundamental representation of SU(N), with the T^a being the generators of the $\mathfrak{su}(N)$ Lie algebra and N being the number of flavors. As written, this is nearly identical to the SU(3) color transformation from Section 1.1.3, but we emphasize this is a transformation in *flavor* space, not *color* space.

The SU(N) vector symmetry only holds so long as $m_1 = m_2 = \cdots = m_N$. Clearly this is not a good approximation in QCD generally, as the first generation quarks have $m_u \sim m_d \sim 1$ MeV while the third generation quarks have $m_t \gg m_b \gg 1$ GeV. Instead one usually restricts themselves to SU(2) or SU(3) flavor symmetry (the former, of course, is more commonly referred to as isospin). In fact, the mass of the first three quarks is smaller than the lightest bound states of hadrons (as well as $\Lambda_{\text{QCD}} \sim 300$ MeV), so these approximations tend to hold fairly well.

For completeness's sake, the currents and divergences are given by

$$V^{\mu,a} = \overline{q}\gamma^\mu T^a q\,, \tag{3.16}$$

$$\partial_\mu V^{\mu,a} = i\overline{q}\gamma^\mu [M, T^a] q\,. \tag{3.17}$$

Although M and T^a do no generally commute, they do commute when T^a is diagonal. For example, when $N = 2$ the generator $T^3 \to \sigma^3$ (the third Pauli matrix) commutes with M, so the current $V^{\mu,3} \sim \overline{u}\gamma^\mu u - \overline{d}\gamma^\mu d$ is conserved. The corresponding charge is, of course, isospin. Similarly for $N = 3$, the currents corresponding to $T^3 \to \lambda^3$ and $T^8 \to \lambda^8$ (the third and eighth Gell-Mann matrices) are conserved. The current $V^{\mu,3}$ is the same as before, and $V^{\mu,8} \sim \overline{u}\gamma^\mu u + \overline{d}\gamma^\mu d - 2\overline{s}\gamma^\mu s$, with Q_8^V known as hypercharge. Generally speaking, isospin and hypercharge can be used to arrange the hadrons into multiplets, even when SU(3) flavor symmetry is only approximate. This is the realization of Gell-Mann's eightfold way [32] at the level of quarks.

SU(N) axial symmetry

Similarly, we consider the SU(N) axial transformation

$$\begin{aligned} q^a \to q'^a &= \left(e^{i\gamma^5\theta_c T^c}\right)^a_{\ b} q^b \\ \overline{q}^a \to \overline{q}'^a &= \left(e^{-i\gamma^5\theta_c T^c}\right)^a_{\ b} \overline{q}^b \end{aligned} \tag{3.18}$$

with currents and divergences

$$A^{\mu,a} = \overline{q}\gamma^\mu\gamma^5 T^a q\,, \tag{3.19}$$

$$\partial_\mu A^{\mu,a} = i\overline{q}\gamma^\mu\gamma^5 \{M, T^a\} q\,. \tag{3.20}$$

Notice that the commutator $[\cdot,\cdot]$ from the previous section has been replaced by an anticommutator $\{\cdot,\cdot\}$, so the divergence never vanishes for any of the generators unless $M = 0$.

The divergence is known as the *partially conserved axial current* (*partially* since, were it not for the non-zero quark masses, the conservation would be exact). Gell-Mann and Lévy [33] showed that this current can be used to explain the decay rate of the charged pion, albeit with the problem formulated in terms of an effective model for the pions and nucleons (this was before Gell-Mann and Zweig proposed the quark model). We will return to this point later.

$\mathbf{SU(N)_L \times SU(N)_R}$ chiral symmetry

As an alternate approach to SU$(N)_V \times$ SU$(N)_A$, we can instead consider the Lagrangian from a chiral perspective. Projecting out the chiral components, Eq. (3.9) becomes

$$\mathcal{L}_{\text{QCD}} = \overline{q}_L \left(i\gamma^\mu D_\mu\right) q_L + \overline{q}_R \left(i\gamma^\mu D_\mu\right) q_R - \overline{q}_L M q_R - \overline{q}_R M q_L - \frac{1}{4} G^a_{\mu\nu} G^{\mu\nu}_a \,. \tag{3.21}$$

We now consider the following transformations of the quark fields.

$$\begin{aligned} q^a_L \to q'^a_L &= \left(e^{i\theta_{c,L}T^c}\right)^a_{\ b} q^b_L \qquad & q^a_R \to q'^a_R &= \left(e^{i\theta_{c,R}T^c}\right)^a_{\ b} q^b_R \\ \overline{q}^a_L \to \overline{q}'^a_L &= \left(e^{-i\theta_{c,L}T^c}\right)^a_{\ b} \overline{q}^b_L \qquad & \overline{q}^a_R \to \overline{q}'^a_R &= \left(e^{-i\theta_{c,R}T^c}\right)^a_{\ b} \overline{q}^b_R \end{aligned} \tag{3.22}$$

We emphasize that the transformations occur in different spaces, i.e. $[U_L, U_R] = 0$ for $U_L \in$ SU$(N)_L$ and $U_R \in$ SU$(N)_R$. We observe see that the kinetic terms maintain the symmetry, while the mass terms explicitly break it. When SU$(N)_L =$ SU$(N)_R$, the symmetry reduces to SU$(N)_V$.

We can recast the SU$(N)_V$ and SU$(N)_A$ currents from before in terms of the chiral fields.

$$\begin{aligned} V^{\mu,a} &= \overline{q}\gamma^\mu T^a q \\ &= \overline{q}_L \gamma^\mu T^a q_L + \overline{q}_R \gamma^\mu T^a q_R \\ &= V^{\mu,a}_L + V^{\mu,a}_R \end{aligned}$$

Here we have used an identity from Appendix A and defined $V_{L/R}^{\mu,a} = \overline{q}_{L/R}\gamma^\mu T^a q_{L/R}$. The $\mathrm{SU}(N)_A$ currents are slightly trickier.

$$\begin{aligned}A^{\mu,a} &= \overline{q}\gamma^\mu\gamma^5 T^a q \\ &= \overline{q}\gamma^\mu(P_R - P_L)T^a q \\ &= \overline{q}\gamma^\mu(P_R^2 - P_L^2)T^a q \\ &= \overline{q}(P_L\gamma^\mu P_R - P_R\gamma^\mu P_L)T^a q \\ &= V_R^{\mu,a} - V_L^{\mu,a}\end{aligned}$$

Spontaneous symmetry breaking of $\mathbf{SU}(N)_L \times \mathbf{SU}(N)_R$

A review of Goldstone's theorem

Goldstone's theorem tells us that if a continuous symmetry is preserved by the Lagrangian but broken by the vacuum, then there exists a massless boson for each broken generator of that symmetry.

To sketch the proof, [4] let us suppose that Q^a is the conserved charge corresponding to some continuous symmetry of the Lagrangian as guaranteed by Noether's theorem. In the language of quantum mechanics, this means that the Hamiltonian H commutes with Q^a, $[H, Q^a] = 0$. Furthermore, when acting on the vacuum $H|\Omega\rangle = 0$ up to some constant (i.e., take $H \to H + c$ if required).

We assume that the vacuum is not invariant under the symmetry, i.e. $Q^a|\Omega\rangle \neq 0$. This means

$$\begin{aligned}&\underbrace{[H, Q^a]}_{=0}|\Omega\rangle = HQ^a|\Omega\rangle - Q^a \underbrace{H|\Omega\rangle}_{=0} = 0 \\ \implies &H\left(Q^a|\Omega\rangle\right) = 0\,.\end{aligned} \tag{3.23}$$

That is, the state $Q^a|\Omega\rangle$ has the same energy as $|\Omega\rangle$. Let us build a state from $Q^a|\Omega\rangle = \int d^3x\, J^{a,0}(\mathbf{x}, t)|\Omega\rangle$ with momentum $\mathbf{p}$.

$$|\eta\rangle = \int d^3x\, e^{-i\mathbf{p}\cdot\mathbf{x}} J^{a,0}(\mathbf{x}, t)\,|\Omega\rangle \tag{3.24}$$

[4] The argument is taken from [34]. However, the explanation provided is not entirely rigorous as it runs afoul of the Fabri-Picasso theorem: $\langle QQ\rangle \sim \mathcal{V}_{\text{space}} \to \infty$, and therefore $Q|\Omega\rangle$ does not belong to the Hilbert space unless the symmetry is unbroken. Nevertheless, the proof can be made rigorous [35].

But this means that as $\mathbf{p} \to 0$, we require $E^2 = p^2 + m^2 \to 0$, so the particle corresponding to $|\eta\rangle$ must be massless. The symmetry is said to be spontaneously broken, and for each generator T^a there must exist a massless boson.

The quark condensate

As a candidate spontaneous symmetry breaking, let us consider the quark condensate $\langle \overline{q}q\rangle$. Quarks and antiquarks are tightly bound by an attractive interaction, so in the chiral limit where $m_q = 0$, the cost for the vacuum to create a $\overline{q}q$-pair is is small. The quark condensate (along with the gluon condensate) therefore comprise the QCD vacuum.

Under a chiral transformation, the quark condensate becomes

$$\langle \overline{q}q\rangle = \langle \overline{q}_L q_R\rangle + \langle \overline{q}_R q_L\rangle \ . \tag{3.25}$$

Thus a global transformation under SU$(N)_L\times$SU$(N)_R$ will change the value of the vacuum, assuming that $\langle \overline{q}q\rangle \neq 0$. (In fact, lattice calculations support our hunch that the quark condensate has a nonzero vacuum expectation value.) The full chiral symmetry is spontaneously broken by the quark condensate down to just the vector part, SU$(N)_L\times$SU$(N)_R \to$SU$(N)_V$, which leaves $\langle \overline{q}q\rangle$ invariant. The broken symmetry is given by the quotient SU$(N) \times$ SU$(N)/$SU$(N) \sim$ SU(N) which has $N^2 - 1$ generators, and therefore we expect there to be $N^2 - 1$ Goldstone bosons. [5]

In the case of isospin, we have $N = 2$, so there are 3 Goldstone bosons. The full theory of QCD does not contain massless hadrons—but it does contain 3 bosons that are significantly lighter than the rest: the neutral and charged pions. We recall that, in addition to being spontaneously broken, chiral symmetry is explicitly broken by a mass term for the quarks. Thus the Goldstone bosons of chiral symmetry breaking are technically pseudo-Goldstone bosons, which are comparably light but not massless.

In the case of SU(3) chiral symmetry breaking, we identify the kaons and η mesons as pseudo-Goldstone bosons, too.

[5]Technically the quotient SU$(N)_L \times$ SU$(N)_R/$SU$(N)_V$ is not a group but a coset space; this distinction will become important later.

The linear-σ model

In low-energy QCD, we do not observe quarks and gluons; instead, we see the lightest hadrons—pions and nucleons, for example. In the 1960s, Gell-Mann and Lévy proposed the linear-σ model to explain the decay of charged pions [33]. In this model, the neutron and proton belong to an isodoublet $N = (p, n)^T$ transforming under SU(2) isospin. Of course, in those days (prior to the quark model) isospin was understood in terms of the proton and neutron; but since the valence quark content of each particle is $p = uud$ and $n = udd$, the difference between a proton and neutron is the difference between a u and d quark, which can be described by an approximate SU(2) flavor symmetry.

We see that the kinetic term is invariant under a global transformation of $\mathrm{SU}(2)_V$ (isospin) and $\mathrm{SU}(2)_A$ (here τ^a are the Pauli matrices).

$$\mathrm{SU}(2)_V: \qquad \overline{N} i\gamma^\mu \partial_\mu N \to \overline{N}' i\gamma^\mu \partial_\mu N' = \overline{N} e^{-i\theta_a \frac{\tau^a}{2}} i\gamma^\mu e^{i\theta_a \frac{\tau^a}{2}} \partial_\mu N \qquad = \overline{N} i\gamma^\mu \partial_\mu N \tag{3.26}$$

$$\mathrm{SU}(2)_A: \qquad \overline{N} i\gamma^\mu \partial_\mu N \to \overline{N}' i\gamma^\mu \partial_\mu N' = \overline{N} e^{i\gamma^5\theta_a \frac{\tau^a}{2}} i\gamma^\mu e^{i\gamma^5\theta_a \frac{\tau^a}{2}} \partial_\mu N \qquad = \overline{N} i\gamma^\mu \partial_\mu N \tag{3.27}$$

However, although the mass term in invariant under $\mathrm{SU}(2)_V$, it is not invariant under $\mathrm{SU}(2)_A$:

$$\mathrm{SU}(2)_V: \qquad m\overline{N}N \to m\overline{N}'N' = m\overline{N} e^{-i\theta_a \frac{\tau^a}{2}} e^{i\theta_a \frac{\tau^a}{2}} N \qquad = m\overline{N}N \tag{3.28}$$

$$\mathrm{SU}(2)_A: \qquad m\overline{N}N \to m\overline{N}'N' = m\overline{N} e^{i\gamma^5\theta_a \frac{\tau^a}{2}} e^{i\gamma^5\theta_a \frac{\tau^a}{2}} N \qquad = m\overline{N}N e^{2i\gamma^5\theta_a \frac{\tau^a}{2}} \tag{3.29}$$

Nevertheless, Gell-Mann and Lévy insisted on keeping the full $\mathrm{SU}(2)_V \times \mathrm{SU}(2)_A \simeq \mathrm{SU}(2)_L \times \mathrm{SU}(2)_R$ symmetry intact. Towards that end, they included a few additional fields in the model, π^a and σ, with the π^a fields playing the role of the pions and (as we will see) the σ field providing a mass for the nucleon after spontaneous symmetry breaking.

We assume that the pion fields transform according to the vector representation of SU(2) and as a pseudoscalar under Lorentz symmetry. Taken together, we write $\pi^a = i\overline{\psi}\gamma^5\tau^a\psi/2$ with ψ a Dirac bispinor. The field σ will transform under the trivial representation of SU(2) and as a scalar under Lorentz symmetry, so $\sigma = \overline{\psi}\psi$. Their transformations are given below.

$$\begin{aligned}
\mathrm{SU}(2)_V: \qquad \pi^a \to \pi'^a &= i\overline{\psi}'\gamma^5\tau^a\psi' \\
&= i\overline{\psi}e^{-i\theta_b\frac{\tau^b}{2}}\gamma^5\tau^a e^{i\theta_b\frac{\tau^b}{2}}\psi \\
&\approx i\overline{\psi}\gamma^5\left(1-i\theta_b\frac{\tau^b}{2}\right)\tau^a\left(1+i\theta_b\frac{\tau^b}{2}\right)\psi \\
&= i\overline{\psi}\gamma^5\left(\tau^a - i\theta_b\left[\frac{\tau^b}{2},\tau^a\right]+O(\theta^2)\right)\psi \\
&\approx \pi^a - \epsilon^{abc}\theta_b\pi_c
\end{aligned} \tag{3.30}$$

$$\begin{aligned}
\mathrm{SU}(2)_A: \qquad \pi^a \to \pi'^a &= i\overline{\psi}'\gamma^5\tau^a\psi' \\
&= i\overline{\psi}e^{i\gamma^5\theta_b\frac{\tau^b}{2}}\gamma^5\tau^a e^{i\gamma^5\theta_b\frac{\tau^b}{2}}\psi \\
&\approx i\overline{\psi}\left(1+i\gamma^5\theta_b\frac{\tau^b}{2}\right)\gamma^5\tau^a\left(1+i\gamma^5\theta_b\frac{\tau^b}{2}\right)\psi \\
&= \bar{i}\psi\left(\gamma^5\tau^a + i\theta_b\left\{\frac{\tau^b}{2},\tau^a\right\}+O(\theta^2)\right)\psi \\
&\approx \pi^a + \theta^a\sigma
\end{aligned} \tag{3.31}$$

Similarly, $\sigma \to \sigma$ under $\mathrm{SU}(2)_V$ and $\sigma \to \sigma + \theta_a\pi^a$ under $\mathrm{SU}(2)_A$. We would like to build terms into the linear-σ model Lagrangian that are invariant under the $\mathrm{SU}(2)_V \times \mathrm{SU}(2)_A$ symmetry using these fields. We note that the squares of these fields transform as follows.

$$\mathrm{SU}(2)_V: \qquad \pi^2 \to \pi^2 \qquad\qquad \sigma^2 \to \sigma^2 \tag{3.32}$$

$$\mathrm{SU}(2)_A: \qquad \pi^2 \to \pi^2 - 2\sigma\theta_a\pi^a \qquad\qquad \sigma^2 \to \sigma^2 + 2\sigma\theta_a\pi^a \tag{3.33}$$

The kinetic terms $(\partial_\mu\pi)^2, (\partial_\mu\sigma)^2$ also transform the same way (remember that these are global transformations). Although the square fields individually do not preserve the $\mathrm{SU}(2)_V \times \mathrm{SU}(2)_A$ symmetry, the sum $\sigma^2 + \pi^2 = |\phi|^2$ does, where we have (for brevity) combined the σ and π fields into the meson matrix $\phi = \mathbb{1}\sigma + i\gamma^5\tau\cdot\pi$.

Finally, we note that the term $\overline{N}\phi N$ is also invariant under these transformations. Putting everything together, we have the Lagrangian for the linear-σ model.

$$\mathcal{L} = \overline{N}\left(i\gamma^\mu\partial_\mu - g\phi\right)N + \frac{1}{2}\left|\partial_\mu\phi\right|^2 - V\left(|\phi|^2\right) \tag{3.34}$$

Notice that we have assumed the pions and σ are massless. We choose the following for our potential, which will generates a mass for the nucleon.

$$V\left(|\phi|^2\right) = -\frac{\mu^2}{2}|\phi|^2 + \frac{\lambda}{4}|\phi|^4 \tag{3.35}$$
$$= -\frac{\mu^2}{2}\left(\sigma^2+\pi^2\right) + \frac{\lambda}{4}\left(\sigma^2+\pi^2\right)^2 \tag{3.36}$$

When $\mu > 0$, the potential is minimized for $|\phi|^2 = \mu^2/\lambda$, which we assume occurs when $\sigma \to v \equiv \mu/\sqrt{\lambda}$ and $\pi^a \to 0$. Now we perturbatively expand around $\sigma = v + \tilde{\sigma}$. Dropping the constant terms from the Lagrangian, this procedure yields

$$\begin{aligned}\mathcal{L} =& \overline{N}\left(i\gamma^\mu\partial_\mu - gv\right)N - g\overline{N}\left(\tilde{\sigma} - i\tau\cdot\pi\gamma^5\right)N + \frac{1}{2}\Big(\left(\partial_\mu\tilde{\sigma}\right)^2 + \left(\partial_\mu\pi\right)\Big)^2 \\ &- \mu^2\tilde{\sigma}^2 - \lambda v\tilde{\sigma}\left(\tilde{\sigma}^2+\pi^2\right) - \frac{\lambda}{4}\left(\tilde{\sigma}^2+\pi^2\right)^2 \ .\end{aligned} \tag{3.37}$$

After spontaneous symmetry breaking, the pions remain massless, while the nucleon picks up a mass gv.

It is instructive to also view this Lagrangian from the perspective of the chiral $\mathrm{SU}(2)_L \times \mathrm{SU}(2)_R$ symmetry. We recall that ψ transforms

$$\psi_L \to L\psi_L \qquad \psi_R \to R\psi_R \tag{3.38}$$

where $L \in \mathrm{SU}(2)_L$ and $R \in \mathrm{SU}(2)_R$. Defining $\Sigma = \sigma + i\tau\cdot\pi$, we see that

$$\begin{aligned}\Sigma &= \sigma + i\tau\cdot\pi \\ &= \overline{\psi}\Big(1 + i\left(\tau^a\right)^2 i\gamma^5\Big)\psi \\ &= \overline{\psi}\left(1-\gamma^5\right)\psi \\ &= \overline{\psi}P_L^2\psi \\ &= \overline{\psi}_R\psi_L \ .\end{aligned}$$

Therefore $\Sigma \to L\Sigma R^\dagger$ under a chiral transformation, making $\mathrm{Tr}\,\Sigma^\dagger\Sigma$ automatically invariant (as well as $\mathrm{Tr}\,\partial_\mu\Sigma^\dagger\partial^\mu\Sigma$). Similar to before, a mass term for the nucleon is not invariant under a chiral transformation as $\overline{N}N \to L^\dagger\overline{N}_L N_R R + R^\dagger\overline{N}_R N_L L$, but this is easily corrected by inserting a Σ and $\Sigma^\dagger$, respectively.

Now we can rewrite the Lagrangian in Eq. 3.34 with the chiral symmetry explicit.

$$\begin{aligned}\mathcal{L} =&\overline{N}_L i\gamma^\mu \partial_\mu N_L + \overline{N}_R i\gamma^\mu \partial_\mu N_R - g\left(\overline{N}_L \Sigma N_R + \overline{N}_R \Sigma^\dagger N_L\right) \\ &+ \frac{1}{4}\operatorname{Tr}\partial_\mu \Sigma^\dagger \partial^\mu \Sigma - V\left(\operatorname{Tr}\Sigma^\dagger\Sigma\right)\end{aligned} \tag{3.39}$$

The potential becomes

$$V\left(\operatorname{Tr}\left\{\Sigma^\dagger\Sigma\right\}\right) = -\frac{\mu}{4}\operatorname{Tr}\left\{\Sigma^\dagger\Sigma\right\} + \frac{\lambda}{16}\operatorname{Tr}\left\{\Sigma^\dagger\Sigma\right\}^2 \tag{3.40}$$

with chiral symmetry breaking occurring when $\operatorname{Tr}\Sigma^\dagger\Sigma = 2\mu^2/\lambda$.

An application: charged pion decay

As mentioned previously, Gell-Mann and Lévi introduced the linear-σ model in order to explain the charged pion decay process $\pi^+ \to \overline{\mu} + \nu_\mu$. We can consider this decay from the perspective of the effective Fermi interaction in which the role of the W^+ boson has been integrated out.

$$\mathcal{L}_{\text{Fermi}} = \frac{G_F}{\sqrt{2}}\left[\overline{u}\gamma^\mu\left(\mathbb{1}-\gamma^5\right)d\right]\left[\overline{\mu}\gamma^\mu\left(\mathbb{1}-\gamma^5\right)\nu_\mu\right] \tag{3.41}$$

The associated scattering matrix element can be factorized into a leptonic and hadronic part, with the leptonic part calculated perturbatively. We focus on the hadronic part, $\langle\Omega|A^\mu|\pi^+\rangle$, in which some current operator A^μ takes the pion to the QCD vacuum Ω.

In fact, we can use the axial current associated with the linear-σ model for the current operator.

$$\begin{aligned}\theta_a A^{\mu,a} &= -\left(\frac{\partial\mathcal{L}}{\partial\partial_\mu N}\delta N + \frac{\partial\mathcal{L}}{\partial\partial_\mu \pi}\delta\pi + \frac{\partial\mathcal{L}}{\partial\partial_\mu \sigma}\delta\sigma\right) \\ &= \overline{N}\gamma^\mu\gamma^5\theta_a\frac{\tau_a}{2}N - \theta_a\pi^a\partial^\mu\sigma - \theta_a\sigma\partial^\mu\pi^a\end{aligned} \tag{3.42}$$

Expanding around $\sigma = \tilde{\sigma} + v$, we find

$$A^{\mu,a} = \overline{N}\gamma^\mu\gamma^5\frac{\tau_a}{2}N - \pi^a\partial^\mu\tilde{\sigma} - \tilde{\sigma}\partial^\mu\pi^a - v\partial^\mu\pi^a\,. \tag{3.43}$$

Since the other terms involve either the σ or nucleon, we only expect the last term to contribute to the matrix element.

$$\langle\Omega|A^{\mu,a}|\pi^+\rangle = -\langle\Omega|v\partial^\mu\pi^+|\pi^+\rangle = -ivp^\mu e^{-ip\cdot x} \tag{3.44}$$

We see that v describes the size of this decay process and is referred to as the *pion decay constant*, f_π. [6]

Next we take the divergence.

$$\langle\Omega|\partial_\mu A^{\mu,a}|\pi^+\rangle = -f_\pi p_\mu p^\mu e^{-ip\cdot x} = -f_\pi m_\pi^2 e^{-ip\cdot x} \tag{3.45}$$

In the limit where $m_\pi \to 0$ the divergence vanishes. Of course, the pion mass is not zero, but it is small compared to other hadronic scales. For that reason, this is know as the *partially* conserved axial current.

Chiral perturbation theory

There is a detail in the linear-σ model we have so far skipped over: what exactly is the σ anyway? Experimentally the closest match seems to be the $\sigma/f_0(500)$ resonance, which is the lightest scalar meson; however, as it lies just above the two pion threshold, it is highly unstable and difficult to observe—in fact, its existence has been doubted and reaffirmed multiple times since its initial measurement in the mid-1960s.

To say the $\sigma/f_0(500)$ resonance has been a source of controversy would be an understatement [36]. Fortunately, it is possible to remove the σ meson from the linear-σ model in what is (perhaps misleadingly) called the nonlinear-σ model, with the leading order term equivalent to the chiral perturbation theory Lagrangian. However, we will sidestep the construction of the nonlinear model and skip straight to the chiral Lagrangian from an effective field theory perspective.

[6] There are two different conventions for the pion decay constant, differing by a factor of $\sqrt{2}$. In this chapter, we use the convention $f_\pi \approx 130$ MeV; in Chapter 5, we use the convention $F_\pi \approx 90$ MeV.

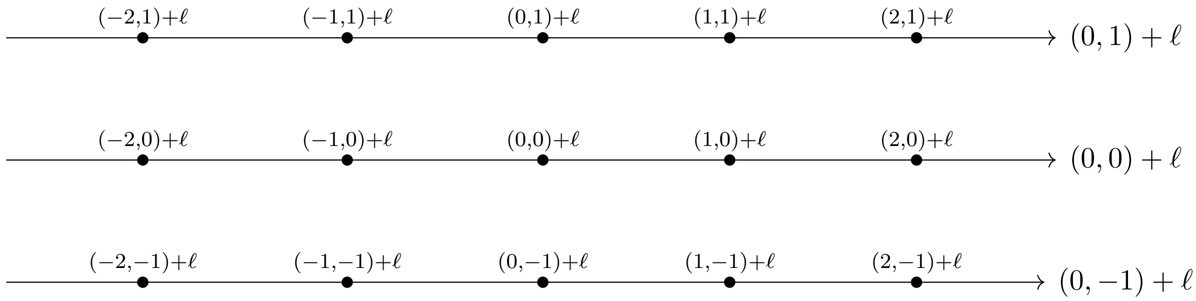

Figure 3.1: An example of a coset space. Let $G = \mathbb{Z} \times \mathbb{Z}$ with addition and $H = \{(n, 0)|n \in \mathbb{Z}\} \subset G$ be the horizontal line ℓ running through the origin. Then gH is a line parallel to ℓ and G/H is the set of all lines parallel to ℓ (including itself). This example also demonstrates that cosets are either disjoint (e.g., parallel lines do not overlap) or overlap entirely (e.g., $(0, 0) + \ell = (0, 1) + \ell$).

Like taxes, inevitable group theory

We recall that the quark condensate (Eq. (3.25)) does not respect chiral symmetry even in the limit of massless quarks.

$$\text{SU}(N)_L : \qquad \langle \overline{q}_L q_R \rangle \to L^\dagger \langle \overline{q}_L q_R \rangle \tag{3.46}$$

$$\text{SU}(N)_R : \qquad \langle \overline{q}_L q_R \rangle \to \langle \overline{q}_L q_R \rangle R \tag{3.47}$$

However, the quark condensate does respect flavor transformations, which gives us the following symmetry breaking pattern.

$$\underbrace{\text{SU}(N)_L \times \text{SU}(N)_R}_{G} \to \underbrace{SU(N)_V}_{H} \tag{3.48}$$

Coleman et al. showed (with generality) that the Goldstone fields ϕ_a distinguish the different elements of the coset space $G/H = \{gH|g \in G\}$ [37, 38]. (See fig. 3.1.) The proceeding algorithm for constructing an effective field theory from a spontaneously broken symmetry is known as coset construction.

We will now sketch the procedure and its consequences (see either [24] or [39] for another perspective). Let $\mathbf{\Phi} = (\phi_1, \ldots, \phi_n)$, where $n = \dim G - \dim H$ is the number of Goldstone bosons, correspond to a configuration of the fields transformed from the Goldstone vacuum, $\mathbf{\Phi}_0$ by $g \in G$. (We note that this is a map $\mathbf{\Phi} : \mathbb{R}^{3,1} \to \mathbb{R}^n$ taking Minkowski space to the field values). Denote the collection of all possible maps

$V = \{\mathbf{\Phi} | \mathbf{\Phi}_0 \xrightarrow{g} \mathbf{\Phi} \quad \forall g \in G\}$. Intuitively, we can think of $\mathbf{\Phi}$ as corresponding to the QFT "mattress" of the Goldstone fields and the space V as corresponding to all possible mattresses.

Typically a transformation by $g \in G$ changes the mattress: $\mathbf{\Phi} \xrightarrow{g} \mathbf{\Phi}'$; however, if the mattress is in a vacuum configuration $\mathbf{\Phi}_0$, a transformation by $h \in H$ will keep the mattress in a vacuum configuration: $\mathbf{\Phi}_0 \xrightarrow{h} \mathbf{\Phi}_0$. In a moment, we will encode this information in the group action $\varphi : G \times V \to V$

$$\varphi(e, \mathbf{\Phi}) = \mathbf{\Phi} \tag{3.49}$$

$$\varphi(g, \varphi(g', \mathbf{\Phi})) = \varphi(gg', \mathbf{\Phi}) \tag{3.50}$$

where $e, g, g' \in G$ and e is the identity element. Note that the group action is not necessarily a representation of the group since we do not require the group action be linear.

The statement that only transformations by $h \in H$ leave the vacuum unchanged subjects the group action to the requirements $\varphi(h, \mathbf{\Phi}_0) = \mathbf{\Phi}_0$ for $h \in H$ and $\varphi(g, \mathbf{\Phi}_0) \neq \mathbf{\Phi}_0$ for $g \notin H$. Consequently, if the transformations $f = gh, f' = gh' \in gH$ belong to the same coset, then they will transform the vacuum in the same way, $\mathbf{\Phi}_0 \xrightarrow{f} \mathbf{\Phi}' \xleftarrow{f'} \mathbf{\Phi}_0$, since

$$\begin{aligned}
\varphi(f, \mathbf{\Phi}_0) &= \varphi\left(fh^{-1}, \varphi(h, \mathbf{\Phi}_0)\right) \\
&= \varphi(g, \mathbf{\Phi}_0) \\
&= \varphi\left(f'h'^{-1}, \varphi(h', \mathbf{\Phi}_0)\right) = \varphi(f', \mathbf{\Phi}_0)\,.
\end{aligned}$$

Moreover, if the transformations belong to different cosets, $f \in gH \neq g'H \ni f'$, then the vacuum transforms differently under each, $\mathbf{\Phi}_0 \xrightarrow{f} \mathbf{\Phi} \neq \mathbf{\Phi}' \xleftarrow{f'} \mathbf{\Phi}_0$. We prove this by contradiction. Assume (to be contradicted) that $\varphi(f, \mathbf{\Phi}_0) = \varphi(f', \mathbf{\Phi}_0)$. Then

$$\mathbf{\Phi}_0 = \varphi(e, \mathbf{\Phi}_0) = \varphi\Big(f^{-1}, \overbrace{\varphi(f, \mathbf{\Phi}_0)}^{\text{assume: } \varphi(f', \mathbf{\Phi}_0)}\Big) = \varphi(f^{-1}f', \mathbf{\Phi}_0) \tag{3.51}$$

but this requires $f^{-1}f' \in H \implies f' \in fH = gH$, which is inconsistent with our original assumptions.

Combining both of these results with their contrapositives, we conclude that

$$\mathbf{\Phi}_0 \xrightarrow{g} \mathbf{\Phi} \xleftarrow{g'} \mathbf{\Phi}_0 \qquad \Longleftrightarrow \qquad gH = g'H\,. \tag{3.52}$$

Thus, given a configuration of the fields $\mathbf{\Phi}$, we can classify the transformation by which coset the transformation belonged to (and vice versa). This is what it means for the Goldstone fields to distinguish the elements of G/H.

In fact, what we have shown is a specific case of the *orbit-stabilizer theorem* [40]. In group theory lingo,

$$\text{Orb}(\mathbf{\Phi}_0) = \left\{ \mathbf{\Phi} \,\middle|\, \mathbf{\Phi}_0 \xrightarrow{g} \mathbf{\Phi} \quad \forall g \in G \right\} = V \qquad \text{(Orbit of } \mathbf{\Phi}_0\text{)} \tag{3.53}$$

$$G_{\mathbf{\Phi}_0} = \left\{ g \in G \,\middle|\, \mathbf{\Phi}_0 \xrightarrow{g} \mathbf{\Phi}_0 \right\} = H \qquad \text{(Stabilizer of } \mathbf{\Phi}_0\text{)} \tag{3.54}$$

The theorem states that $\mathbf{\Phi}_0 \xrightarrow{g} \mathbf{\Phi} \xleftarrow{g'} \mathbf{\Phi}_0$ if and only if $gH = g'H$. A consequence of this theorem is that the map φ must define a bijection between G/H and Orb$(\mathbf{\Phi}_0)$.

We summarize the critical results:

1. The action of g on $\mathbf{\Phi}$ is not unique up to compositions by $h \in H$ since $\mathbf{\Phi} \xrightarrow{g} \mathbf{\Phi}' \xleftarrow{gh} \mathbf{\Phi}$.

2. Because there is an isomorphism between the elements of G/H and the elements $\mathbf{\Phi} \in V$, we can associate with each transformation of the Goldstone fields a representative element of the coset space.

3. An action built from the group elements will remain spontaneously broken so long as the group elements transform per the group action $\varphi(g, \varphi(g', \mathbf{\Phi}_0)) = \varphi(gg', \mathbf{\Phi}_0) = \varphi(gg'h, \mathbf{\Phi}_0)$.

4. Specifically in the case of a Lie algebra, we can write $f = \exp\{i\phi_a t^a\} \in G$ so that the fields transform nonlinearly per $f \xrightarrow{g} gf = f'h$ where $h \in H$.

Implications for QCD

Now we apply these results to the Goldstone bosons of QCD, i.e. the pions. Let $(L, R) \in \text{SU}(N)_L \times \text{SU}(N)_R$ and $(V, V) \in SU(N)_V$ (recall that $\text{SU}(N)_V$ is the realization $\text{SU}(N)_L = \text{SU}(N)_R$, hence the tuple). Given $g = (L, R), g' = (L', R') \in G$, we can chain these transformations together in the following manner

$$g'g = (L', R')(L, R) = (L'L, R'R)\,. \tag{3.55}$$

But the conclusion of the previous section is that a transformation of the fields by g is the same as a transformation of the fields by $gh \in gH$.

$$g'gh = \overbrace{(L', R')}^{g'}\overbrace{(L, R)}^{g}\overbrace{(L^\dagger, L^\dagger)(L'^\dagger, L'^\dagger)}^{h} \tag{3.56}$$

$$= \underbrace{(L', R')}_{g'}\underbrace{(\mathbb{1}, RL^\dagger)}_{\tilde{g}}\underbrace{(L'^\dagger, L'^\dagger)}_{\tilde{h}} = (\mathbb{1}, R'RL^\dagger L'^\dagger) \tag{3.57}$$

That is, the action of $g \to g'g$ on the Goldstone fields is equivalent to the action of $g \to g'\tilde{g}\tilde{h}$. This motivates the following transformation law (we swap the primes).

$$(\mathbb{1}, U) \to (\mathbb{1}, RUL^\dagger) \tag{3.58}$$

For shorthand we have written $U = R'L'^\dagger$, which could be any element of SU(N).

When written in this manner, it is manifestly clear that $\tilde{g}$ is parameterized by $N^2 - 1$ real numbers—exactly the number of Goldstone fields. Moreover, we know how to construct U by exponentiating some generators of the Lie algebra $\mathfrak{su}(N)$ for some parameters α_a, which again is parameterized by $N^2 - 1$ real numbers. This procedure yields the following exponential representation

$$U = e^{2i\alpha_a T^a/F} \,. \tag{3.59}$$

In the case of $N = 2$, we replace the parameters α_a with the pion fields π_a.

$$2\alpha_a T^a \overset{\text{SU(2)}}{=} \pi_a \tau^a = \begin{bmatrix} \pi_3 & \pi_1 - i\pi_2 \\ \pi_1 + i\pi_2 & -\pi_3 \end{bmatrix} = \begin{bmatrix} \pi^0 & \sqrt{2}\pi^+ \\ \sqrt{2}\pi^- & -\pi^0 \end{bmatrix} \tag{3.60}$$

(The constant F a dimensionful quantity needed to keep the exponent dimensionless.) In the case of $N = 3$, we would include the kaons and η meson. (The cases for $N > 3$ are not physically relevant, as these are not good approximate symmetries.) Notice that the transformation of the pion fields is a nonlinear realization of chiral symmetry.

The chiral Lagrangian

Now we use this matrix to construct terms in the chiral Lagrangian. First, we promote U from being a constant matrix to a matrix that depends on x—clearly this is necessary if U is going to describe our pions fields. Using the cyclic property of the trace, it is evident that terms like

$$\mathrm{Tr}\left\{(UU^\dagger)^n\right\} \to \mathrm{Tr}\left\{(RUL^\dagger LU^\dagger R^\dagger)^n\right\} = \mathrm{Tr}\left\{(UU^\dagger)^n\right\} \tag{3.61}$$

are invariant under chiral transformations. However, these particular terms won't appear in the chiral Lagrangian: since U is unitary, these are constant terms.

Instead, we will construct terms from derivatives of U. We note that

$$\partial_\mu U \to \partial_\mu U' = \partial_\mu(RUL^\dagger) = R\partial_\mu UL^\dagger \tag{3.62}$$

because these are global transformations. This gives us the candidates for the leading order (LO) contributions to the chiral perturbation theory Lagrangian,

$$\mathrm{Tr}\left\{\partial_\mu U\partial^\mu U^\dagger\right\} \quad \partial^\mu\,\mathrm{Tr}\left\{\partial_\mu UU^\dagger\right\} \quad \mathrm{Tr}\left\{\partial^2 UU^\dagger\right\}. \tag{3.63}$$

However, these terms either vanish or are equivalent up to a total derivative.

$$\mathrm{Tr}\left\{\partial_\mu UU^\dagger\right\} = 0 \tag{3.64}$$

$$\partial^\mu\,\mathrm{Tr}\left\{\partial_\mu UU^\dagger\right\} = \mathrm{Tr}\left\{\partial^2 UU^\dagger\right\} + \mathrm{Tr}\left\{\partial_\mu U\partial^\mu U^\dagger\right\} \tag{3.65}$$

Therefore the first term is given by

$$\mathcal{L}^{(2)} \supset \frac{F^2}{4}\,\mathrm{Tr}\left\{\partial_\mu U\partial^\mu U^\dagger\right\} \tag{3.66}$$

where the superscript in $\mathcal{L}^{(2)}$ reminds us of the number of derivatives of U. Here we have included a factor of $F^2/4$ to correct the mass dimension and normalize the kinetic term. The parameter F is again related to the pion decay constant; although we won't show that here, this fact shouldn't be too surprising since we constructed the linear-σ model as a prototype for chiral perturbation theory. We can verify the normalization and mass dimension by defining $\phi = 2\alpha_a T^a$ and expanding the term. [7]

$$\begin{aligned}
\mathcal{L}^{(2)} &\supset \frac{F^2}{4}\,\mathrm{Tr}\left\{\partial_\mu\left[1+\frac{i\phi}{F}+\frac{1}{2}\left(\frac{i\phi}{F}\right)^2+\cdots\right]\partial^\mu\left[1-\frac{i\phi}{F}+\frac{1}{2}\left(\frac{-i\phi}{F}\right)^2+\cdots\right]\right\} \\
&= \frac{F^2}{4}\,\mathrm{Tr}\left\{\frac{1}{F^2}\partial_\mu\phi\partial^\mu\phi+\frac{1}{F^3}\left[\partial_\mu\phi\phi+\phi\partial_\mu\phi,\partial^\mu\phi\right]-\frac{1}{4F^4}\left(\partial_\mu\phi\phi+\phi\partial_\mu\phi\right)^2\right\} \\
&= \frac{1}{2}(\partial_\mu\alpha_a)^2+\frac{1}{6F^2}\left(\alpha_a\alpha^a\partial_\mu\alpha_b\partial^\mu\alpha^b-\alpha_a\alpha_b\partial_\mu\alpha^a\partial^\mu\alpha^b\right)+\cdots
\end{aligned} \tag{3.67}$$

The expansion begins with a kinetic term for the Goldstone fields as expected, while the term with an odd mixture of ϕ and its derivatives drops out.

While Eq. (3.66) contributes to the chiral Lagrangian, it is only the lowest order term, as it contains the fewest derivatives of the Goldstone fields and, more generally, the lowest dimension operators when expanded. Indeed, there are infinitely many terms we could construct by taking the traces of products of U and its derivatives which respect the group symmetry; we expect to be able to sort these terms by some power-counting scheme such that $\mathcal{L}_\chi = \mathcal{L}^{(2)} + \mathcal{L}^{(4)} + \cdots$. For example, a term like $(\mathrm{Tr}\,\partial_\mu U\partial^\mu U)^2/F^2 \subset \mathcal{L}^{(4)}$ is not redundant but rather competes with $\mathcal{L}^{(2)}$ at the next order in the expansion given in Eq. (3.67).

In chiral perturbation theory, we expand in powers of p/Λ_χ, where p is the Goldstone boson momentum and $\Lambda_\chi \approx 4\pi F \sim 1$ GeV is the chiral symmetry scale (the appearance of F is obvious; the geometric factor of 4π emerges when evaluating loop integrals). When we later include the explicit breaking of chiral symmetry by the mass terms, we include the Goldstone masses in our power-counting such that $p/\Lambda_\chi \sim m/\Lambda_\chi$.

Including a mass term

Recall that chiral symmetry is explicitly broken by the mass of the quarks in the full theory,

$$\mathcal{L}_{\mathrm{QCD}} \supset \sum_f m_f\left(\overline{q}_{f,L}q_{f,R}+\overline{q}_{f,R}q_{f,L}\right)\,. \tag{3.68}$$

[7] We employ the following SU(N) identities:

$$\mathrm{Tr}\left\{T^a\right\}=0\,,\quad \mathrm{Tr}\left\{T^aT^b\right\}=\delta^{ab}/2\,,\quad \mathrm{Tr}\left\{T^aT^aT^bT^b\right\}=\delta^{ab}\,,\quad T^aT^bT^a=-\frac{1}{2N}T^a\,.$$

We could add a term like $m^2 F^2 \operatorname{Tr}(U^\dagger + U) \approx 16 - 2m^2\alpha_a^2$ to provide a mass m for each of the pseudo-Goldstone bosons. However, we would also like to have the flexibility to allow the pseudo-Goldstone bosons to have different masses.

A useful trick is to promote the mass matrix $M = \operatorname{diag}(m_1, \cdots, m_N)$ to a *spurion* field which transforms like U, i.e. $M \to RML^\dagger$. This procedure makes it easy to construct terms that appear invariant under the group symmetry, but which are nevertheless violated since the spurions are not real. This gives us the lowest mass term in the chiral Lagrangian and, with it, the full expression for $\mathcal{L}^{(2)}$.

$$\mathcal{L}^{(2)} = \frac{F^2}{4} \operatorname{Tr}\left\{\partial_\mu U \partial^\mu U^\dagger\right\} + \frac{F^2 B}{2} \operatorname{Tr}\left\{MU^\dagger + UM^\dagger\right\} \tag{3.69}$$

Notice that we have included a new parameter in our effective field theory, B.

Let us now specialize to the case of SU(2) so that $M = \operatorname{diag}(m_u, m_d)$ and expand the explicit chiral symmetry breaking term.

$$\begin{aligned}
\mathcal{L}^{(2)} &\supset \frac{F^2 B}{2} \operatorname{Tr}\left\{MU^\dagger + UM^\dagger\right\} \\
&= \frac{F^2 B}{2} \operatorname{Tr}\left\{M\left(1 - \frac{i\phi}{F} - \frac{\phi^2}{2F^2} + \cdots\right) + \left(1 + \frac{i\phi}{F} - \frac{\phi^2}{2F^2} + \cdots\right) M^\dagger\right\} \\
&\overset{\text{SU(2)}}{=} F^2 B\,(m_u + m_d) - \frac{B}{2}(m_u + m_d)(\pi_0^2 + 2\pi^+\pi^-) + \cdots
\end{aligned} \tag{3.70}$$

We can drop the constant term. Since $m_u \approx m_d$ (and exactly so in the isospin limit), we denote $\hat{m} = (m_u + m_d)/2$. Thus we conclude

$$m_\pi^2 \approx 2B\hat{m}\,. \tag{3.71}$$

Notably, the pion mass dependence on the quark masses is not linear. If we specialize to SU(3), we find that for the other Goldstone bosons

$$m_K^2 \approx B(\hat{m} + m_s) \qquad m_\eta^2 \approx \frac{2}{3}B(\hat{m} + 2m_s)\,. \tag{3.72}$$

(The expression for the pion is unchanged.) This allows us to relate the mass of the Goldstone bosons to each other in the following manner,

$$4m_K^2 \approx 3m_\eta^2 + m_\pi^2\,, \tag{3.73}$$

or alternatively, relate the ratio of the quark masses to the masses of the Goldstone bosons,

$$\frac{\hat{m}}{m_s} \approx \frac{m_\pi^2}{2m_K^2 - m_\pi^2} \approx \frac{1}{26} \tag{3.74}$$

Collectively these equation are known as the Gell-Mann–Oakes–Renner (GMOR) relations [41]. [8]

Extending chiral perturbation theory to baryons

The spectrum of QCD contains more than just pions, kaons, and the η—there are also baryons and (non-pseudo-Goldstone) mesons, which are generally referred to as matter fields. The extension of chiral perturbation theory to baryons was first worked out in [42, 43]. The result—heavy baryon chiral perturbation theory—separates the matter fields into "light" and "heavy" components such that the heavy components can be integrated out and the light components become massless in the chiral limit [44].

As an example, we quote the result for SU(2) heavy baryon χPT where the matter fields are just the nucleons and are packaged as an isodoublet $\psi_N = (p, n)^T$ [24, 45]. After the "light" and "heavy" fields have been separated out, the resulting Lagrangian is

$$\mathcal{L}_{\pi N}^{(1)} = \overline{\psi}_N \left(i\gamma^\mu \partial_\mu - M + \frac{g_A}{2}\gamma^\mu \gamma_5 u_\mu \right) \psi_N \tag{3.75}$$

with covariant derivative $D_\mu = \partial_\mu + \Gamma^\mu$ and Γ^μ the chiral connection. To preserve the chiral symmetry, we require the fields/operators transform like

$$\begin{aligned} \psi_N &\to K\psi_N \\ D_\mu \psi_N &\to K D_\mu \psi_N \\ u_\mu &\to K u_\mu K^\dagger \end{aligned} \tag{3.76}$$

where $K = \sqrt{RUL^\dagger} R\sqrt{U}$ and $U = u_\mu u^\mu$ is the matrix field previously introduced when deriving the (meson) chiral Lagrangian.

[8] Technically the GMOR relations include one more relation that relates the quark condensate to B. The easiest way to see this is by *not* dropping the constant term in Eq. (3.70). It turns out that the fields are minimized when $\phi = 0$, so $\langle \mathcal{H}_\chi \rangle = F^2 B\hat{m}$ (see [24], e.g.). But we also know that $\hat{m}(\overline{u}u + \overline{d}d) \subset \mathcal{H}_{\text{QCD}}$. Taking the derivative of both with respect to $\hat{m}$ and then equating their vacuum expectation values, we find that $F^2 B = \langle \overline{u}u + \overline{d}d \rangle$ (the light quark condensate).

Similar to how $\mathcal{L}^{(2)}$ is the just the lowest order meson contribution to the chiral Lagrangian, this is just the lowest order nucleon contribution to the chiral Lagrangian. We note that there are two new LECs—M, the nucleon mass in the chiral limit, and g_A, the axial charge, which can be shown to be $g_A \approx g_{\pi N} F_\pi / M_N$ (the Goldberger-Treiman relation [46]).

Scale Setting

Quantities generated on the lattice are dimensionless; however, many observables that we're interested in studying are not. To convert our dimensionless observables generated on the lattice into dimensionful quantities, we must introduce a scale. This process is known as *scale setting*.

The work described in this section resulted in the following publication.

N. Miller et al., Phys. Rev. D 103, 054511 (2021), arXiv:2011.12166 [hep-lat].

Measuring dimensionful observables on the lattice

As motivation for scale setting, let us review how to extract the mass of a baryon from the lattice. In Chapter 1, we saw how to calculate the correlator of two observables using the Euclidean path integral.

$$\langle O_2(t) O_1(0) \rangle = \frac{1}{Z_0} \int \mathcal{D}[q, \overline{q}] \mathcal{D}[U] \, e^{-S_F[q,\overline{q},U] - S_G[U]} O_2[q_{(t)}, \overline{q}_{(t)}, U_{(t)}] O_1[q_{(0)}, \overline{q}_{(0)}, U_{(0)}] \tag{4.1}$$

This (Euclidean) path integral is sampled using Monte-Carlo to determine the two-point function on the lattice. However, there is another way one might defined the correlation function. As operators (rather than functionals), the correlation function is defined as

$$\langle O_2(t) O_1(0) \rangle = \lim_{T \to \infty} \frac{1}{Z_T} \text{tr} \left\{ e^{-(T-t)\hat{H}} \hat{O}_2 e^{-t\hat{H}} \hat{O}_1 \right\} \tag{4.2}$$

where $Z_T = \text{tr} \left[e^{-T\hat{H}} \right]$. From this definition, we see that by introducing a complete set of energy eigenstates, we can rewrite this correlation function in terms of its energy spectrum.

$$\langle O_2(t) O_1(0) \rangle = \sum_{m,n} \langle m | e^{-(T-t)\hat{H}} \hat{O}_2 | n \rangle \langle n | e^{-t\hat{H}} \hat{O}_1 | m \rangle \tag{4.3}$$

$$\approx \sum_{n} \langle 0 | \hat{O}_2 | n \rangle \langle n | \hat{O}_1 | 0 \rangle \, e^{-tE_n} \qquad \text{as } T \to \infty \tag{4.4}$$

The above formula is quite general, but it doesn't tell us how to calculate the mass of some particular baryon. To do that, we replace $\hat{O}_1, \hat{O}_2$ with operators that create a baryon from the vacuum at $t = 0$, which is then destroyed at $t = t$.

$$\langle O_2(t)O_1(0)\rangle \to \langle\Omega|B(t)B^\dagger(0)|\Omega\rangle \tag{4.5}$$

Here Ω is the QCD vacuum and $B^\dagger$ is an operator that creates an excitation with the quantum numbers of the specific baryon we're interested in studying.

To summarize, we can estimate the mass of a baryon with

$$\langle\Omega|B(t = an_t)B^\dagger(0)|\Omega\rangle \approx \sum_n A_n e^{-(n_t)(aE_n)}\,. \tag{4.6}$$

The expression on the left-hand side is simulated on the lattice via (4.1) for different values of t; the parameters A_n, aE_n on the right-hand side are determined by an n-state fit. Notice that we have substituted $t = an_t$ since the separations in time, like the separations in space, are discretized. In fact, we do not even need to know what the times are: if L_t is the "length" of the lattice in the t-direction, then we only require $n_t \in \{0, 1, \ldots, L_t/a\}$. The parameters we extract from this fit are therefore purely dimensionless.

Most lattices are simulated with quark masses tuned away from their physical (experimental) values; we therefore expect the baryon mass to differ from the experimental value also. If we know the lattice spacing, we can convert the dimensionless parameter from the two-point function fit into a dimensionful parameter. Reintroducing factors of c and $\hbar$ temporarily, we must calculate

$$E_0^{\text{phys}} = \frac{\hbar c}{a}(aE_0)^{\text{latt}}\,. \tag{4.7}$$

But here's the snag: we generally do not know the lattice spacing *a priori*.

Lattice spacing dependence of the coupling

Recall that QCD has $N_f + 1$ degrees of freedom: one per each fermion flavor (up, down, strange, charm, bottom, and top) plus the gauge coupling g. On the lattice, one usually simulates less than the full $N_f = 6$ theory, as the heavier quarks play a negligible roll in the low-energy regime. In this work, we simulate $N_f = 2 + 1 + 1$ quarks (here the 2 denotes that the up and down quarks are degenerate, i.e. we take the isospin limit). Thus we have 3+1 parameters we must tune.

To set the quark masses, we can tune the masses until the ratio of the masses of hadrons with different quark content agree with their physical values, e.g. by tuning the ratios m_π/M_p, m_K/M_p, and m_{D_s}/m_p until they agree with the PDG (see the next section).

For the gauge coupling, we realize that even in quark-less QCD (i.e., gluons only) we must still determine the running coupling constant which changes according to the renormalization scale through a process known as dimensional transmutation. Since the only dimensionful quantity available is the lattice spacing, determining the lattice spacing must be equivalent to determining g.

Physical versus theory scales

The most obvious candidates for scale setting are observables known precisely from experiment, e.g. the nucleon mass. Scale setting observables which depend on comparison with experiment are known as *physical* scales. Ideally a scale setting observable should be precise and easy to generate on the lattice, yet also have small systematics and depend only weakly on the quark mass [47] (a weak quark mass dependence minimizes errors from extrapolation or quark mass mistuning). However, physical scales tend to lack one of those desirable properties, so they are not ideal for scale setting.

To rectify this deficiency, lattice QCD practitioners have invented *theory* scales. Unlike physical scales, theory scales are impractical—if not outright impossible—to measure with experiment alone. Nevertheless, they can easily be measured on the lattice. We give an example of a physical scale and a theory scale below.

A physical scale: scale setting with the proton

As an example of scale setting with a physical scale, let us consider scale setting with the proton loosely following the procedure described in [48]. We assume that we have already extracted the pion, kaon, and proton masses from their associated two-point functions on multiple ensembles, spanning multiple quark masses but only at a single lattice spacing. For illustration, suppose we use the following Taylor ansätze in the quark masses (in general, more sophisticated expressions can be derived using chiral perturbation theory).

$$\begin{aligned} am_\pi &= c_\pi^{(0)} + \sum_{n,f} c_\pi^{(n,f)} am_{q_f} \\ am_K &= c_K^{(0)} + \sum_{n,f} c_K^{(n,f)} am_{q_f} \\ aM_p &= c_p^{(0)} + \sum_{n,f} c_p^{(n,f)} am_{q_f} \end{aligned} \tag{4.8}$$

Finally, let us assume that we're working in the isospin limit ($u = d$) and that the contribution from the charm quark is negligible such that $f \in \{u, s\}$ in the sum above.

To determine the lattice spacing, we must first fit the above expressions to determine the low energy constants $c_{\{\pi,K,p\}}^{(n,f)}$. We would like to know which values of m_{q_f} cause the mass expressions to match the experimental values; we achieve this by solving for $m_{q_f^*}$ such that

$$\left.\frac{am_\pi}{aM_p}\right|_{m_{q_f^*}} = \frac{m_\pi^{\text{exp}}}{M_p^{\text{exp}}} \qquad \text{and} \qquad \left.\frac{am_K}{aM_p}\right|_{m_{q_f^*}} = \frac{m_K^{\text{exp}}}{M_p^{\text{exp}}} \,. \tag{4.9}$$

Finally the lattice spacing a is found by extrapolating aM_p to "physical" quark masses and comparing against the experimental value.

$$a = \left.\frac{aM_p^{\text{fit}}}{M_p^{\text{exp}}}\right|_{m_{q_f^*}} \tag{4.10}$$

We then repeat this procedure for each lattice spacing.

A theory scale: scale setting with the Sommer parameter r_0

As hinted at before regarding physical scales, there is a flaw with using the proton for scale setting: the proton correlator has a nasty signal-to-noise problem. To understand why, consider the variance of the proton correlator

$$\text{Var}\left[C(t)\right] = \underbrace{\text{E}\left[C(t)C^\dagger(t)\right]}_{\sim\langle(uud)(\overline{uud})\rangle} - \text{E}\left[C(t)\right]^2 \,. \tag{4.11}$$

The first term tells us that the variance is sensitive to the particles formed from 3 quarks and 3 anti-quarks. It is possible for a proton-antiproton pair to form, but this is rather heavy ($\sim 2M_p$). A much lighter (and hence more energetically favorable) configuration is 3 pions, so we expect $\langle |C(t)|^2\rangle \sim e^{-3m_\pi t}$. This term will be much larger than the second term in Eq. (4.11), so the signal-to-noise ratio is approximately given by

$$\frac{\mathrm{E}\left[C(t)\right]}{\sqrt{\mathrm{Var}\left[C(t)\right]}} \sim e^{-\left(M_p-\frac{3}{2}m_\pi\right)t} \tag{4.12}$$

We expect the signal-to-noise ratio to shrink with lattice time. In fact, this is an issue with all baryons, albeit to varying degrees; mesons, however, do not suffer so, as the lightest combinations of quarks in the first term of Eq. (4.11) will still be mesonic.

As an alternative to scale setting using baryon masses, Sommer proposed a scale setting technique using the static QCD potential [49]. Compared to scale setting with a baryon, there is no signal-to-noise problem. We note that the static quark potential is given by [8]

$$V(r) = A + \frac{B}{r} + \sigma r \tag{4.13}$$

where the B/r term corresponds to a Coulomb-like potential and the σr term corresponds to the string tension/confinement (for reference, $\sigma \approx 900$ MeV/fm; the constant term A is included for completeness, but it is irrelevant for our purposes). This effects a force between two static quarks,

$$F(r) = \frac{d}{dr}V(r) = -\frac{B}{r^2} + \sigma\,. \tag{4.14}$$

(Convention omits the negative sign in the derivative.) We would like to use this potential to set the scale; however, we would also like to avoid an extrapolation in r. To that end, we instead consider

$$r_0^2 F(r_0) = c\,. \tag{4.15}$$

with a fixed value of $r = r_c$. When $m_q \gg \Lambda_{\mathrm{QCD}}$, we can estimate the effect of this potential by using the (nonrelativistic) Schrödinger equation [50], which can then be compared to experimental measurements of $\bar{c}c$ and $\bar{b}b$ states. Sommer suggested setting $c = 1.65$, which would correspond to $r_0 \approx 0.49$ fm. Solving for r_0, we find that

$$r_0 = \sqrt{\frac{c+B}{\sigma}}\,. \tag{4.16}$$

Dividing both sides by the lattice spacing a and rearranging the equation, we have the following relation

$$a = r_0 \sqrt{\frac{\sigma a^2}{c + B}}\,. \tag{4.17}$$

Notice that B and σa^2 are both dimensionless quantities, suggesting that they might be accessible on the lattice. Let us now focus on determining these parameters.

We begin by noting (see Chapter 3 of [8] for details) that the static quark potential is related to the expectation value of the Wilson loop $W_{\mathcal{L}}$, a generalization of the plaquette (Eq. (1.38)) to more general paths.

$$\langle W_{\mathcal{L}} \rangle \approx C e^{-tV(r)} = C e^{-(n_t)(aV(an))} \tag{4.18}$$

Here we have substituted r, t for the lattice values: $r = an$ and $t = an_t$. Suffice it to say that the expression on the left-hand side of this equation can be readily calculated on the lattice. By varying n_t (but fixing n), we can fit this equation to determine the parameters C and $aV(r = an)$. We then repeat this process varying n such that we extract values of the potential $aV(r = an)$ for $n \in \{0, 1, \dots, L/a\}$.

Finally we fit $aV(an)$ as a function of n to determine B and σa^2.

$$aV(an) = Aa + \frac{B}{n} + \sigma a^2 n \tag{4.19}$$

These parameters can then be substituted into Eq. (4.17), thus determining a.

Scale setting with the gradient flow

In our work, we use a theory scale derived from gradient flow instead of the static potential. In addition to being cheap to compute and highly precise, the gradient flow-derived scales, in contrast to the potential-derived scales, have an expression in chiral perturbation theory. But first we should describe what gradient flow actually is.

We define a gradient flow field B_μ which diffuses according to [51]

$$\dot{B}_\mu = D_\nu G_{\nu\mu} \qquad\qquad B_\mu|_{t=0} = A_\mu \tag{4.20}$$

$$G_{\mu\nu} = \partial_\mu B_\nu - \partial_\nu B_\mu + [B_\mu, B_\nu] \qquad\qquad D_\mu = \partial_\mu + [B_\mu, \cdot\,] \tag{4.21}$$

where A_μ is the QCD gauge field, B_μ describes the flow of A_μ, and $\dot{B}_\mu$ denotes the derivative of B_μ with respect to the flow time t. Critically, the flow time has mass dimension -2, making it possible for us to use it to set the scale. Observe that these flow equations must drive the gauge fields towards stationary points of the action.

Now we define $E = \frac{1}{4} G^a_{\mu\nu} G^{\mu\nu}_a$, which reduces to the gluonic energy density in the limit $t \to 0$. So long as the flow time satisfies $a \ll \sqrt{8t_0} \ll aL$, we can approximate the expectation value as

$$\langle E \rangle = \frac{3}{4\pi t^2} \alpha_\mathrm{S}(Q^2) \left(1 + k_1 \alpha_\mathrm{S}(Q^2) + \cdots \right) \tag{4.22}$$

where $\alpha_\mathrm{S}(Q^2)$ is the running coupling. The left-hand side is something we can calculate on the lattice for relatively cheap since it doesn't depend on the fermion action.

If we multiply this quantity by the flow time squared t^2, we see that quantity is proportional to the coupling at leading-order. This is the motivation for defining the gradient flow scales t_0 and w_0. Empirically this quantity is observed to be nearly constant around $t^2 \langle E \rangle = 0.3$, so we define t_0 to be the flow time at which this condition is satisfied.

$$t^2 \langle E(t) \rangle \Big|_{t = t_{0,\mathrm{orig}}} = 0.3 \tag{4.23}$$

$$W_\mathrm{orig} = t \frac{d}{dt} \left(t^2 \langle E(t) \rangle \right) \Big|_{t = w^2_{0,\mathrm{orig}}} = 0.3 \tag{4.24}$$

Here we have also included a related quantity, w_0, which ameliorates artifacts introduced by the transition of $\langle E \rangle$ from a $1/t^2$ dependence to a $1/t$ dependence at larger flow times (including times near t_0) [52]. These equations are how the gradient scales were originally defined (hence the subscript "orig").

Additionally, Fodor et al. [53] proposed the following "improved" definitions (still at tree level) which remove some of the lattice spacing dependence of these scales.

$$\left. \frac{t^2 \langle E(t) \rangle}{1 + \sum_n C_{2n} \frac{a^{2n}}{t^n}} \right|_{t = t_{0,\mathrm{imp}}} = 0.3 \tag{4.25}$$

$$t \frac{d}{dt} \left(\frac{t^2 \langle E(t) \rangle}{1 + \sum_n C_{2n} \frac{a^{2n}}{t^n}} \right) \Bigg|_{t = w^2_{0,\mathrm{imp}}} = 0.3 \tag{4.26}$$

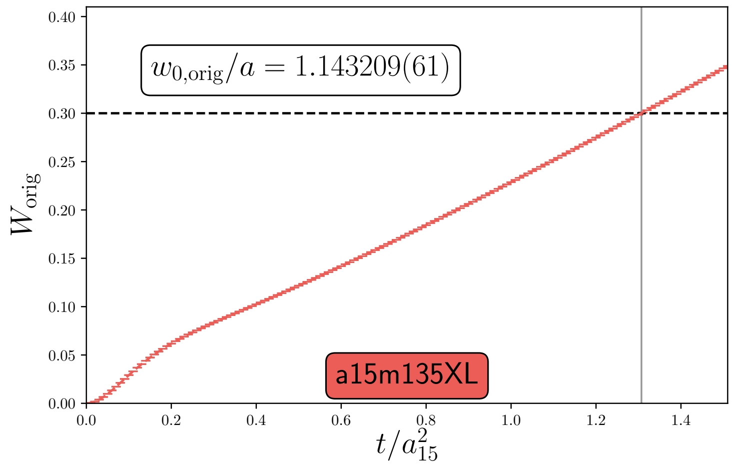

Figure 4.1: Measuring w_0/a on one of the ensembles. Notice that the derivative is practically constant near the point at which $W_{\text{orig}} = 0.3$ Figure from [54].

Here the C_{2n} coefficients are just some rational numbers that were determined in [53].

Finally, because $\langle E\rangle$ is just the kinetic gauge term, it is automatically invariant under chiral transformations. This implies the existence of a chiral expansion for $\langle E\rangle$, which in turn yields a chiral expansion for t_0 and w_0.

Project goals

Ultimately we would like to calculate the gradient flow scales w_0 and t_0, which will allow us to set the scale of our lattice. We accomplish this task by generating the gradient flow scales on each lattice ensemble (each of which is tuned for a different light quark/pion mass and have different lattice spacing sizes), then extrapolate from those lattice ensembles down to the physical point. [1]

However, we cannot extrapolate directly the gradient flow scales—these are dimensionful quantities, after all. Instead we need to construct dimensionless quantities from the gradient flow scales and some dimensionful observable. For example, consider w_0, which has the following N^{2}LO χPT expression [55]. [2]

$$w_0 = w_{0,\text{ch}} \left(1 + c_1\epsilon_\pi^2 + c_2\epsilon_\pi^4 + c_3\epsilon_\pi^4 \log \epsilon_\pi^2\right) \tag{4.27}$$

[1] See Appendix B for the ensemble data as well as a discussion of our lattice action.

[2] Throughout this thesis, we will assume the renormalization scale in loop integrals (logarithms) is chosen such that $\mu = \Lambda_\chi = 4\pi F_\pi$ unless otherwise noted. This choice has limited impact on our extrapolations other than shuffling the values of the LECs. See Appendix E.

(Here we have defined the expansion parameter $\epsilon_\pi = m_\pi/\Lambda_\chi$, where $\Lambda_\chi = 4\pi F_\pi$ is the chiral cutoff. The parameters c_i and $w_{0,\text{ch}}$ are low-energy constants, with $w_{0,\text{ch}}$ in particular being the value of w_0 in the chiral limit, i.e. $m_q = 0$.) On the lattice, we do not generate w_0; instead we generate the dimensionless quantity w_0/a. If we divide both sides by the lattice spacing, we might think we have something more amenable to a fit.

$$\frac{w_0}{a} = \frac{w_{0,\text{ch}}}{a}\left(1 + c_1\epsilon_\pi^2 + c_2\epsilon_\pi^4 + c_3\epsilon_\pi^4 \log\epsilon_\pi^2\right) \tag{4.28}$$

There are a couple problems with this approach, however. First there is the obvious question: what does it even mean to extrapolate this quantity to the physical point, which includes the limit $a = 0$? Since w_0 is finite, the quantity on the right-hand side will blow up. The proposal to extrapolate w_0/a to the continuum limit is a non-starter.

Second, we have changed the low-energy constant (LEC) $w_{0,\text{ch}}$ to $w_{0,\text{ch}}/a$. Notably, this LEC now also depends on the lattice spacing. Thus Eq. (4.28) is only useful if we're fitting ensembles that have (approximately) the same lattice spacing.

However, none of these comments are meant to imply that Eq. (4.28) is useless. On the contrary, we can use Eq. (4.28) to determine the lattice spacings if we've already determined w_0 by some other method through the relation

$$a = \left.\frac{w_0}{(w_0/a)^{\text{fit}}}\right|_{\text{physical point}}. \tag{4.29}$$

But first we must determine w_0. Notice that if we multiply w_0 by an observable with mass dimension 1—the Ω baryon mass, for example—then we will have something dimensionless. But like w_0, we do not directly generate M_Ω on a lattice but rather aM_Ω; however, we see that the factors of a will cancel. Therefore if we instead extrapolate the quantity $(w_0/a)(aM_\Omega) = w_0 M_\Omega$ to the physical point, we can determine w_0 by calculating

$$w_0 = \left.\frac{(w_0 M_\Omega)^{\text{fit}}}{M_\Omega^{\text{exp}}}\right|_{\text{physical point}}. \tag{4.30}$$

That is, we use M_Ω as the physical scale when calculating the theory scale w_0.

The example of using M_Ω is not arbitrary—that is, in fact, the physical scale we use in this project. One might wonder why we would use a baryonic quantity, which admittedly suffers from an aforementioned signal-to-noise issue, as opposed to some mesonic quantity like F_π. In fact, some collaborations do use F_π as the physical scale when calculating the gradient flow scales. However, the Ω baryon, being composed of

Scheme	a_{15}/fm	a_{12}/fm	a_{09}/fm	a_{06}/fm
$t_{0,\mathrm{orig}}/a^2$	0.1284(10)	0.10788(83)	0.08196(64)	0.05564(44)
$t_{0,\mathrm{imp}}/a^2$	0.1428(10)	0.11735(87)	0.08632(65)	0.05693(44)
$w_{0,\mathrm{orig}}/a$	0.1492(10)	0.12126(87)	0.08789(71)	0.05717(51)
$w_{0,\mathrm{imp}}/a$	0.1505(10)	0.12066(88)	0.08730(70)	0.05691(51)

Table 4.1: Determinations of the lattice spacing for four different scale setting schemes using Eq. (4.29). Notice that the lattice spacing is scheme dependent. However, the result of an extrapolation to the physical (continuum) point is *not* scheme dependent; different schemes simply shuffle the LECs around.

three valence s quarks, has weak light quark dependence unlike F_π. Moreover, when calculating the variance of the correlation function per Eq. (4.11), we form pairs of kaons instead of pions. Thus the signal-to-noise falls as $\exp[-(M_\Omega - 3m_K/2)t]$, which is slower than other baryons.

Extrapolating the gradient flow scales to the physical point

We perform fits of $w_0 m_\Omega$ and $\sqrt{t_0} m_\Omega$ in order to determine the gradient flow scales w_0 and t_0, which we can then use for scale setting. The chiral expansion for $\sqrt{t_0}$ is identical to that of w_0 given in Eq. 4.28, other than the LECs being different. For convenience, let us separate out the observable into two pieces,

$$(w_0 M_\Omega)^{\mathrm{fit}} = (w_0 M_\Omega)^{\mathrm{chiral}} + (w_0 M_\Omega)^{\mathrm{disc}}\,, \tag{4.31}$$

and analyze them separately.

General remarks on the procedure for extrapolating observables are available in Appendix C.

Chiral models

The chiral expansion for M_Ω was worked out to N^{3}LO in [56].

$$\begin{aligned} M_\Omega =& M_0 + \alpha_2 \epsilon_\pi^2 \Lambda_\chi + \left(\alpha_4 + \beta_4 \log \epsilon_\pi^2\right) \epsilon_\pi^4 \Lambda_\chi \\ &+ \left(\alpha_6 + \beta_4 \log \epsilon_\pi^2 + \gamma_6 \left(\log \epsilon_\pi^2\right)^2\right) \epsilon_\pi^6 \Lambda_\chi \end{aligned} \tag{4.32}$$

$\lvert\mathbf{n}\rvert$	1	$\sqrt{2}$	$\sqrt{3}$	$\sqrt{4}$	$\sqrt{5}$	$\sqrt{6}$	$\sqrt{7}$	$\sqrt{8}$	$\sqrt{9}$	$\sqrt{10}$
c_n	6	12	8	6	24	24	0	12	30	24

Table 4.2: Finite volume weight factors for the first few finite volume modes.

We multiply this expression with that for the gradient flow scales to yield the χPT expression for the combined quantity.

$$
\begin{aligned}
(w_0 M_\Omega)^{\text{chiral}} =& w_{0,\text{ch}} M_0 && \text{(LO)} \\
&+ c_l \epsilon_\pi^2 + c_s \epsilon_s^2 && \text{(NLO)} \\
&+ \left[c_{ll} + c_{ll,g} \log(\epsilon_\pi^2)\right] \epsilon_\pi^4 + c_{ls} \epsilon_\pi^2 \epsilon_s^2 + c_{ss} \epsilon_s^4 && \text{(N}^2\text{LO)} \\
&+ \left[c_{lll} + c_{lll,g} \log(\epsilon_\pi) + c_{lll,g^2} \log^2(\epsilon_\pi)\right] \epsilon_\pi^6 && \text{(N}^3\text{LO)} \\
&+ c_{lls} \epsilon_\pi^4 \epsilon_s^2 + c_{lss} \epsilon_\pi^2 \epsilon_s^4 + c_{sss} \epsilon_s^6
\end{aligned}
\tag{4.33}
$$

The strange quark dependence is parameterized by $\epsilon_s = (2m_K^2 - m_\pi^2)/\Lambda_\chi$. We reiterate that the expression for $\sqrt{t_0} M_\Omega$ is identical other than the LECs.

We consider two choices for Λ_χ when model averaging: either Λ_χ, as is typically chosen in χPT, or $\Lambda_\chi = M_\Omega$, taking inspiration from [57].

Discretization effects

The lattice spacing corrections are a simple Taylor Ansatz, as explained in Appendix C. There is some ambiguity in the definition of the expansion parameter ϵ_a (e.g., $\epsilon_a = a/2w_0$ or $\epsilon_a = a/2\sqrt{t_0}$); however, this choice impacts the final extrapolation at less than a fraction of a standard deviation, so we choose $\epsilon_a = w_0/2a$.

The finite volume corrections require us to modify the logarithms (associated with loop integrals in χPT) in the following manner [58, 59]. The single logarithms become

$$
\log \epsilon_\pi^2 \to \log \epsilon_\pi^2 + 4k_1(m_\pi L) \tag{4.34}
$$

where

$$
k_1(x) = \sum_{|\mathbf{n}|\neq 0} c_n \frac{K_1\left(x|\mathbf{n}|\right)}{x|\mathbf{n}|} \tag{4.35}
$$

and K_1 is a modified Bessel function of the second kind and the c_n are given in Table 4.2. Meanwhile the two-loop integrals, manifest in the $(\log \xi)^2$ terms, are modified slightly differently. These become

$$\begin{aligned} \Big[\log \xi_l\Big]^2 &\to \Big[\log \xi_l + 4k_1(m_\pi L)\Big]^2 - \Big[\log \xi_l\Big]^2 \\ &\approx 8k_1(m_\pi L) \log \xi_l \end{aligned} \tag{4.36}$$

with the approximation being valid for our range of $m_\pi L$.

Additionally, there is a radiative correction $\alpha_s a^2$ for our sea quark action that scales as $\log a$ [60].

Results & conclusions

We summarize the choice of models we average over in the following table; the impact of these choices is demonstrated in Fig. 4.4. (The model averaging procedure is described in Appendix C.)

$\times 2$:	Taylor or χPT
$\times 2$:	Expand to N^{2}LO or N^{3}LO
$\times 2$:	Include/exclude finite volume corrections
$\times 2$:	Include/exclude radiative corrections $\alpha_s a^2$
$\times 2$:	Choice of $\Lambda_\chi \in \{4\pi F_\pi, M_\Omega\}$
32 :	Total choices

Overall, we find that our model average is largely insensitive to these choices. We note that it is unnecessary to include either the finest lattice spacing ensemble (`a06m310L`) or the smaller-than-physical strange quark mass ensemble (`a12m220ms`) in order to achieve the precision reported in this work; however, excluding either ensemble does shift the central value of the model average, albeit less than 1σ.

We find that our model average is insensitive to the choice of χPT- or Taylor-type fit as well as the order at which the expansion in truncated. Nevertheless, the choice for $\Lambda_\chi = 4\pi F_\pi$ (the typical χPT choice) is favored by a Bayes factor of roughly 150.

Below we report the values for the extrapolations to the physical point using $\epsilon_a = a/2w_0$. The full paper [54] lists the results for an alternate choice for the definition of ϵ_a, but the difference is barely perceptible so we omit it here.

$$
\begin{aligned}
\sqrt{t_0} M_\Omega &= 1.2051(82)^s(15)^\chi(46)^a(00)^V(21)^{\text{phys}}(61)^M \\
&= 1.205(12)\,, \\
\frac{\sqrt{t_0}}{\text{fm}} &= 0.1422(09)^s(02)^\chi(05)^a(00)^V(02)^{\text{phys}}(07)^M \\
&= 0.1422(14)\,,
\end{aligned}
$$

$$
\begin{aligned}
w_0 M_\Omega &= 1.4483(82)^s(15)^\chi(45)^a(00)^V(26)^{\text{phys}}(18)^M \\
&= 1.4483(97) \\
\frac{w_0}{\text{fm}} &= 0.1709(10)^s(02)^\chi(05)^a(00)^V(03)^{\text{phys}}(02)^M \\
&= 0.1709(11)\,.
\end{aligned}
$$

The uncertainties have been split by type: statistics (s), chiral model (χ), lattice spacing (a), finite volume (V), physical point input (phys), and model uncertainty (M). For w_0, the largest contribution to our error budget comes from statistics, suggesting a clear path forward for improving our result. In contrast, for t_0 the model selection uncertainty is comparable to the statistical uncertainty, with the former source of error primarily arising from different ways of modeling the discretization effects.

In future work we will likely need to incorporate the effects of isospin breaking (QCD + QED) if we wish to significantly reduce our uncertainty budget (for example, as was performed in [61]). As scale setting is necessary for converting any dimensionful observable calculated on the lattice into physical units, it is imperative that the uncertainty introduced by scale setting be minimized to the greatest extent possible. For now, however, we expect the contribution from scale setting to be subdominant when calculating such observables.

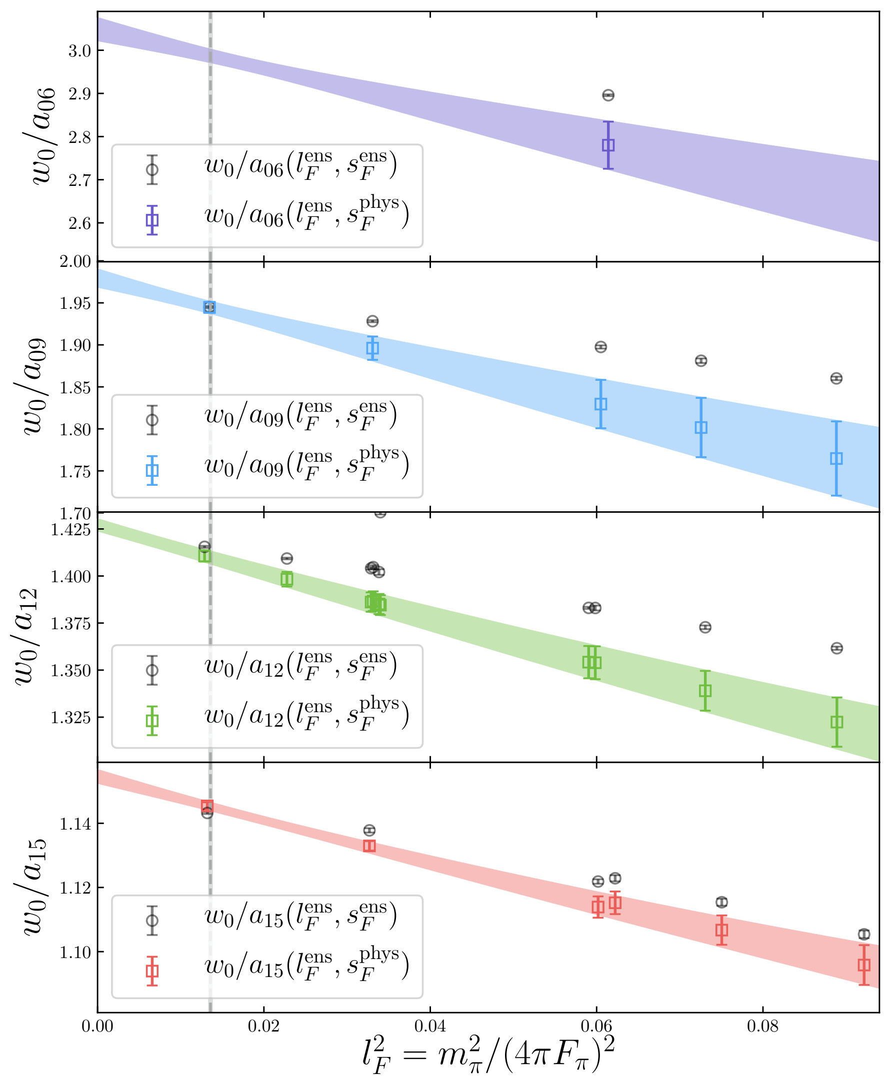

Figure 4.2: Results of interpolating (or in the case of w_0/a_{06}, extrapolating) w_0/a to the physical pion mass using Eq. 4.28. The square data have been “shifted” such that the dependence is only on $\epsilon_\pi^2 = l_F^2$; the black data are the original data (see Appendix C). Multiplying $w_0/(w_0/a_{15})$ yields the lattice spacing on a given ensemble (see Table 4.1). Figure from [54].

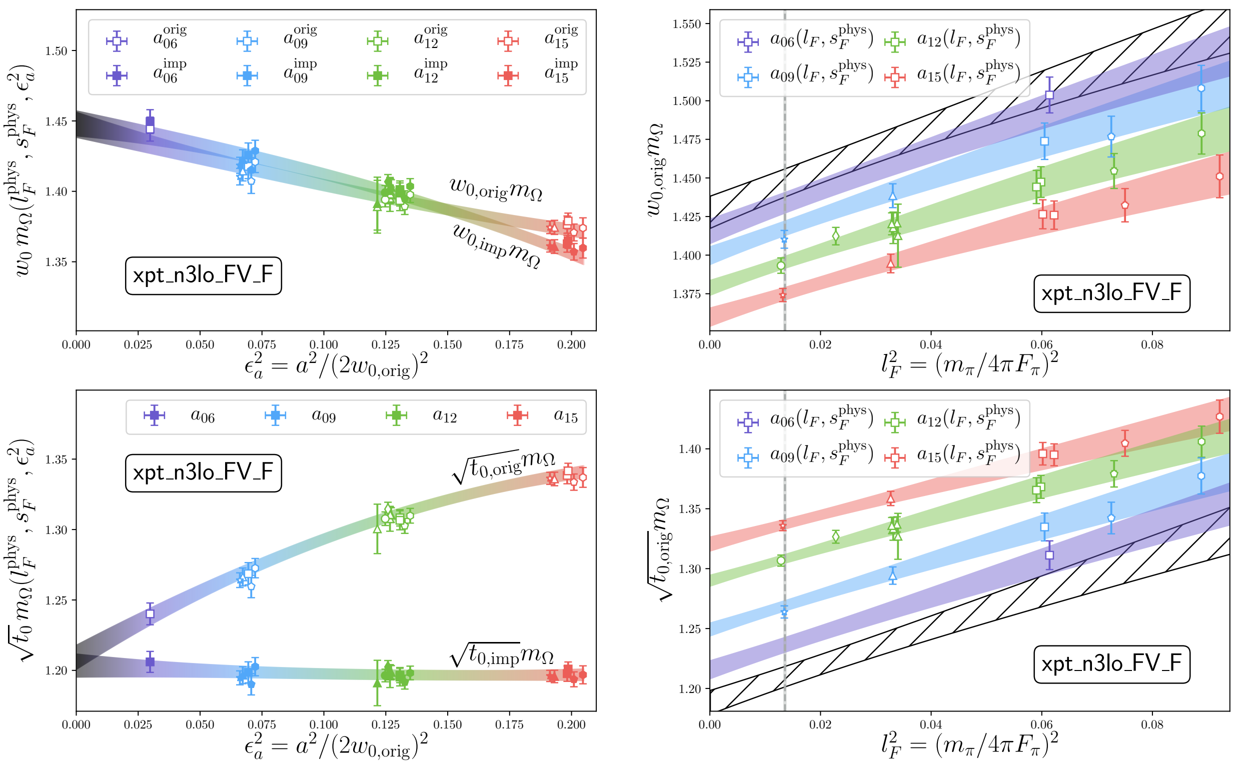

Figure 4.3: Extrapolations of $w_0 M_\Omega$ and $\sqrt{t_0} M_\Omega$ using the tree-level and improved definitions of the gradient flow scales. Here $l_F = \epsilon_\pi$. Notably, we see that $\sqrt{t_0} M_\Omega$ approaches the continuum limit in drastically different manners depending on which version of t_0 is used. However, the continuum values agree to within a fraction of a sigma, demonstrating that observables should agree in the continuum limit independent of scheme even if their values on a particular ensemble do not. Figure from [54].

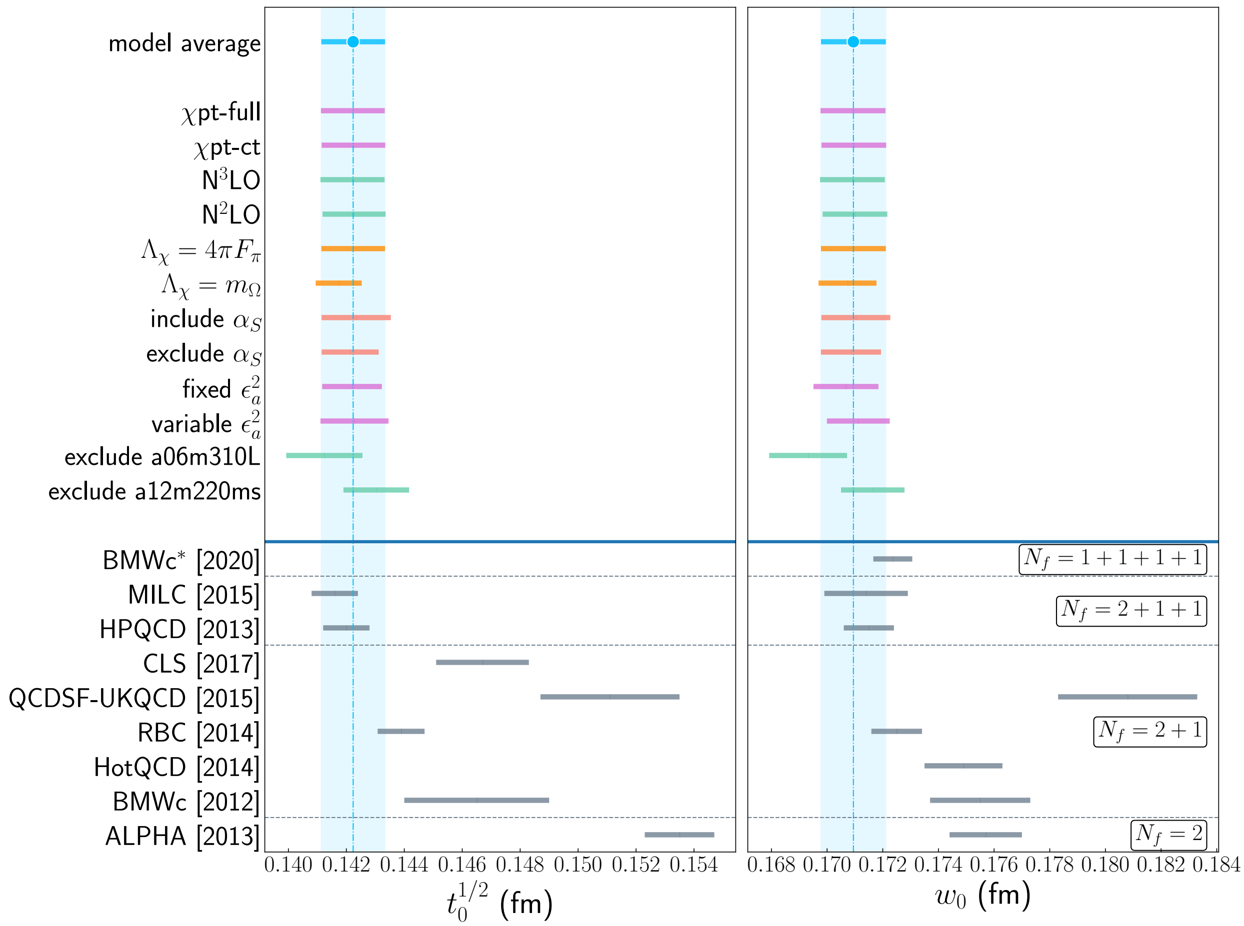

Figure 4.4: Model breakdown and comparison using the scale-improved, gradient flow derived quantities (i.e., $\sqrt{t_{0,\text{imp}}}m_\Omega$, $w_{0,\text{imp}}m_\Omega$). The vertical band is our model average. **χpt-full**: χPT model average, including $\log(\epsilon_\pi^2)$ corrections. **χpt-ct**: χPT model average with counterterms only, excluding $\log(\epsilon_\pi^2)$ corrections. **N^{3}LO/N^{2}LO**: model average restricted to specified order. **Λ_χ**: model average with specified chiral cutoff. **incl./excl. α_S**: model average with/without α_S corrections. **fixed/variable ϵ_a^2**: model average using two different definitions of ϵ_a^2. **excl. a06m310L**: model average excluding $a = 0.06$ fm ensemble (`a06m310L`). **excl. a12m220ms**: model average excluding small strange quark mass ensemble (`a12m220ms`). **Below solid line**: results from other collaborations: BMWc [2020] [61], MILC [2015] [62], HPQCD [2013] [63], CLS [2017] [64], QCDSF-UKQCD [2015] [65], RBC [2014] [66], HotQCD [2014] [67], BMWc [2012] [68] and ALPHA [2013] [69]. Figure from [54].

Ratio of Pseudoscalar Decay Constants, F_K/F_π

The ratio F_K/F_π is known as a *gold-plated* quantity in lattice QCD, being something that's easily calculable on the lattice and thus useful as a benchmark in comparing the fermion actions used by different collaborations. Moreover, precisely knowing the ratio allows one to determine the ratio of the Cabibbo-Kobayashi-Maskawa matrix elements $|V_{us}|$ and $|V_{ud}|$, as we will explain.

The work described in this chapter culminated in the following publication

N. Miller et al., Phys. Rev. D 102, 034507 (2020), arXiv:2005.04795 [hep-lat].

Connection to the Cabibbo-Kobayashi-Maskawa matrix

The Cabibbo-Kobayashi-Maskawa (CKM) matrix characterizes the extent to which the quarks eigenstates of the strong interaction can be thought of as a quark eigenstates of the weak interaction. In a universe where the quark eigenstates of the weak and strong interaction are the same, the CKM matrix is the identity; we are evidently not in that universe (quarks can change flavors through the weak interaction), and indeed the CKM matrix reflects that deviation from unity. Per the PDG [70] (and slightly overestimating some uncertainties to simplify the notation),

$$\begin{bmatrix} |V_{ud}| & |V_{us}| & |V_{ub}| \\ |V_{cd}| & |V_{cs}| & |V_{cb}| \\ |V_{td}| & |V_{ts}| & |V_{tb}| \end{bmatrix} = \begin{bmatrix} 0.97401(11) & 0.22650(48) & 0.00361(11) \\ 0.22636(48) & 0.97320(11) & 0.04053(83) \\ 0.00854(23) & 0.03978(82) & 0.99917(04) \end{bmatrix} . \tag{5.1}$$

Since the standard model requires the CKM matrix to be unitary, we can derive constraints on the rows and columns of this matrix. We will concentrate in particular on the top-row unitarity condition,

$$|V_{ud}|^2 + |V_{us}|^2 + |V_{ub}|^2 = 1\,. \tag{5.2}$$

We make the following observations regarding these matrix elements:

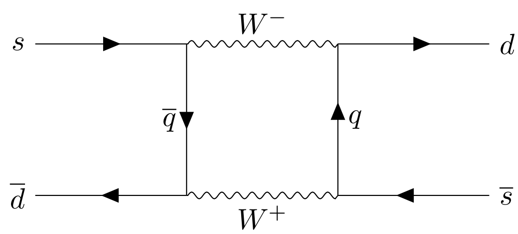

Figure 5.1: A kaon box diagram. Here q is an up-type quark (i.e., $q \in \{u, c, t\}$). Because the quark eigenstates are different in the strong and weak interactions, a K^0 can spontaneously change into a $\overline{K}^0$. Consequently, kaon decays do not conserve CP.

1. Of the three matrix elements in this relation, $|V_{ud}|$ is the most precisely known. Here $|V_{ud}|$ is extracted using superallowed beta decays, in which one calculates a comparative half-life for some nucleus, which can then be averaged with the comparative half-lives from several different nuclei [71]; the dominant uncertainty comes from the radiative and nuclear structure corrections as predicted by theory [72].

2. Historically $|V_{us}|$ was determined by assuming SU(3) flavor symmetry, which allowed one to estimate the form factors by relating the decays of different baryons in the baryon octet [71]. However, as SU(3) flavor symmetry is broken by $\sim$15%, this leads to a comparably poor estimate. These days one determines $|V_{us}|$ instead by using either leptonic ($K_{\ell 2}$) or semi-leptonic ($K_{\ell 3}$) kaon decays in conjunction with a lattice estimate of the associated form factor(s) [73].

3. Finally, the last matrix element in this relation, $|V_{ub}|$, is determined from semi-leptonic B decays; however, it is largely irrelevant for top-row unitarity tests, as its central value is small enough to be eclipsed by the uncertainty of the other two. Thus the top-row unitarity condition is primarily a test between $|V_{ud}|$ and $|V_{us}|$.

In summary, $|V_{us}|$ is essential for checking top-row unitarity. Additionally, in the Wolfenstein $(\lambda, A, \overline{\rho}, \overline{\eta})$ parameterization of the CKM matrix [74], $|V_{us}| = \lambda$ and thus affects all the other entries of the CKM matrix.

In this work, we determine $|V_{us}|$ through the leptonic decay $K \to l\overline{\nu}_l$ by using the lattice and experimental input. We begin with the charge-changing Lagrangian for the weak interaction [71],

$$\mathcal{L}_{\text{CC}} = -\frac{G_F}{\sqrt{2}} V_{km} \overline{u}^k \gamma_\mu \left(1 - \gamma^5\right) d^m \bar{l} \gamma^\mu \left(1 - \gamma^5\right) \nu + \text{ h.c.} \tag{5.3}$$

We can now write down the transition matrix element for a pseudoscalar—for example, the pion—decaying into two leptons.

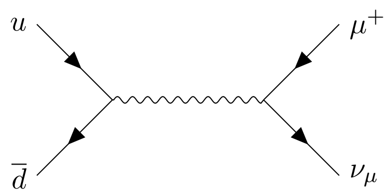

$$= \frac{G_F}{\sqrt{2}} V_{ud} \underbrace{\langle 0|\overline{d}\gamma_\mu\gamma^5 u|\pi(p)\rangle}_{i\sqrt{2}p_\mu F_\pi} l\gamma^\mu \left(1-\gamma^5\right)\overline{\nu}_l \tag{5.4}$$

Fermi's golden rule allows us to relate the decay rates to the spin-averaged transition matrix element. To wit, $d\Gamma \sim \langle |T|^2 \rangle \, d\phi$, with ϕ a phase space factor. Consequently, we expect $\Gamma(\pi \to l\overline{\nu}_l) \sim |V_{ud}|^2 F_\pi^2$. A similar argument can be made for $|V_{us}|$.

Calculating F_K/F_π on the lattice

Marciano [75, 76] showed how to relate the ratio the decay rates to the ratio of the decay constants exactly, which allows us to extract the ratio $|V_{us}|^2/|V_{ud}|^2$.

$$\frac{\Gamma(K \to l\,\overline{\nu}_l)}{\Gamma(\pi \to l\,\overline{\nu}_l)} = \left(\frac{F_K}{F_\pi}\right)^2 \frac{|V_{us}|^2}{|V_{ud}|^2} \frac{m_K(1-m_l^2/m_K^2)^2}{m_\pi(1-m_l^2/m_\pi^2)^2} \left[1+\frac{\alpha}{\pi}(C_K - C_\pi)\right] \tag{5.5}$$

The decay rates Γ and masses are well-determined from experiment. The last factor (in brackets) accounts for radiative electroweak corrections, but it contributes little to the calculation due to the factor of α.

The pseudoscalar decay constants themselves are defined as follows,

$$\langle 0|\overline{d}\gamma_\mu\gamma_5 u|\pi^+(p)\rangle = i\sqrt{2}p_\mu F_{\pi^+} \qquad \langle 0|\overline{s}\gamma_\mu\gamma_5 u|K^+(p)\rangle = i\sqrt{2}p_\mu F_{K^+}\,. \tag{5.6}$$

That is, they are related to the expectation value for the respective pseudoscalar particle to return to the (QCD) vacuum, which occurs by the action of its antiparticle on the state. This particular combination of gamma matrices ensures the antiparticle is a pseudoscalar also.

On the lattice, we can relate these decay constants to the correlation functions through the following Ward identity [77].

$$F_{q_1q_2} = Z_{q_1q_2}^{(PS)} \frac{m_{q_1} + m_{q_2} + m_{q_1}^{(res)} + m_{q_2}^{(res)}}{\sqrt[3]{E_{q_1q_2}}} \tag{5.7}$$

Here $m_q^{(res)}$ is the residual mass of quark q (a quantity particular to Möbius domain wall fermions, which characterizes the breaking of chiral symmetry), $E_{q_1q_2}$ is the ground state energy of the meson (q_1q_2), and $Z^{\text{PS}}_{q_1q_2}$ is the wavefunction overlap. The latter two quantities are determined from correlator fits, whereas the other quantities are known *a priori*. (Refer to Appendix D for a nuanced discussion of correlator fits.)

Extrapolation functions

The goal of this project is to determine the ratio F_K/F_π, which will allow us to estimate the ratio $|V_{us}|/|V_{ud}|$; doing so will require us to generate the quantity F_K/F_π on each lattice and then extrapolate the observable to the physical point.

As in Chapter 4, we separate our fit function into a chiral piece and discretization piece.

$$\left(\frac{F_K}{F_\pi}\right)^{\text{fit}} = \left(\frac{F_K}{F_\pi}\right)^{\text{chiral}} + \left(\frac{F_K}{F_\pi}\right)^{\text{disc}} \tag{5.8}$$

Chiral models

The SU(3) χPT expression for F_K/F_π to N^{2}LO is [78]

$$\begin{aligned}
\left(\frac{F_K}{F_\pi}\right)^{\chi\text{PT-expanded}} =& 1 + \frac{5}{8}\epsilon_\pi^2 \log \epsilon_\pi^2 - \frac{1}{4}\epsilon_K^2 \log \epsilon_K^2 - \frac{3}{8}\epsilon_\eta^2 \log \epsilon_\eta^2 + 4(4\pi)^2 L_5 \left(\epsilon_K^2 - \epsilon_\pi^2\right) && \text{(NLO)} \\
&+ \epsilon_K^4 F_F\left(\frac{\epsilon_\pi^2}{\epsilon_K^2}\right) + \hat{K}_1^r \left(\log \epsilon_\pi^2\right)^2 + \hat{K}_2^r \log \epsilon_\pi^2 \log \epsilon_K^2 && (\text{N}^2\text{LO}) \\
&+ \hat{K}_3^r \log \epsilon_\pi^2 \log \epsilon_\eta^2 + \hat{K}_4^r \left(\log \epsilon_K^2\right)^2 + \hat{K}_5^r \log \epsilon_K^2 \log \epsilon_\eta^2 + \hat{K}_6^r \left(\log \epsilon_\eta^2\right)^2 \\
&+ \hat{C}_1^r \log \epsilon_\pi^2 + \hat{C}_2^r \log \epsilon_K^2 + \hat{C}_3^r \log \epsilon_\eta^2 + \hat{C}_4^r \,. && (5.9)
\end{aligned}$$

where $\epsilon_p = m_p/\Lambda_\chi$. Let us refer to this as the *χPT-expanded* expression for F_K/F_π. Clearly this chiral expression is significantly more complicated than the chiral expression for $w_0 M_\Omega$ (recall that one reason for choosing w_0 as a scale setting quantity was for its weak pion dependence). We will break down these terms by order in the next few sections.

Compared to our chiral extrapolation of $w_0 M_\Omega$ before, we have an additional constraint on F_K/F_π: in the SU(3) flavor limit, we expect $F_K/F_\pi = 1$. Indeed, the expression above satisfies this condition, and it is easily verified to NLO using the GMOR relation (Eq. 3.74).

However, rather than use the expanded expression, we can instead calculate F_K and F_π individually, then calculate the ratio (of course, the decay constants themselves are dimensionful quantities, but this is irrelevant once we take the ratio). In this case, we instead use

$$\left(\frac{F_K}{F_\pi}\right)^{\chi\text{PT-ratio}} = \frac{F_K^{\chi\text{PT}}}{F_\pi^{\chi\text{PT}}} \tag{5.10}$$

where to NLO [79]

$$F_K^{\chi\text{PT}} = F_0 \left[1 - \frac{3}{8}\epsilon_\pi^2 \log \epsilon_\pi^2 - \frac{3}{4}\epsilon_K^2 \log \epsilon_K^2 - \frac{3}{8}\epsilon_\eta^2 \log \epsilon_\eta^2 + 4\epsilon_\pi^2 (4\pi)^2 L_4 + 4\epsilon_K^2 (4\pi)^2 (L_5 + 2L_4)\right] , \tag{5.11}$$

$$F_\pi^{\chi\text{PT}} = F_0 \left[1 - \epsilon_\pi^2 \log \epsilon_\pi^2 - \frac{1}{2}\epsilon_K^2 \log \epsilon_K^2 + 4\epsilon_\pi^2 (4\pi)^2 (L_4 + L_5) + 8\epsilon_K^2 (4\pi)^2 L_4\right] . \tag{5.12}$$

Let us refer to this as the *χPT-ratio* expression for F_K/F_π.

We also attempted to fit F_K/F_π using mixed-action effective field theory [80], an extension of χPT to the sea-quark sector. However, the weights were orders of magnitude worse for this class of fits and were ultimately excluded from the analysis, so we omit a discussion of them here. Refer to the full paper for details [81].

In this work we also consider the choices $\mu = \Lambda_\chi \in 4\pi\{F_\pi, F_K, \sqrt{F_\pi F_K}\}$ as different proxies for the chiral cutoff/renormalization scale. Note that we use a sliding renormalization scale (e.g., using the value of F_π on an ensemble) and not a fixed renormalization scale (e.g., using the physical point value of F_π). Different choices (without counterterms) are expected to shift the LECs but not the final extrapolated value. Corrections for these different choices are worked out in Appendix E.

Chiral models: NLO

Appearing in the NLO χPT expressions Eqs. (5.9), (5.11), and (5.12) are the Gasser-Leutwyler LECs L_4 and L_5. These LECs are the coefficients in the next leading term in the chiral Lagrangian, e.g.

$$\mathcal{L}^{(4)} \supset L_5 \,\mathrm{Tr}\left[\partial_\mu U \partial^\mu U^\dagger \left(M U^\dagger + U M^\dagger\right)\right] . \tag{5.13}$$

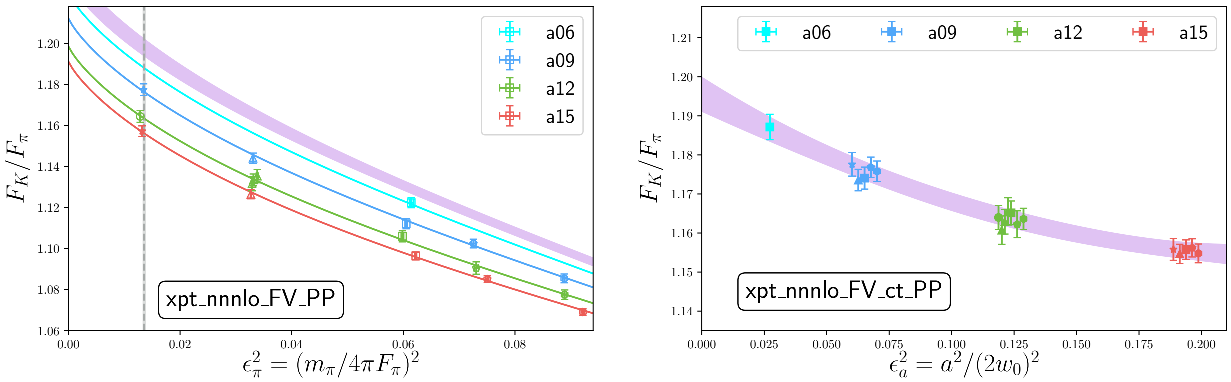

Figure 5.2: Example extrapolation as a function of the light quark mass (left) and lattice spacing (right). Figure from [81].

Even though we could model our expression for F_K/F_π as a Taylor expansion plus χPT-motivated log terms, using the explicit χPT expression allows us to determine the Gasser-Leutwyler LECs, which can be reused for other χPT calculations.

Comparing the χPT-expanded and χPT-ratio models, we observe that there is an advantage to the expanded form: L_4 is eliminated at NLO.

Finally, we note that although we typically prior our LECs when fitting as $\mathcal{O}(1)$ (that is, we assume our effective field theory is "natural"), we note that the Gasser-Leutwyler coefficients have been measured to be much smaller, roughly $\mathcal{O}(10^{-3})$.

Chiral models: N^{2}LO

The N^{2}LO corrections can be broadly classified into four categories: pure Taylor, single logs, double-logs, and a "sunset" term, the last of which comes from evaluating a sunset integral.

$$\delta\left(\frac{F_K}{F_\pi}\right)^{\chi\text{PT-expanded}}_{\text{N}^2\text{LO}} = \delta\left(\frac{F_K}{F_\pi}\right)^{\text{Taylor}}_{\text{N}^2\text{LO}} + \delta\left(\frac{F_K}{F_\pi}\right)^{\text{log}}_{\text{N}^2\text{LO}} + \delta\left(\frac{F_K}{F_\pi}\right)^{\text{log}^2}_{\text{N}^2\text{LO}} + \delta\left(\frac{F_K}{F_\pi}\right)^{\text{sunset}}_{\text{N}^2\text{LO}} \tag{5.14}$$

The Taylor terms can be modeled in a straightforward fashion: one could simply write $\sum_p \alpha_p \epsilon_p^2(\epsilon_K^2 - \epsilon_\pi^2)$. However, since the χPT-expanded expression is known to N^{2}LO, we could instead rewrite the α_p coefficients in terms of the Gasser-Leutwyler coefficients; this is encapsulated in the term

$$\delta\left(\frac{F_K}{F_\pi}\right)^{\text{Taylor}}_{\text{N}^2\text{LO}} = \hat{C}_4^r\,. \tag{5.15}$$

In addition to the Gasser-Leutwyler constants, however, this term also includes the coefficients of $\mathcal{L}^{(6)}$.

The single log dependence is captured by the remaining $\hat{C}_i^r$.

$$\delta\left(\frac{F_K}{F_\pi}\right)^{\text{log}}_{\text{N}^2\text{LO}} = \hat{C}_1^r \log \epsilon_\pi^2 + \hat{C}_2^r \log \epsilon_K^2 + \hat{C}_3^r \log \epsilon_\eta^2 \tag{5.16}$$

Only the Gasser-Leutwyler LECs appear in these terms.

The double-log terms are entirely determined, with no LECs appearing inside $\hat{K}_i^r$.

$$\begin{aligned}\delta\left(\frac{F_K}{F_\pi}\right)^{\log^2}_{\text{N}^2\text{LO}} =& \hat{K}_1^r \left(\log \epsilon_\pi^2\right)^2 + \hat{K}_2^r \log \epsilon_\pi^2 \log \epsilon_K^2 + \hat{K}_3^r \log \epsilon_\pi^2 \log \epsilon_\eta^2 \\ &+ \hat{K}_4^r \left(\log \epsilon_K^2\right)^2 + \hat{K}_5^r \log \epsilon_K^2 \log \epsilon_\eta^2 + \hat{K}_6^r \left(\log \epsilon_\eta^2\right)^2\end{aligned} \tag{5.17}$$

The remaining term arises comes from the sunset integral.

$$\delta\left(\frac{F_K}{F_\pi}\right)^{\text{sunset}}_{\text{N}^2\text{LO}} = \epsilon_K^4 F_F \left(\frac{\epsilon_\pi^2}{\epsilon_K^2}\right) \tag{5.18}$$

The analytic result is quite complicated but was worked out in [78]. In our extrapolation routine, we include these terms using a Python wrapper for the software package `CHIRON` [82].

We can use N^{2}LO chiral corrections for the ratio-type models also so long as we subtract off the N^{2}LO cross terms that come from Taylor expanding

$$\frac{F_K}{F_\pi} = \frac{1 + \delta F_K^{\text{NLO}}}{1 + \delta F_\pi^{\text{NLO}}} \,. \tag{5.19}$$

Thus

$$\delta\left(\frac{F_K}{F_\pi}\right)^{\chi\text{PT-expanded}}_{\text{N}^2\text{LO}} = \delta\left(\frac{F_K}{F_\pi}\right)^{\text{chiral}}_{\text{N}^2\text{LO}} + \delta F_\pi^{\text{NLO}} \delta F_K^{\text{NLO}} - \left(F_\pi^{\text{NLO}}\right)^2 \,. \tag{5.20}$$

Chiral models: N^{3}LO

Corrections at N^{3}LO are pure Taylor counterterms (with the appropriate factor of $\epsilon_K^2 - \epsilon_\pi^2$). Although simple, we find that these terms are useful in obtaining a good quality fit.

Discretization effects

The discretization corrections for F_K/F_π are nearly identical to those we included for $w_0 M_\Omega$ in Chapter 4. That is, for the finite volume corrections we again modify the logs as

$$\log \epsilon_\pi^2 \to \log \epsilon_\pi^2 + 4k_1(m_\pi L) \tag{5.21}$$

using the coefficients given in Table 4.2. We omit the N^{2}LO finite volume corrections in which the double-log terms are modified, as we find our fits are insensitive to these corrections when fitting this particular observable.

The lattice spacing corrections are also modified to ensure that $F_K/F_\pi \to 1$ in the SU(3) flavor limit. We again require that the discretization terms include a factor of $\epsilon_K^2 - \epsilon_\pi^2$, which consequently means that the lowest-order lattice spacing corrections must enter at $\mathcal{O}(\epsilon^4)$. Similarly, if we choose to include the radiative α_s correction, it also contributes at $\mathcal{O}(\epsilon^4)$.

Results & conclusions

We include the following models in our model average. A representative model is shown in Fig. 5.2.

$\times 3:$	Choice of $\mu = \Lambda_\chi \in 4\pi\{F_\pi, F_K, \sqrt{F_\pi F_K}\}$
$\times 2:$	Choice of χPT-expanded or χPT-ratio for chiral model
$\times 2:$	Include/exclude χPT corrections at N^{2}LO
$\times 2:$	Include/exclude α_s discretization correction
$24:$	Total choices

The impact of these differences is shown in Figs. 5.3 and 5.4. Notably, we find that simply using Taylor counterterms at N^{2}LO (but keeping the χPT-motivated terms at NLO) is strongly preferred over a full χPT fit, suggesting our data is insufficient to discern the chiral logs. Further, as mentioned previously, results from mixed-action χPT fared no better than regular χPT , with the most discernible difference being a tanking of the Bayes factor. Fits using the canonical choice $\Lambda_\chi = 4\pi F_\pi$ contribute the most to the model average, whereas those using $\Lambda_\chi = 4\pi F_K$ (the largest deviation from the canonical choice) contribute the least. Nevertheless, the difference on the extrapolation is less than 1σ.

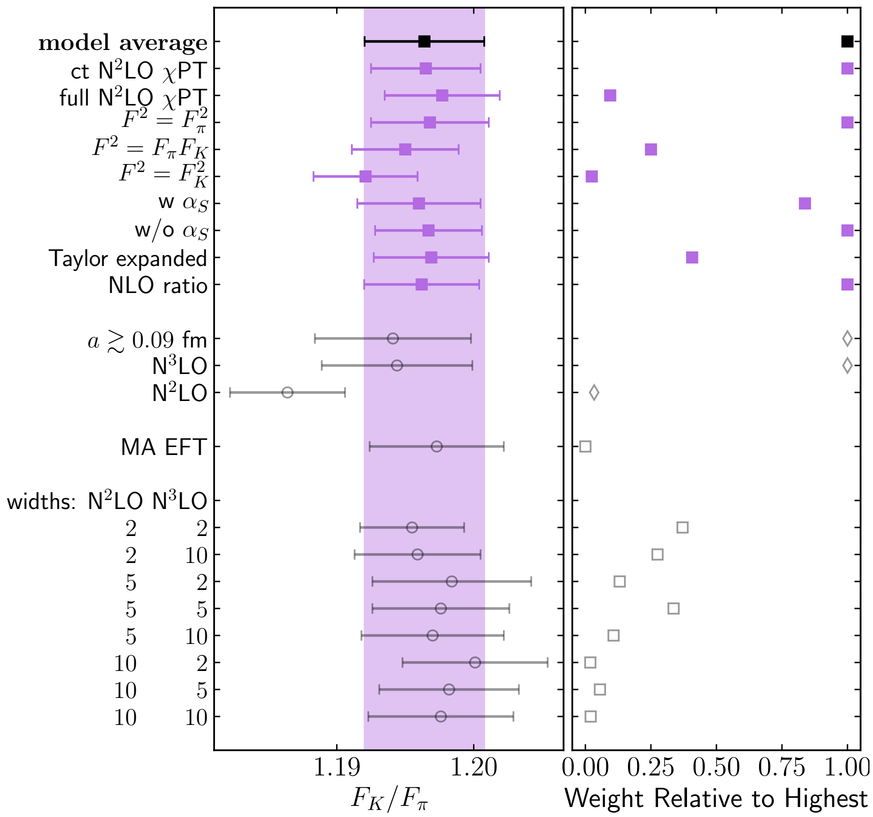

Figure 5.3: Model comparison. The left panel shows the result of the model average for given restrictions on the models, while the right side shows the relative weight of the model. Only models that include the same set of ensembles can be compared; thus the fits with gray triangles (denoting fits in which the finest lattice spacing ensemble is excluded) should only be compared among themselves. We see that the mixed-action EFT fits produce a similar result as our model average despite having negligibly small weight and being excluded from the model average. The final model average is relatively insensitive to our choice of priors. Figure from [81].

We report a final model-averaged result of

$$\begin{aligned} \frac{F_K}{F_\pi} &= 1.1964(32)^s(12)^\chi(20)^a(01)^V(15)^{\text{phys}}(12)^M \\ &= 1.1964(44)\,. \end{aligned} \tag{5.22}$$

separated into statistical (s), chiral (χ), lattice spacing (a), finite volume (V), physical point input (phys), and model selection (M) uncertainties.

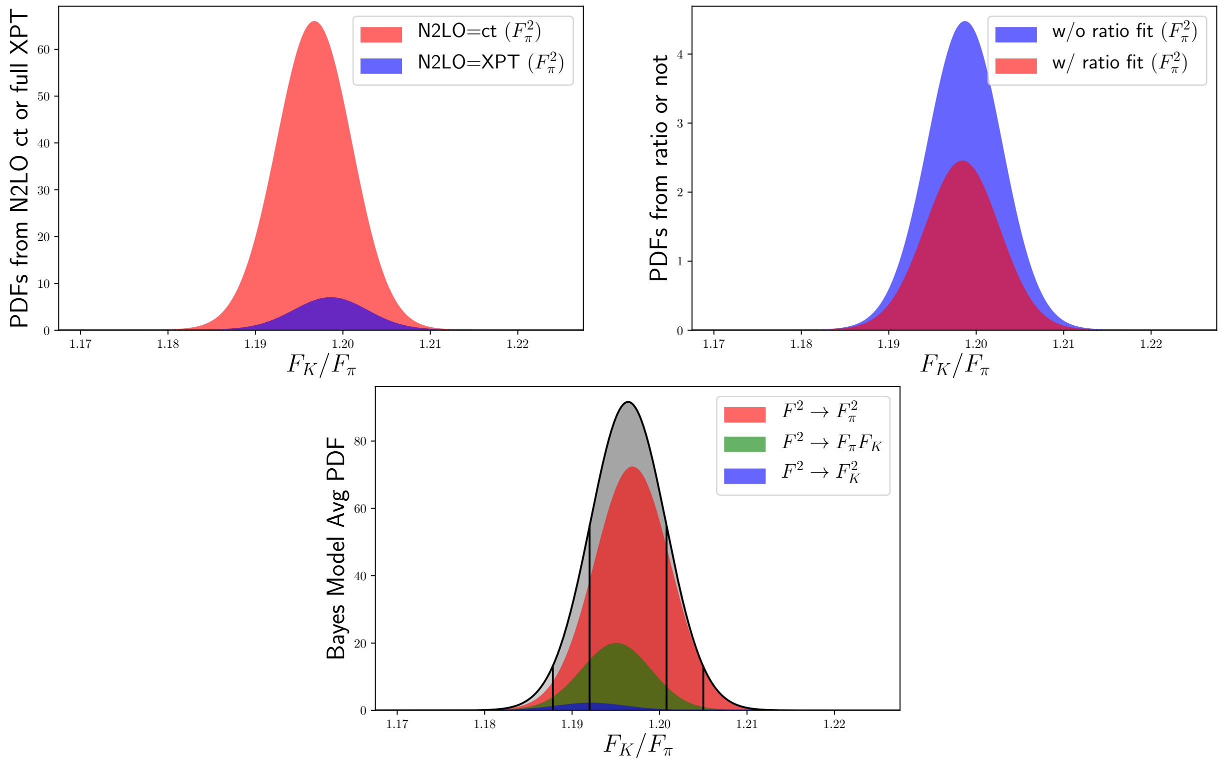

Figure 5.4: Histograms for some of the model averaging choices. Besides showing the relative weights, these plots also demonstrate the distribution of values. Figure from [81].

Additionally, we also estimate the SU(2) isospin-breaking correction [83].

$$\delta_{\text{SU(2)}} = \sqrt{3}\epsilon_{\text{SU(2)}} \left[-\frac{4}{3}(F_K/F_\pi - 1) + \frac{4}{3(4\pi F)^2} \left(m_K^2 - m_\pi^2 - m_\pi^2 \log \frac{m_k^2}{m_\pi^2} \right) \right] \tag{5.23}$$

Here $\epsilon_{\text{SU(2)}} = \sqrt{3}/(4R)$, $R = 35.7(2.6)$ per FLAG [73], the masses are the physical values, and F_K/F_π is the extrapolated result. With $\delta_{\text{SU(2)}}$ in hand, we can compare our value of F_K/F_π determined on the lattice to the corrected charged ratio $F_K^\pm/F_\pi^\pm$ through

$$\frac{F_K^\pm}{F_\pi^\pm} = \frac{F_K}{F_\pi}\sqrt{1 + \delta_{\text{SU(2)}}}\,. \tag{5.24}$$

The corrected charge ratio $F_K^\pm/F_\pi^\pm$, as opposed to F_K/F_π, is the quantity compiled by FLAG. We find that

$$\begin{aligned} \frac{F_K^\pm}{F_\pi^\pm} &= 1.1942(44)(07)^{\text{isospin}} \\ &= 1.1942(45)\,. \end{aligned} \tag{5.25}$$

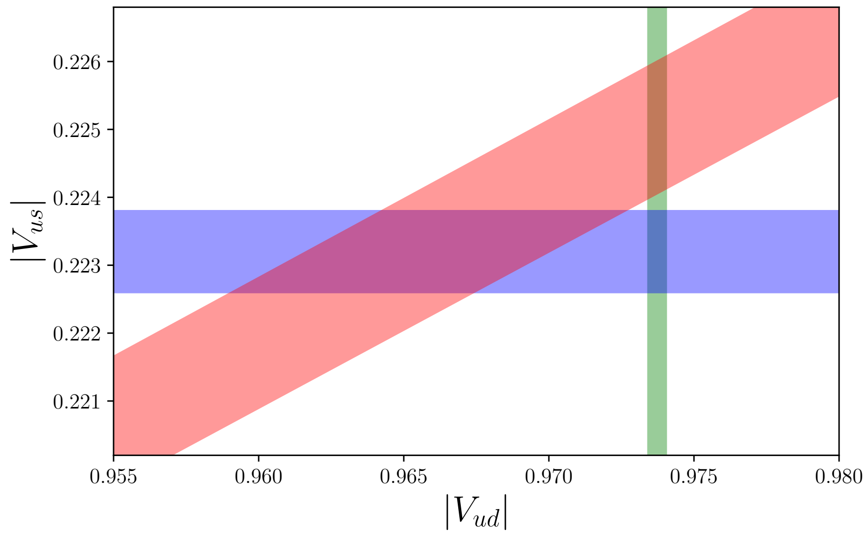

Figure 5.5: Plot of $|V_{us}|/|V_{ud}|$ (red band). The blue band is the global average for $|V_{us}|$ using lattice determinations of $f^+(0)$ plus semi-leptonic kaon decays. The green band is the global average for $|V_{ub}|$ using superallowed beta decays. The figure from [81] has been updated with more recent averages.

Next we check the top-row unitarity condition and determine the CKM matrix element $|V_{us}|$. From Eq. (5.5), we have

$$\frac{|V_{us}|}{|V_{ud}|}\frac{F_K^\pm}{F_\pi^\pm} = 0.2760(4) \implies \frac{|V_{us}|}{|V_{ud}|} = 0.2311(10) \tag{5.26}$$

using global averages from the PDG [72] and our model-averaged result.

With our ratio $|V_{us}|/|V_{us}|$, we can either determine $|V_{us}|$ (using the global averages from superallowed beta decay) or $|V_{ud}|$ (using the other lattice determination of $|V_{us}|$ from semi-leptonic kaon decays, $K_{\ell 3}$).

$$|V_{us}| = 0.2252(9) \qquad \text{(w/ } \beta) \tag{5.27}$$

$$|V_{ud}| = 0.9658(49) \qquad \text{(w/ } K_{\ell 3}) \tag{5.28}$$

Although the $|V_{us}|$ result from F_K/F_π is comparable to the result from $f^+(0)$ (see Fig. 5.5), the result for $|V_{ud}|$ is significantly less precise than superallowed beta decay result, $|V_{ud}| = 0.97373(31)$, as one might expect.

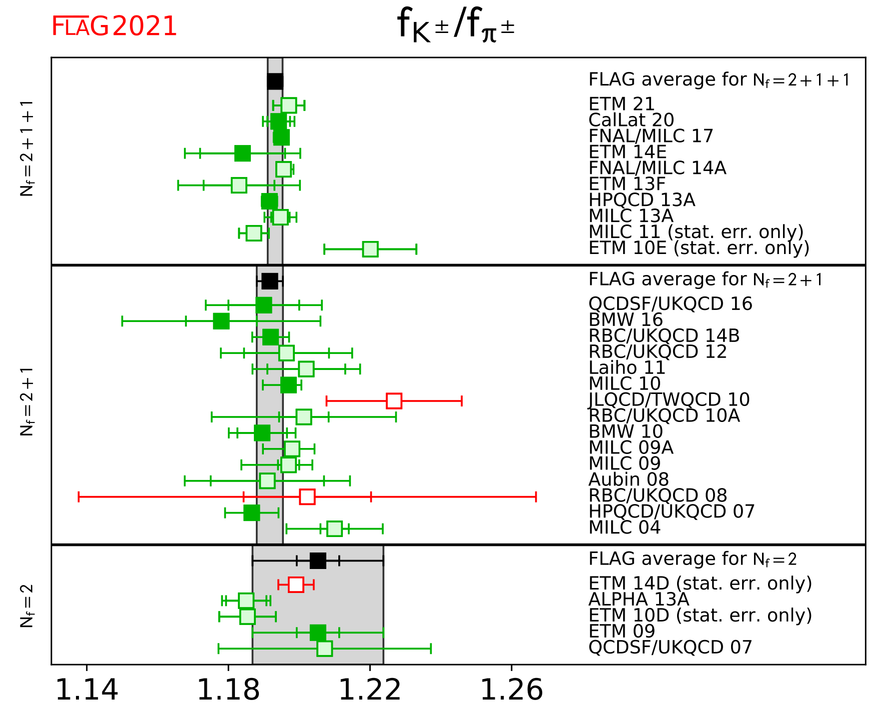

Figure 5.6: Results from various collaborations: FNAL/MILC 17 [84], QCDSF/UKQCD 16 [85], HPQCD 13A [63], ETM 14E [86], RBC/UKQCD 14B [87], MILC 10 [88], BMW 10 [76], ETM 09 [89], HPQCD/UKQCD 07 [90]. We find that our result (CalLat 20) lies in good agreement. Taken from FLAG [73].

Finally, we check the top-row unitarity condition either assuming the semi-leptonic kaon decay results for $|V_{us}|$ or the superallowed beta decay value for $|V_{ud}|$.

$$|V_u| = 0.99880(77) \qquad \text{(w/ } \beta) \tag{5.29}$$

$$|V_u| = 0.9826(96) \qquad \text{(w/ } K_{\ell 3}) \tag{5.30}$$

We have incorporated the PDG average $|V_{ub}| = 3.82(24) \times 10^{-3}$, but we note its contribution is minuscule. Either procedure results in some tension with the top-row unitarity condition.

We finish this chapter my recalling a second motivation for calculating F_K/F_π: being a gold-plated quantity, it is relatively easy to calculate on the lattice and therefore serves as an important benchmark for testing the convergence of different discretizations of the QCD action. Moreover, as we intend to continue to use this action for other calculations, we must verify that our action converges, too. We find that our result agrees with others (Fig. 5.6).

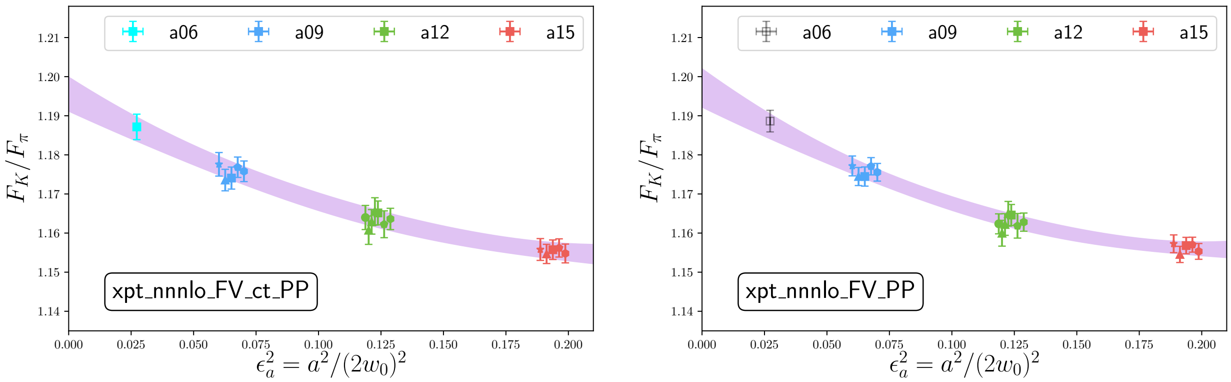

Figure 5.7: A representative fit which includes the finest lattice spacing ensemble (left) and a different fit which excludes that ensemble (right). We find that the finest lattice spacing ensemble, although helpful for guiding the extrapolation, is not necessary. Figure from [81].

In addition, we find that our action does not require the finest lattice ensemble to obtain our level of precision, which is not true of all actions (see Figs. 5.3 and 5.7).

The hyperon spectrum

Hyperons are a class of baryons containing strange quarks but no heavier quarks. In this chapter we discuss how hyperon decays can be used to determine $|V_{us}|$ in a manner orthogonal to F_K/F_π, and we present some preliminary calculations of the mass spectrum for the cascades, Ξ and Ξ^*, as a stepping stone for a future determination of the hyperon transition matrix elements.

The work described in this chapter was presented at the 38th International Symposium on Lattice Field Theory and accompanied with the following proceeding.

> N. Miller et al., in 38th International Symposium on Lattice Field Theory (2022) arXiv:2201.01343 [hep-lat].

Background: $|V_{us}|$ from hyperon decays

In the previous chapter we showed how to determine the CKM matrix element $|V_{us}|$ using leptonic kaon decays ($K_{\ell 2}$) and F_K/F_π. But this is not the only way to determine $|V_{us}|$; there is a competing technique using semi-leptonic kaon decays ($K_{\ell 2}$) and a lattice calculation of the 0-momentum form factor $f^+(0)$.

Unfortunately, there is some tension in the two kaon-based methods (see Fig. 6.1), with the two kaon-derived values for $|V_{us}|$ differ by roughly 2σ. We previously mentioned that $|V_{us}|$ was estimated historically using hyperon decays and assuming SU(3) flavor symmetry. However, with the lattice we don't need to make these assumptions—we can instead directly calculate the relevant hadronic matrix elements.

A lattice determination of the hyperon transition matrix elements, nevertheless, presents its own set of challenges: the signal is baryonic, not mesonic, and thus inherently noisier than the kaon-based methods; and unlike the kaon determinations where only a single form factor (or ratio of form factors) need be determined, there are multiple form factors in hyperon decays that must be accounted for.

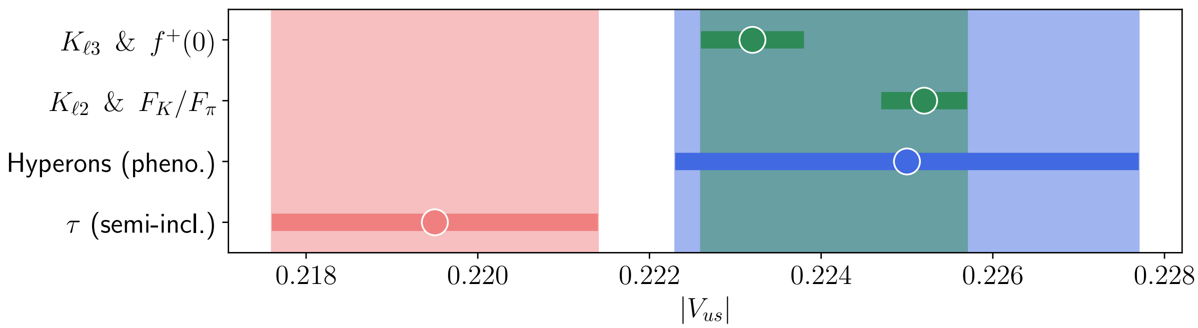

Figure 6.1: Determinations of $|V_{us}|$ from different sources. The two kaon-derived estimates are taken from FLAG [73]; the phenomenological hyperon-derived value is taken from the Particle Data Group [72] (specifically [91]); the semi-inclusive τ-derived average is taken from the Heavy Flavor Averaging Group [92]. Note that $K_{\ell 2}$ & F_K/F_π only determine the ratio $|V_{us}|/|V_{ud}|$, so here we have also assumed the Particle Data Group average for $|V_{ud}|$. The green band spans the minimum/maximum values of $|V_{us}|$ from kaon decays. Figure from [93].

To get an idea of how this works, let us write down the transition matrix element T for the semi-leptonic baryon decay $B_1 \to B_2 + l^- + \overline{\nu}_l$ [71].

$$T = \frac{G_{\mathrm{F}}}{\sqrt{2}} V_{us} \left[\overbrace{\langle B_2 | \overline{u} \gamma_\mu \gamma^5 s | B_1 \rangle}^{\text{axial-vector}} - \overbrace{\langle B_2 | \overline{u} \gamma_\mu s | B_1 \rangle}^{\text{vector}} \right] \bar{l} \gamma^\mu (1 - \gamma^5) \nu_l \tag{6.1}$$

The transition matrix element can then be related to the decay widths to extract $|V_{us}|$, which depends on two hadronic matrix elements. By projecting out the Lorentz structure, we obtain the form factors.

$$\langle B_2 | \overline{u} \gamma_\mu \gamma^5 s | B_1 \rangle = g_A(q^2) \gamma_\mu \gamma^5 + \underbrace{\cancel{\frac{f_{\mathrm{T}}(q^2)}{2M} i \sigma_{\mu\nu} q^\nu \gamma^5}}_{G\text{-parity}} + \frac{f_{\mathrm{P}}(q^2)}{2M} q_\mu \gamma^5 \tag{6.2}$$

$$\langle B_2 | \overline{u} \gamma_\mu s | B_1 \rangle = g_V(q^2) \gamma_\mu + \frac{f_{\mathrm{M}}(q^2)}{2M} i \sigma_{\mu\nu} q^\nu + \overbrace{\cancel{\frac{f_{\mathrm{S}}(q^2)}{2M}}}^{\text{CVC}} q_\mu \tag{6.3}$$

In total there are six form factors, though one can reduce the total to four by invoking the conserved vector current (CVC) hypothesis and appealing to G-parity (a generalization of C-parity to multiplets [94]). Given recent measurements of the hyperon decay widths from the LHCb experiment [95], we believe we can extract a competitive hyperon-derived value of $|V_{us}|$ so long as we can determine the transition form factors to $\sim 1\%$.

Before we can calculate all the hyperon transition form factors, however, we will undertake a few more modest goals: first we will calculate the hyperon mass spectrum and then the hyperon axial charges. As our final result for these observables will depend upon an extrapolation based on $SU(2)$ χPT for hyperons [56, 96, 97], it is prudent to study the convergence pattern of this effective field theory (EFT) and to benchmark our results with the experimental measurements of the hyperon masses. Prior to having precise lattice QCD results for hyperon quantities, $SU(3)$ baryon chiral perturbation theory (χPT) was utilized to relate the otherwise numerous low-energy-constants (LECs) describing various processes involving hyperons. However, $SU(3)$ heavy baryon χPT generally does not exhibit a converging expansion [98, 99, 100]. Lattice QCD can be used to determine the more extensive set of LECs that arise in $SU(2)$ (heavy) baryon χPT for hyperons, thus providing the theory with predictive power. The benefit of checking the heavy baryon χPT predictions using the masses are twofold: first, experimental measurements are readily available; second, masses are relatively easy to calculate on the lattice.

The next step will be to calculate the hyperon axial charges. The leading order LECs that contribute to the hyperon axial charges also describe the pion exchange between hyperons as well as the radiative pion-loop corrections to the hyperon spectrum. Therefore a precise determination of the axial charges will improve the determination of other observables derived from these Lagrangians. These same hyperon axial charge LECs will also be important for understanding the hyperon-nucleon interactions germane in light hyper-nuclei and possibly for understanding the role of hyperons in neutron stars.

Project goals & lattice details

The eventual goal of this program is to calculate the hyperon transition matrix elements as motivated by the previous section. To perform these calculations, we employ an EFT for hyperons as derived in [56, 96, 97] that relies on heavy baryon χPT. The first goal of this project is to test the convergence of the EFT employed in this work. To that end, we will first calculate the hyperon mass spectrum, which we determine by taking the chiral mass formula derived from this EFT and extrapolating to the physical point. Later we will calculate the hyperon axial charges and the other transition form factors, which will allow us to determine the transition matrix elements.

The hyperon spectrum has been calculated numerous times, for example in [48, 101]. There has been comparatively less work on the hyperon axial charges. The first lattice determination of the hyperon axial

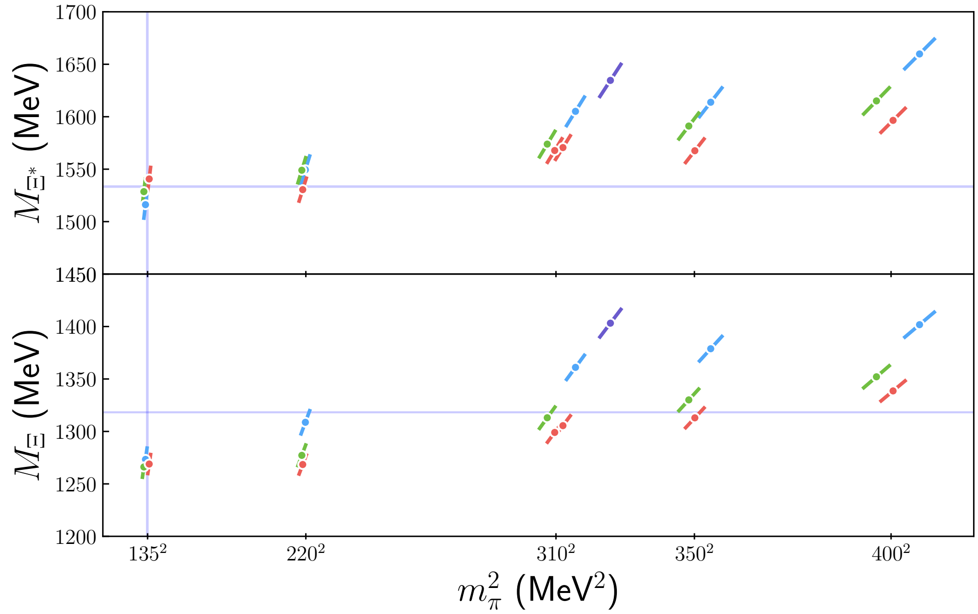

Figure 6.2: M_Ξ as a function of m_π^2 for each of our ensembles. Here the lattice spacings range from ~ 0.06 fm (purple) to ~ 0.15 fm (red). We convert from lattice units to physical units by scale setting with M_Ω and the gradient flow scale w_0 as explained in Chapter 4. The violet bands denote the physical point values of each observable; for M_Ξ in particular, discrepancies between the physical pion mass ensembles and the physical point vanish once the strange quark mistuning and lattice spacing effects are accounted for. Figure from [93].

charges occurred in 2007 but only involved a single lattice spacing [102]; a calculation involving a physical pion mass ensemble and an extrapolation to the continuum limit didn't occur until 2018 [103]. However, that work only employed a Taylor extrapolation, not a χPT-motivated extrapolation to the continuum limit. Moreover, our work will benefit from the inclusion of three lattice spacings at the physical pion mass (four in total).

Extrapolation details

Let us consider the strangeness $S = 2$ hyperons, i.e. the (strange) cascades. The chiral expressions for the mass formulae are as follows

$$
\begin{aligned}
M_{\Xi}^{(\chi)} = \;& M_{\Xi}^{(0)} + \sigma_{\Xi}\Lambda_\chi\epsilon_\pi^2 \\
& - \frac{3\pi}{2} g_{\pi\Xi\Xi}^2 \Lambda_\chi \epsilon_\pi^3 \\
& - g_{\pi\Xi^*\Xi}^2 \Lambda_\chi \mathcal{F}(\epsilon_\pi, \epsilon_{\Xi\Xi^*}, \mu) \\
& + \frac{3}{2} g_{\pi\Xi^*\Xi}^2 (\sigma_\Xi - \overline{\sigma}_\Xi)\Lambda_\chi\epsilon_\pi^2 \mathcal{J}(\epsilon_\pi, \epsilon_{\Xi\Xi^*}, \mu) \\
& + \alpha_{\Xi}^{(4)} \Lambda_\chi \epsilon_\pi^4 \log \epsilon_\pi^2 + \beta_{\Xi}^{(4)} \Lambda_\chi \epsilon_\pi^4
\end{aligned}
\qquad
\begin{aligned}
M_{\Xi^*}^{(\chi)} = \;& M_{\Xi^*}^{(0)} + \overline{\sigma}_{\Xi}\Lambda_\chi\epsilon_\pi^2 \\
& - \frac{5\pi}{6} g_{\pi\Xi^*\Xi^*}^2 \Lambda_\chi \epsilon_\pi^3 \\
& - \frac{1}{2} g_{\pi\Xi^*\Xi}^2 \Lambda_\chi \mathcal{F}(\epsilon_\pi, -\epsilon_{\Xi\Xi^*}, \mu) \\
& + \frac{3}{4} g_{\pi\Xi^*\Xi}^2 (\overline{\sigma}_\Xi - \sigma_\Xi)\Lambda_\chi\epsilon_\pi^2 \mathcal{J}(\epsilon_\pi, -\epsilon_{\Xi\Xi^*}, \mu) \\
& + \alpha_{\Xi^*}^{(4)} \Lambda_\chi \epsilon_\pi^4 \log \epsilon_\pi^2 + \beta_{\Xi^*}^{(4)} \Lambda_\chi \epsilon_\pi^4
\end{aligned}
$$

where the non-analytic functions correspond to loop diagrams in SU(2) heavy baryon χPT and are defined as so

$$\mathcal{F}(\epsilon_\pi, \epsilon, \mu) = -\epsilon\left(\epsilon^2 - \epsilon_\pi^2\right) R\left(\frac{\epsilon_\pi^2}{\epsilon^2}\right) - \frac{3}{2}\epsilon_\pi^2 \epsilon \log\left(\epsilon_\pi^2 \frac{\Lambda_\chi^2}{\mu^2}\right) - \epsilon^3 \log\left(4\frac{\epsilon^2}{\epsilon_\pi^2}\right), \tag{6.4}$$

$$\mathcal{J}(\epsilon_\pi, \epsilon, \mu) = \epsilon_\pi^2 \log\left(\epsilon_\pi^2 \frac{\Lambda_\chi^2}{\mu^2}\right) + 2\epsilon^2 \log\left(4\frac{\epsilon^2}{\epsilon_\pi^2}\right) + 2\epsilon^2 R\left(\frac{\epsilon_\pi^2}{\epsilon^2}\right), \tag{6.5}$$

$$R(x) = \begin{cases} \sqrt{1-x}\log\left(\frac{1-\sqrt{1-x}}{1+\sqrt{1-x}}\right), & 0 < x \leq 1 \\ 2\sqrt{x-1}\arctan\left(\sqrt{x-1}\right), & x > 1 \end{cases} \tag{6.6}$$

and we have defined the small parameters

$$\epsilon_\pi = \frac{m_\pi}{\Lambda_\chi} \qquad \epsilon_{\Xi\Xi^*} = \frac{M_{\Xi^*}^{(0)} - M_{\Xi}^{(0)}}{\Lambda_\chi}$$

with again the chiral scale/renormalization scale set at $\Lambda_\chi = 4\pi F_\pi$.

From glancing at the chiral expressions, we can immediately glean a few insights. First, in this EFT, baryons of the same strangeness will share many common LECs. Thus we see an immediate advantage of a chiral extrapolation over independent Taylor extrapolations of each: simultaneously fitting both mass formulae will result in more precise determinations of the LECs, which in turn will lead to more precise extrapolations to the physical point. Second, when we later include the axial charges in our analysis, we

$+1:$	Taylor $\mathcal{O}(m_\pi^2)$
$+1:$	χPT $\mathcal{O}(m_\pi^3)$
$+3:$	Taylor $\mathcal{O}(m_\pi^4) + \chi$PT $\{0,\, \mathcal{O}(m_\pi^3),\, \mathcal{O}(m_\pi^4)\}$
$5:$	chiral choices

$\times 5:$	chiral choices
$\times 2:$	$\{\mathcal{O}(a^2), \mathcal{O}(a^4)\}$
$\times 2:$	incl./excl. strange mistuning
$\times 2:$	natural priors or empirical priors
$40:$	total choices

Table 6.1: Models employed in this work.

see that our analysis will benefit twice: once from simultaneously fitting the two and three point functions, thereby improving our determination for the energies on each lattice [104], and later when performing the extrapolation to the physical point. Finally, the LECs are manifestly dimensionless as written, other than the constant terms $M_\Xi^{(0)}$ and $M_{\Xi^*}^{(0)}$. Indeed, the only other dimensionful quantity in the expansion is the cutoff Λ_χ.

Results

We explore a range of models (summarized in Table 6.1) with the models weighted according to their Bayes factors and averaged per the procedure described in Appendix C. There are five choices for the chiral expansion. We begin by considering a pure Taylor extrapolation to leading order (LO), i.e. $\mathcal{O}(m_\pi^2)$. Next we consider extensions of the LO fit to next-to-leading-order (NLO), i.e. χPT $\mathcal{O}(m_\pi^3)$ terms. At N^{2}LO, should we choose to include terms of this order, we consider either a pure Taylor term with or without the inclusion of χPT terms up to $\mathcal{O}(m_\pi^4)$. Regardless of the pion mass extrapolation, we assume the observables have common LECs per the chiral expression above. Fig. 6.3 explores the impact of these different models.

Next we explore corrections specific to the lattice, starting with lattice discretization corrections up to $\mathcal{O}(a^4)$. We also explore the impact of our simulated strange quark mass being slightly mistuned from the physical value.

The priors for the axial charges are set from either experiment or prior lattice calculations [96] but with appreciable (20%) width. The remaining dimensionless LECs are independently priored per the Gaussians $\mathcal{N}(0, 2^2)$ as is commensurate with "naturalness" expectations. The dimensionful constant terms $M_\Xi^{(0)}$ and $M_{\Xi^*}^{(0)}$ are the exception here and are priored at the physical value of $M_\Xi^{(0)}$ with a 20% width. We have labeled these the *natural priors*. We have also explored an alternative set of priors derived from the empirical Bayes method (see Appendix C).

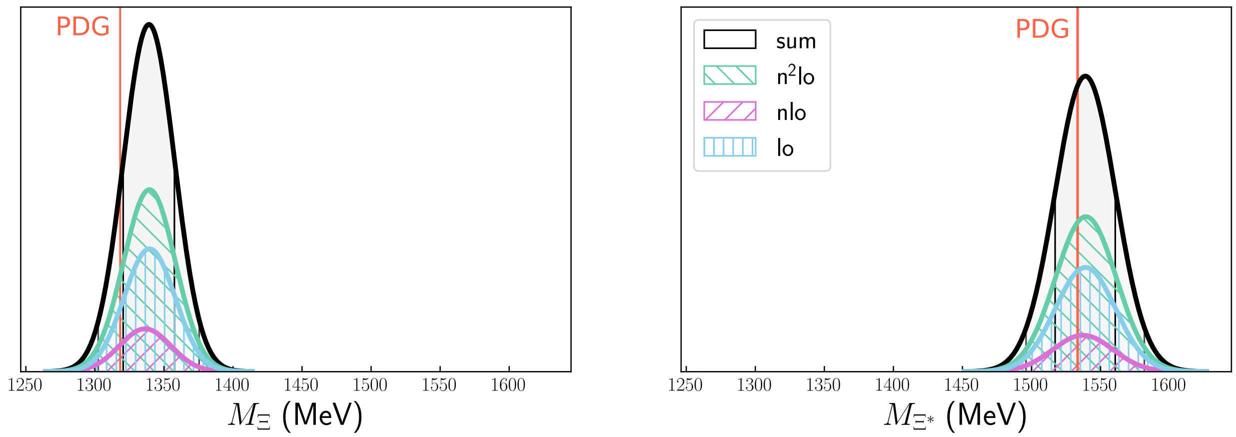

Figure 6.3: Truncation of the chiral expansion to different orders in the pion mass. We have adopted a "data-driven" analysis, i.e. we give no *a priori* weight to any of the different chiral models. Although the LO fit only comprises 1/5 of the total models used in this analysis (see Table 6.1), they still contribute more to the model average than the 2/5 of models that truncate at NLO instead. Further, the LO fits contribute almost as much as 2/5 of models that include N^{2}LO terms. The vertical red band is the Particle Data Group average [72]. Figure from [93].

After model averaging, we report the masses to be

$$M_\Xi = 1339(17)^{\mathrm{s}}(02)^{\chi}(05)^{a}(00)^{\mathrm{phys}}(01)^{\mathrm{M}}\ \mathrm{MeV} \qquad = 1339(18)\ \mathrm{MeV} \tag{6.7}$$

$$M_{\Xi^*} = 1542(20)^{\mathrm{s}}(03)^{\chi}(06)^{a}(00)^{\mathrm{phys}}(03)^{\mathrm{M}}\ \mathrm{MeV} \qquad = 1542(21)\ \mathrm{MeV} \tag{6.8}$$

Again we have separated the errors as induced by statistics (s), chirality (χ), lattice discretization (a), physical point input (phys), and model averaging (M). We have not yet calculated the finite volume corrections.

In this precursory work, we find that a LO Taylor fit describes the data approximately as well as an N^{2}LO χPT fit. Indeed, including the nonanalytic ϵ_π^3 term and chiral logarithms at NLO tanks the weight of the fit, while some cancellation between the NLO and N^{2}LO terms appears to yield an extrapolated value for the masses virtually identical to the LO results. So far the chiral terms introduced by heavy baryon χPT do not appear to be useful in guiding our extrapolation; however, knowing the relationship between the LECs contained in different observables might still prove helpful yet.

The nucleon sigma term

In this chapter, we present work on a calculation of the nucleon sigma term. For reference, it is defined as

$$\sigma_{\pi N} = \hat{m} \langle N|(\overline{u}u + \overline{d}d)|N\rangle \tag{7.1}$$

where $\hat{m} = (m_u + m_d)/2$. The nucleon sigma term $\sigma_{\pi N}$ measures the contribution to the nucleon mass by the explicit breaking of chiral symmetry. It also has implications in certain classes of dark matter searches, as we will explain shortly.

A callback to the linear-σ model

If the name sounds familiar, it's because we already encountered the sigma term back in Chapter 3 when we discussed the linear-σ model (Eq. 3.34). We assumed there was a particle like $\sigma = \overline{\psi}\psi$ (a Lorentz scalar), which after spontaneous symmetry breaking caused the nucleon to gain a mass term (gv). However, there still remained an interaction with $\tilde{\sigma} = \sigma - v$.

$$\mathcal{L} \supset -\overline{N}(gv + g\tilde{\sigma})N \tag{7.2}$$

If we now include a term $-\epsilon\sigma$ in the potential that explicitly breaks the symmetry (analogous to the explicit symmetry breaking by the quark masses), the potential (Eq. 3.35) becomes [25]

$$V(\pi, \sigma) = -\frac{\mu^2}{2}\left(\sigma^2 + \pi^2\right) + \frac{\lambda}{4}\left(\sigma^2 + \pi^2\right)^2 - \epsilon\sigma \tag{7.3}$$

with a new minimum at $\sigma \to v \approx v_0 + \epsilon/(2\lambda v_0)$ and $\pi \to 0$ where $v_0 = \mu/\sqrt{\lambda}$ was the original minimum. Notably, the pion mass is now non-zero,

$$m_\pi^2 \approx \left.\frac{\partial^2 V}{\partial \sigma^2}\right|_{(\sigma,\pi)\to(v,0)} = \frac{\epsilon}{v_0}\,. \tag{7.4}$$

This is essentially a statement of the GMOR relation for the linear-σ model. Finally, we see that the nucleon mass term also picks up a small correction.

$$g v_0 \overline{N} N \to g \left(v_0 + \frac{\epsilon}{2\lambda v_0} \right) \overline{N} N \tag{7.5}$$

If we reinterpret σ as the light quarks $\overline{u}u + \overline{d}d$, we see that this correction describes the contribution to the nucleon mass from explicit chiral symmetry breaking, which is exactly what $\sigma_{\pi N}$ is meant to measure. In fact, this expression suggests that at leading order $\sigma_{\pi N} \sim m_\pi^2$, a prediction also supported by chiral perturbation theory.

Relevance to dark matter searches

Among the simplest extensions to the Standard Model is the so-called minimal supersymmetric Standard Model (MSSM), which in the process of solving the Higgs hierarchy problem [105], could also explain the abundance of dark matter in the universe by way of weakly interacting massive particles. Specifically, the lightest supersymmetric particle, the neutralino χ, would be the dark matter candidate. The MSSM Lagrangian describes the interaction of this particle with nucleons through the terms [106]

$$\begin{aligned} \mathcal{L}_{\text{MSSM}} \supset & \alpha_{1f} \left(\overline{\chi} \gamma_\mu \gamma^5 \chi \right) \left(\overline{q}_f \gamma^\mu q_f \right) + \alpha_{2f} \left(\overline{\chi} \gamma_\mu \gamma^5 \chi \right) \left(\overline{q}_f \gamma^\mu \gamma^5 q_f \right) + \alpha_{3f} \left(\overline{\chi} \chi \right) \left(\overline{q}_f q_f \right) \\ & + \alpha_{4f} \left(\overline{\chi} \gamma^5 \chi \right) \left(\overline{q}_f \gamma^5 q_f \right) + \alpha_{5f} \left(\overline{\chi} \chi \right) \left(\overline{q}_f \gamma^5 q_f \right) + \alpha_{6f} \left(\overline{\chi} \gamma^5 \chi \right) \left(\overline{q}_f q_f \right) \end{aligned} \tag{7.6}$$

which are summed over the quark flavors. The terms can be classified as velocity-independent (α_{2f}, α_{3f} coefficients) and velocity-dependent (the rest). For direct dark matter searches like the LUX-ZEPLIN experiment [107], these terms are suppressed by a factor of $(v/c)^2 \sim 10^{-8}$, with v roughly the relative speed between the Earth and the Sun, and are therefore largely irrelevant. (For indirect searches like Super-Kamiokande [108], however, these velocity-dependent terms are more important).

Of the two velocity-independent terms, one is spin-dependent (α_{2f}) and the other spin-independent (α_{3f}). Let us focus on the spin-independent term. The cross section is given by [109]

$$\sigma_{\text{SI}} = \frac{4 m_r^2}{\pi} \left[Z f_p + (A - Z) f_n \right]^2 . \tag{7.7}$$

with A the mass number, Z the proton number, and m_r the neutralino-nucleon reduced mass. Buried in the definitions of f_p and f_n lies the dependence on the *flavor* sigma terms.

$$\frac{f_N}{M_N} = \sum_{f=u,d,s} f_{T_f}^{(N)} \frac{\alpha_{3f}}{m_f} + \frac{2}{27} f_{TG}^{(N)} \sum_{q=c,b,t} \frac{\alpha_{3f}}{m_f} \tag{7.8}$$

where $N = p, n$ and

$$m_N f_{T_f}^{(N)} = \langle N | m_f \overline{q}_f q_f | N \rangle \tag{7.9}$$

$$f_{TG}^{(N)} = 1 - \sum_{q=u,d,s} f_{T_f}^{(N)} . \tag{7.10}$$

The importance of the sigma terms here shouldn't be understated—the nucleon sigma term is currently the largest source of uncertainty when calculating the spin-independent neutralino-nucleon cross section; the authors of said uncertainty analysis literally plead for a campaign to better determine the sigma term [109].

Measuring $\sigma_{\pi N}$ via the Feynman-Hellman theorem

There are two techniques one can employ on the lattice to calculate the sigma term. First there is the direct method. Notice that Eq. 7.1 is just a matrix element. We can calculate it on the lattice by having a nucleon at the source and sink and then inserting a quark current in the middle. In principle this is straightforward, but it does suffer disadvantages; in particular, this requires fitting a baryonic 3-point function and dealing with all the ensuing messiness.

Alternatively, one can relate the sigma term to the nucleon mass via the Feynman-Hellmann theorem [115, 116], which means one fewer thing to generate on the lattice. The theorem states that given a Hermitian operator H depending on a real parameter λ with normalized eigenvectors $|\psi(\lambda)\rangle$ and eigenvalues $E(\lambda)$,

$$\left\langle \psi(\lambda) \middle| \frac{\partial}{\partial \lambda} H(\lambda) \middle| \psi(\lambda) \right\rangle = \frac{\partial E}{\partial \lambda} . \tag{7.11}$$

Let's apply this theorem to the nucleon. In particular, we know that the QCD Hamiltonian has a term like

$$\begin{aligned} \mathcal{H}_{\text{QCD}} &\supset m_u \overline{u} u + m_d \overline{d} d \\ &= \hat{m}(\overline{u} u + \overline{d} d) + \frac{1}{2} \delta_m (\overline{u} u - \overline{d} d) \end{aligned} \tag{7.12}$$

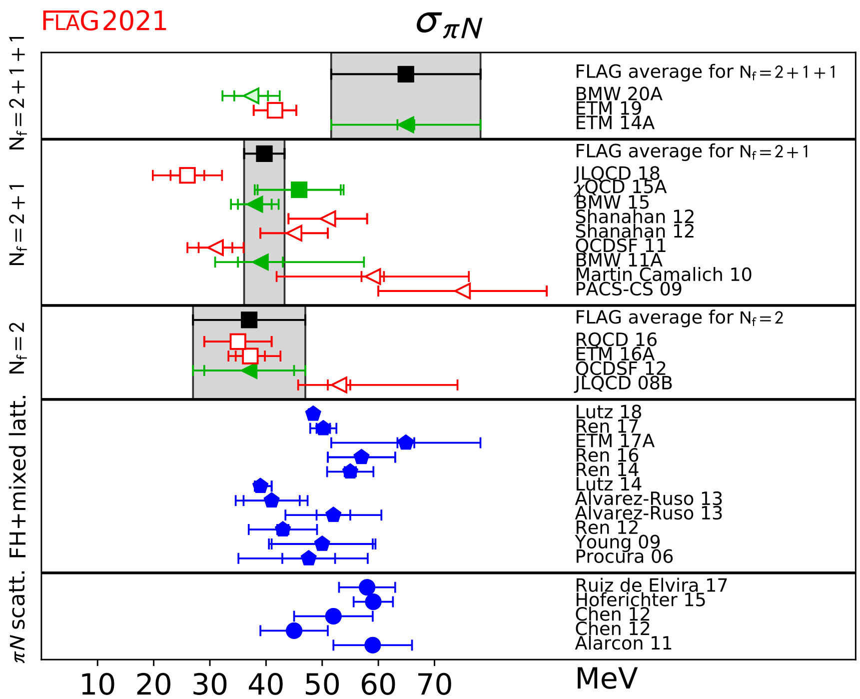

Figure 7.1: Estimates of $\sigma_{\pi N}$ from the lattice and phenomenology. The phenomenological results are denoted by the blue circles; the lattice results are in green and red, with the green values (QCDSF 12 [110], χQCD 15A [111], BMW 15 [112], BMW 11A [112], ETM 14A [113]) passing the FLAG criteria for being "reasonably consistent". In addition, Gupta et al. [114] have a recent result near the center of ETM 14A but with tighter error bars. In summary, most lattice calculations are around ~ 40 MeV, whereas most phenomenological results are around ~ 55 MeV. Figure from FLAG [73].

where we have defined $\hat{m} = (m_u + m_d)/2$ and $\delta_m = m_d - m_u$. With normalized eigenstates $|N\rangle$ and eigenvalues M_N, we find that

$$\left\langle N \middle| \frac{\partial}{\partial \hat{m}} \left[\hat{m} \left(\overline{u}u + \overline{d}d \right) \right] \middle| N \right\rangle = \frac{\partial M_N}{\partial \hat{m}} . \tag{7.13}$$

Comparing this result with Eq. 7.1 yields the desired result.

$$\sigma_{\pi N} = \hat{m} \frac{\partial M_N}{\partial \hat{m}} \tag{7.14}$$

However, this technique isn't without tradeoffs. Although now the sigma term can be calculated using only the nucleon correlator, the quoted result will be dependent on the *derivative* of the nucleon mass fit. It is not just sufficient that our different fit models converge to the same value at the physical point; they must approach the physical point at the same rate.

Finagling an expression for the sigma term

Recasting the nucleon mass derivative into something more manageable

Although we could, in principle, use Eq. 7.14 to determine the nucleon sigma term, it is not a convenient expression for calculations on the lattice. Instead of taking a derivative with respect to $\hat{m}$, we would prefer to take a derivative with respect m_π or (better yet) $\epsilon_\pi = m_\pi/\Lambda_\chi$, as these are the data we have readily available.

As a starting point, we can of course write

$$\hat{m}\frac{\partial M_N}{\partial \hat{m}} = \hat{m}\frac{\partial m_\pi^2}{\partial \hat{m}}\frac{\partial M_N}{\partial m_\pi^2} \,. \tag{7.15}$$

To NLO, [1] the pion mass can be perturbatively related to $\hat{m}$ by

$$m_\pi^2 \approx 2B\hat{m}\left(1+\delta_{m^2}\right) \qquad \Longrightarrow \qquad \hat{m} \approx \frac{m_\pi^2}{2B}\left(1-\delta_{m^2}\right) \tag{7.16}$$

where δ_{m^2} is the NLO correction. Therefore to NLO

$$\begin{aligned}
\hat{m}\frac{\partial m_\pi^2}{\partial \hat{m}} &\approx \frac{m_\pi^2}{2B}\left(1-\delta_{m^2}\right)\frac{\partial}{\partial \hat{m}}\Big[2B\hat{m}\left(1+\delta_{m^2}\right)\Big] \\
&= m_\pi^2\Big(1-\delta_{m^2}\Big)\Big(1+\delta_{m^2}+\hat{m}\frac{\partial \delta_{m^2}}{\partial \hat{m}}\Big) \\
&\approx m_\pi^2\left(1+\hat{m}\frac{\partial \delta_{m^2}}{\partial \hat{m}}\right)
\end{aligned} \tag{7.17}$$

At this point we need the expression for δ_{m^2} [117],

$$\delta_{m^2} = \frac{1}{2}\frac{2B\hat{m}}{(4\pi F)^2}\left[\log\left(\frac{2B\hat{m}}{\mu^2}\right)+4\bar{l}_3^r(\mu)\right] \,, \tag{7.18}$$

[1] Unfortunately the literature defines "LO" differently for meson χPT ($\mathcal{O}(1)$) versus baryon χPT ($\mathcal{O}(\epsilon^2)$). We will stick with the literature here. If an expression mixes baryon and meson χPT expressions (e.g., M_N/F_π), we will use the baryon power-counting scheme. We will refer to the $\mathcal{O}(1)$ contributions in baryon χPT as LLO ("less-than-leading order").

which has partial derivative

$$\begin{aligned}
\frac{\partial \delta_{m^2}}{\partial \hat{m}} &= \frac{1}{2}\frac{2B}{(4\pi F)^2}\left[\log\left(\frac{2B\hat{m}}{\mu^2}\right) + 1 + 4\bar{l}_3^r(\mu)\right] \\
&\approx \frac{1}{2}\frac{2B}{(4\pi F)^2}\left[\log\left(\frac{2B\hat{m}}{\mu^2}\right) + 1 - \left(\bar{l}_3 + \log\frac{m_\pi^2}{\mu^2}\right)\right] \\
&\approx \frac{1}{2}\frac{2B}{(4\pi F)^2}\left(1 - \bar{l}_3\right) \\
&\approx \frac{1}{2}\frac{\epsilon_\pi^2}{\hat{m}}\left(1 - \bar{l}_3\right)
\end{aligned} \tag{7.19}$$

where in the second line we have related the renormalized LEC $\bar{l}_3^r(\mu)$ to the barred LEC $\bar{l}_3$ by [118]

$$\bar{l}_i^r = \frac{\gamma_i}{2}\left[\bar{l}_i + \log\left(\frac{m_\pi^2}{\mu^2}\right)\right] \qquad \text{where } \gamma_3 = -\frac{1}{2} \text{ and } \gamma_4 = 2\,. \tag{7.20}$$

In the third line we have combined the logarithms by rounding to NLO, and in the fourth line we have rounded to NLO again after approximating $2B\hat{m} \approx m_\pi^2$ and $F \approx F_\pi$.

Putting everything together, we get an expression for the nucleon sigma term to NLO that doesn't explicitly depend on $\hat{m}$,

$$\sigma_{\pi N} \approx m_\pi^2\left[1 + \frac{1}{2}\epsilon_\pi^2\left(1 - \bar{l}_3\right)\right]\frac{\partial M_N}{\partial m_\pi^2}\,. \tag{7.21}$$

Next we would like to rewrite the derivative with respect to ϵ_π instead of m_π^2. Rewriting the derivative as

$$\frac{\partial M_N}{\partial m_\pi^2} = \frac{1}{2\epsilon_\pi}\frac{\partial \epsilon_\pi^2}{\partial m_\pi^2}\frac{\partial M_N}{\partial \epsilon_\pi}\,, \tag{7.22}$$

we find that we must calculate

$$\frac{\partial \epsilon_\pi^2}{\partial m_\pi^2} = \frac{1}{(4\pi F_\pi^2)}\left[1 - 2\frac{m_\pi^2}{F_\pi}\frac{\partial F_\pi}{\partial m_\pi^2}\right]\,. \tag{7.23}$$

At this point it's evident that we also require the partial derivative $\partial F_\pi / \partial m_\pi^2$. The chiral expression for F_π to NLO is [117]

$$F_\pi \approx F(1 + \delta_F) \quad \implies \quad F \approx F_\pi(1 - \delta_F) \tag{7.24}$$

where δ_F is the NLO piece,

$$\delta_F = \frac{2B\hat{m}}{(4\pi F)^2}\left[-\log\left(\frac{2B\hat{m}}{\mu^2}\right) + \bar{l}_4^r(\mu)\right]. \tag{7.25}$$

Now we write simplify the derivative

$$\begin{aligned}
\frac{\partial F_\pi}{\partial m_\pi^2} &\approx F\frac{\partial \delta_F}{\partial m_\pi^2} \\
&\approx F\frac{\partial}{\partial m_\pi^2}\left\{\frac{m_\pi^2}{(4\pi F)^2}\left[-\log\left(\frac{m_\pi^2}{\mu^2}\right) + \bar{l}_4^r(\mu)\right]\right\} \\
&= F\frac{1}{(4\pi F)^2}\left[-1 - \log\left(\frac{m_\pi^2}{\mu^2}\right) + \bar{l}_4^r(\mu)\right] \\
&= F\frac{1}{(4\pi F)^2}\left[-1 - \log\left(\frac{m_\pi^2}{\mu^2}\right) + \left(\bar{l}_4 + \log\left(\frac{m_\pi^2}{\mu^2}\right)\right)\right] \\
&= F\frac{1}{(4\pi F)^2}\left(-1 + \bar{l}_4\right) \\
&\approx F_\pi\frac{\epsilon_\pi^2}{m_\pi^2}\left(-1 + \bar{l}_4\right).
\end{aligned} \tag{7.26}$$

which means

$$\begin{aligned}
\frac{\partial \epsilon_\pi^2}{\partial m_\pi^2} &= \frac{1}{(4\pi F_\pi^2)}\left[1 - 2\frac{m_\pi^2}{F_\pi}\frac{\partial F_\pi}{\partial m_\pi^2}\right] \\
&\approx \frac{1}{(4\pi F_\pi^2)}\left[1 + 2\epsilon_\pi^2\left(1 - \bar{l}_4\right)\right]
\end{aligned} \tag{7.27}$$

Combining everything yields the desired result

$$\begin{aligned}
\sigma_{\pi N} &\approx \frac{1}{2}\epsilon_\pi\left[1 + \frac{1}{2}\epsilon_\pi^2\left(1 - \bar{l}_3\right)\right]\left[1 + 2\epsilon_\pi^2\left(1 - \bar{l}_4\right)\right]\frac{\partial M_N}{\partial \epsilon_\pi} \\
&\approx \frac{1}{2}\epsilon_\pi\left[1 + \epsilon_\pi^2\left(\frac{5}{2} - \frac{1}{2}\bar{l}_3 - 2\bar{l}_4\right)\right]\frac{\partial M_N}{\partial \epsilon_\pi}.
\end{aligned} \tag{7.28}$$

Accounting for the Gasser-Leutwyler LECs

Inspecting Eq. 7.28, we find that the only dimensionful quantity is M_N. This is not technically an issue for us since we have completed our scale setting (Chapter 4). However, we would prefer to avoid introducing a scale as much as possible, since introducing a scale correlates data across ensembles via that scale (ensembles are otherwise uncorrelated).

Moreover, we find that at NLO we require determinations of $\bar{l}_3$ and $\bar{l}_4$, which are the Gasser-Leutwyler LECs defined at a different scale μ (see Eq. (7.20)). These LECs are compiled in FLAG, but they are also accessible with our lattice data; in fact, it would behoove us to calculate these, too, for reasons that will be evident shortly.

Observe we can expand the derivative in Eq. 7.28 as so

$$\frac{\partial M_N}{\partial \epsilon_\pi} = \Lambda_\chi \frac{\partial (M_N/\Lambda_\chi)}{\partial \epsilon_\pi} + \frac{M_N}{\Lambda_\chi}\frac{\partial \Lambda_\chi}{\partial \epsilon_\pi}\,, \tag{7.29}$$

resulting in the following expression for the sigma term,

$$\sigma_{\pi N} \approx \frac{1}{2}\epsilon_\pi \left[1 + \epsilon_\pi^2 \left(\frac{5}{2} - \frac{1}{2}\bar{l}_3 - 2\bar{l}_4\right)\right] \left[\Lambda_\chi \frac{\partial (M_N/\Lambda_\chi)}{\partial \epsilon_\pi} + \frac{M_N}{\Lambda_\chi}\frac{\partial \Lambda_\chi}{\partial \epsilon_\pi}\right]\,. \tag{7.30}$$

Recall that we set $\Lambda_\chi = 4\pi F_\pi$. Clearly this form for the sigma term requires us to additionally fit F_π. One might object to this strategy: although we removed the scale setting requirement for M_N, now we have a scale setting requirement for F_π!

However, given the choice between a difficult fit of M_N and a difficult fit of F_π, the latter is preferred. Fitting F_π requires only SU(2) (meson) χPT, which has been rather successful; fitting M_N, in contrast, requires SU(2) heavy baryon χPT, which converges more slowly.

Furthermore, as we will see when we discuss the results of this analysis, splitting the terms this way has interesting consequences on where the bulk of the contribution to the sigma term comes from (to preview: not the nucleon part!).

Project goals

To summarize, we can determine $\sigma_{\pi N}$ through the following procedure:

1. Fit M_N/Λ_χ in lattice units (since we have lattice data for both of these observables).

2. Fit F_π in physical units (using our scale setting results).

3. Extract the $\bar{l}_4$ LECs from the F_π fit.

4. Calculate the derivatives.

5. Combine all results (plus the FLAG result for $\bar{l}_3$) to determine $\sigma_{\pi N}$ using Eq. (7.28).

Note that in this preliminary work we do not determine $\bar{l}_3$, as this requires us to fit m_π also. However, our collaboration plans to include the m_π fit in future work.

Extrapolation functions

Fit function for F_π

Again, we separate our fit function as $F_\pi^{\text{fit}} = F_\pi^{\text{chiral}} + F_\pi^{\text{disc}}$. The SU(2) χPT expression for F_π to $\mathcal{O}(\epsilon^4)$ is given by

$$F_\pi^{\text{chiral}} \approx F_0 \left[1 + \epsilon_\pi^2 \left(-\log \epsilon_\pi^2 + \bar{l}_4^r\right) + \epsilon_\pi^4 \left(\frac{5}{4} \log^2 \epsilon^2 + \alpha_F^{(4)} \log \epsilon_\pi^2 + \beta_F^{(4)}\right)\right] \tag{7.31}$$

Notice that the expression recorded here is much simpler than the one from Chapter 5—we are employing SU(2) χPT this time, not SU(3) χPT . For now we do not include finite volume corrections (as we haven't yet worked these out for the baryons), so F_π^{disc} only contains terms that are a Taylor expansion in the lattice spacing.

We will need the reciprocal of this expression soon for M_N/Λ_χ, so we note it now.

$$\begin{aligned} \frac{1}{F_\pi} \approx \frac{1}{F_0}\Big[&1 - \epsilon_\pi^2 \left(-\log \epsilon_\pi^2 + \bar{l}_4^r\right) \\ &+ \epsilon_\pi^4 \left(\left(\bar{l}_4^r\right)^2 - \beta_F^{(4)} - \left(\alpha_F^{(4)} + 2\bar{l}_4^r\right) \log \epsilon_\pi^2 - \frac{1}{4}\left(\log \epsilon_\pi^2\right)^2\right)\Big] . \end{aligned} \tag{7.32}$$

Fit function for M_N

We first note the SU(2) heavy baryon χPT expression for M_N [119],

$$\begin{aligned} M_N^{\text{chiral}} = \;& M_N^{(0)} && \text{(LLO)} \\ &+ \beta_N^{(2)} \Lambda_\chi \epsilon_\pi^2 && \text{(LO)} \\ &- \frac{3\pi}{2} g_{\pi NN}^2 \Lambda_\chi \epsilon_\pi^3 - \frac{4}{3} g_{\pi N\Delta}^2 \Lambda_\chi \mathcal{F}(\epsilon_\pi, \epsilon_{N\Delta}, \mu) && \text{(NLO)} \\ &+ \gamma_N^{(4)} \Lambda_\chi \epsilon_\pi^2 \mathcal{J}(\epsilon_\pi, \epsilon_{N\Delta}, \mu) && \text{(N}^2\text{LO)} \\ &\quad + \alpha_N^{(4)} \Lambda_\chi \epsilon_\pi^4 \log \epsilon_\pi^2 + \beta_N^{(4)} \Lambda_\chi \epsilon_\pi^4 . \end{aligned} \tag{7.33}$$

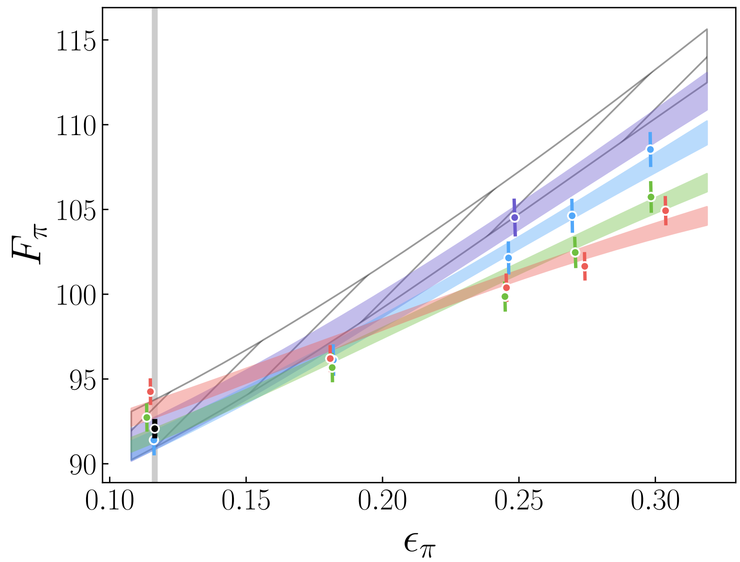

Figure 7.2: Pion mass dependence of F_π. The red, green, blue, and purple bands denote a lattice spacing of roughly $0.15, 0.12, 0.09, 0.06$ fm, respectively. The hashed band is the extrapolation in the continuum ($a = 0$) limit. Note the non-trivial lattice spacing dependence, as evident by the crossing of the different pion spacings near $\epsilon_\pi \approx 0.18$.

Charge	Value	Source
$g_{\pi NN}$	1.27	CalLat
$g_{\pi N\Delta}$	-1.48	Expt.
$g_{\pi\Delta\Delta}$	-2.20	SU(3)

Table 7.1: Predicted/measured values of the axial charges per [120, 96]. The SU(3) predictions are obtained by three-flavor heavy baryon χPT as outlined in [121].

We recall that the non-analytic functions are defined as so

$$\mathcal{F}(\epsilon_\pi, \epsilon_\Delta, \mu) = -\epsilon_\Delta \left(\epsilon_\Delta^2 - \epsilon_\pi^2\right) R\left(\frac{\epsilon_\pi^2}{\epsilon_\Delta^2}\right) - \frac{3}{2}\epsilon_\pi^2 \epsilon_\Delta \log\left(\epsilon_\pi^2 \frac{\Lambda_\chi^2}{\mu^2}\right) - \epsilon_\Delta^3 \log\left(4\frac{\epsilon_\Delta^2}{\epsilon_\pi^2}\right), \tag{7.34}$$

$$\mathcal{J}(\epsilon_\pi, \epsilon_\Delta, \mu) = \epsilon_\pi^2 \log\left(\epsilon_\pi^2 \frac{\Lambda_\chi^2}{\mu^2}\right) + 2\epsilon_\Delta^2 \log\left(4\frac{\epsilon_\Delta^2}{\epsilon_\pi^2}\right) + 2\epsilon_\Delta^2 R\left(\frac{\epsilon_\pi^2}{\epsilon_\Delta^2}\right), \tag{7.35}$$

$$R(x) = \begin{cases} \sqrt{1-x}\log\left(\frac{1-\sqrt{1-x}}{1+\sqrt{1-x}}\right), & 0 < x \leq 1 \\ 2\sqrt{x-1}\arctan\left(\sqrt{x-1}\right), & x > 1 \end{cases}. \tag{7.36}$$

We have left the renormalization scale dependence explicit here. These terms depend on the masses of the nucleon and the Δ resonance. For M_N, we use the lattice value; for M_Δ, we use the PDG value. The estimates for the axial charges are listed in Table 7.1.

As written, it is clear that the factors of Λ_χ will cancel in all but the LLO term when multiplying Eq. (7.33) by Eq. (7.32).

$$\begin{aligned}
\left(\frac{M_N}{\Lambda_\chi}\right)^{\text{chiral}} = & \overbrace{\frac{M_N^{(0)}}{\Lambda_\chi}}^{\text{starts at LLO}} && \text{(LLO)} \\
& + \beta_N^{(2)} \epsilon_\pi^2 && \text{(LO)} \\
& - \frac{3\pi}{2} g_{\pi NN}^2 \epsilon_\pi^3 - \frac{4}{3} g_{\pi N\Delta}^2 \mathcal{F}(\epsilon_\pi, \epsilon_{N\Delta}, \mu) && \text{(NLO)} \\
& + \gamma_N^{(4)} \epsilon_\pi^2 \mathcal{J}(\epsilon_\pi, \epsilon_{N\Delta}, \mu) && \text{(N}^2\text{LO)} \\
& \quad + \alpha_N^{(4)} \epsilon_\pi^4 \log \epsilon_\pi^2 + \beta_p^{(4)} \epsilon_\pi^4
\end{aligned} \tag{7.37}$$

For a Taylor-type fit, we can drop the non-analytic functions as well as the $\mathcal{O}(\epsilon^3)$ term (which is not analytic in ϵ^2). Additionally we treat the LLO term as a constant. Otherwise we should expand the LLO term, whose contributions are in green.

$$\begin{aligned}
\left(\frac{M_N}{\Lambda_\chi}\right)^{\text{chiral}} = & c_0 && \text{(LLO)} \\
& + \left(\beta_N^{(2)} - c_0 \bar{\ell}_4^r\right) \epsilon_\pi^2 + c_0 \epsilon_\pi^2 \log \epsilon_\pi^2 && \text{(LO)} \\
& - \frac{3\pi}{2} g_{\pi NN}^2 \epsilon_\pi^3 - \frac{4}{3} g_{\pi N\Delta}^2 \mathcal{F}(\epsilon_\pi, \epsilon_{N\Delta}, \mu) && \text{(NLO)} \\
& + \left(\beta_N^{(4)} + c_0 \left(\bar{\ell}_4^r\right)^2 - c_0 \beta_F^{(4)}\right) \epsilon_\pi^4 + \gamma_N^{(4)} \epsilon_\pi^2 \mathcal{J}(\epsilon_\pi, \epsilon_{N\Delta}, \mu) && \text{(N}^2\text{LO)} \\
& \quad - \frac{1}{4} c_0 \epsilon_\pi^4 \left(\log \epsilon^2\right)^2 + \left(\alpha_N^{(4)} - c_0 \alpha_F^{(4)} - 2 c_0 \bar{\ell}_4^r\right) \epsilon_\pi^4 \log \epsilon_\pi^2
\end{aligned} \tag{7.38}$$

We note that unless we simultaneously fit M_N/Λ_χ with F_π, we will not be able to disentangle some of these LECs, for example c_0, $\bar{l}_4^r$, and $\beta_N^{(2)}$. In this case we can instead fit $\tilde{\beta}_p^{(2)} = (c_0 \bar{l}_4^r + \beta_p^{(2)})$. If we combine the other LECs in this manner, then the only functional differences between the two equations (ignoring the LLO term in Eq. (7.37)) are the extra $\log \epsilon_\pi^2$ term at LO and $(\log \epsilon_\pi^2)^2$ term at N^{2}LO.

As a final caveat regarding the chiral expression, we comment that the $\mathcal{J}$ term at N^{2}LO probably cannot be resolved without simultaneously fitting the Δ, which presents its own problems. For now we drop this term from our fits.

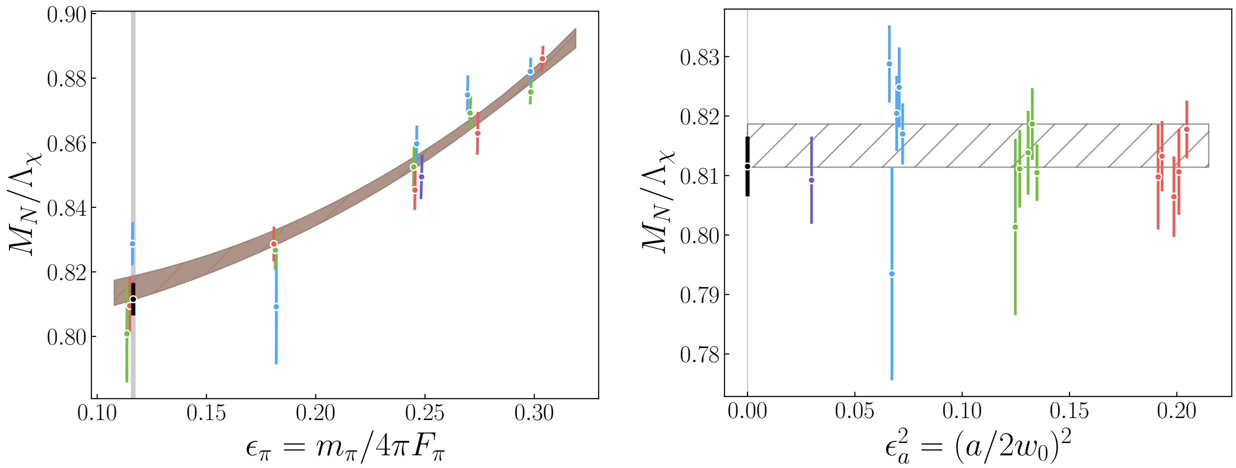

Figure 7.3: Example extrapolation as a function of the pion mass (left) and lattice spacing (right). Notice that, unlike the F_π extrapolation, the fit of M_N/Λ_χ has virtually no lattice spacing dependence.

Finally, the only discretization corrections we consider for now are counterterms in the lattice spacing starting at $\mathcal{O}(\epsilon^2)$. However, as is clear from Eq. 7.3, we could drop these terms; there is no appreciable lattice spacing dependence here.

Derivatives of fit functions

Once we have fit our extrapolation functions, we must take the derivative with respect to ϵ_π (while keeping track of the correlations for purposes of error propagation). The most straightforward way to calculate this derivative is by taking the derivative of Eq. (7.33), but we will separate out the M_N/Λ_χ and Λ_χ derivatives so we can estimate their individual contributions to $\sigma_{\pi N}$.

$$
\begin{aligned}
\epsilon_\pi \Lambda_\chi \frac{\partial (M_N/\Lambda_\chi)}{\partial \epsilon_\pi} = \epsilon_\pi \Lambda_\chi \Bigg\{ & \overbrace{-\frac{M_p^{(0)}}{\Lambda_\chi^2}\frac{\partial \Lambda_\chi}{\partial \epsilon_\pi}}^{\text{starts at LLO}} && \text{(LLO)} \\
& + 2\beta_p^{(2)}\epsilon_\pi && \text{(LO)} \\
& - \frac{9\pi}{2} g_{\pi pp}^2 \epsilon_\pi^2 - \frac{4}{3} g_{\pi p\Delta}^2 \partial_{\epsilon_\pi} \mathcal{F}(\epsilon_\pi, \epsilon_{p\Delta}) && \text{(NLO)} \\
& + \gamma_p^{(4)} \Big[2\epsilon_\pi \mathcal{J}(\epsilon_\pi, \epsilon_{p\Delta}) + \epsilon_\pi^2 \partial_{\epsilon_\pi} \mathcal{J}(\epsilon_\pi, \epsilon_{p\Delta}) \Big] && \text{(N}^2\text{LO)} \\
& \quad + \alpha_p^{(4)} \Big[4\epsilon_\pi^3 \log \epsilon_\pi^2 + 2\epsilon_\pi^3 \Big] + 4\beta_p^{(4)} \epsilon_\pi^3 \Bigg\}
\end{aligned}
\tag{7.39}
$$

The derivatives of the non-analytic functions are listed below.

$$\frac{\partial \mathcal{F}}{\partial \epsilon_\pi} = \frac{2\epsilon_\Delta^3}{\epsilon_\pi} - 3\epsilon_\Delta\epsilon_\pi \log\left(\epsilon_\pi^2\right) - 3\epsilon_\Delta\epsilon_\pi + \left(\frac{2\epsilon_\pi^3}{\epsilon_\Delta} - 2\epsilon_\Delta\epsilon_\pi\right) R'\left(\frac{\epsilon_\pi^2}{\epsilon_\Delta^2}\right) + 2\epsilon_\Delta\epsilon_\pi R\left(\frac{\epsilon_\pi^2}{\epsilon_\Delta^2}\right) \tag{7.40}$$

$$\frac{\partial \mathcal{J}}{\partial \epsilon_\pi} = -\frac{4\epsilon_\Delta^2}{\epsilon_\pi} + 4\epsilon_\pi R'\left(\frac{\epsilon_\pi^2}{\epsilon_\Delta^2}\right) + 2\epsilon_\pi \log\left(\epsilon_\pi^2\right) + 2\epsilon_\pi \tag{7.41}$$

$$R'(x) = \begin{cases} \frac{1}{x} - \frac{\log\left(\frac{1-\sqrt{1-x}}{\sqrt{1-x}+1}\right)}{2\sqrt{1-x}} & 0 < x < 1 \\ 2 & x = 1 \\ \frac{1}{x} + \frac{\tan^{-1}\left(\sqrt{x-1}\right)}{\sqrt{x-1}} & x > 1 \end{cases} \tag{7.42}$$

The Λ_χ derivative at LLO can be combined with the Λ_χ derivative in Eq. (7.30). Expanding to the first non-zero term, we have

$$\begin{aligned} \epsilon_\pi \left(\frac{M_N}{\Lambda_\chi} - \frac{M_p^{(0)}}{\Lambda_\chi}\right) \frac{\partial \Lambda_\chi}{\partial \epsilon_\pi} &\approx \epsilon_\pi \left(\beta_p^{(2)} \epsilon_\pi^2\right) \left(2\epsilon_\pi (\bar{l}_4 - 1)\Lambda_\chi\right) \qquad\qquad (7.43) \\ &= 2\beta_p^{(2)} (\bar{l}_4 - 1)\Lambda_\chi \epsilon_\pi^4 \,. \qquad\qquad (\mathrm{N^2LO}) \end{aligned}$$

Results

In this preliminary exploration for $\sigma_{\pi N}$, we consider a mere 4 models: Taylor terms to $\mathcal{O}(\epsilon^4)$ with either zero, LO, NLO, or N^{2}LO χPT corrections. The discretization errors are modeled at $\mathcal{O}(\epsilon^2)$ for the F_π fits, with the posterior for the discretization LECs compatible with zero for the M_N/Λ_χ fits. We omit higher order discretization counterterms as these tank the weights. These models are compared in Fig. 7.4. After averaging, we find

$$M_N = 951.5(5.4)^{\mathrm{s}}(1.7)^{\chi}(0.0)^{a}(5.8)^{\mathrm{phys}}(3.8)^{\mathrm{M}}\ \mathrm{MeV} \qquad = 951.5(9.0)\ \mathrm{MeV} \tag{7.44}$$

$$\sigma_{\pi N} = 47.6(1.8)^{\mathrm{s}}(1.7)^{\chi}(0.0)^{a}(0.6)^{\mathrm{phys}}(5.2)^{\mathrm{M}}\ \mathrm{MeV} \qquad = 47.6(5.9)\ \mathrm{MeV} \tag{7.45}$$

As previously hinted at, we can make an amusing observation if we split the sigma term in the following manner.

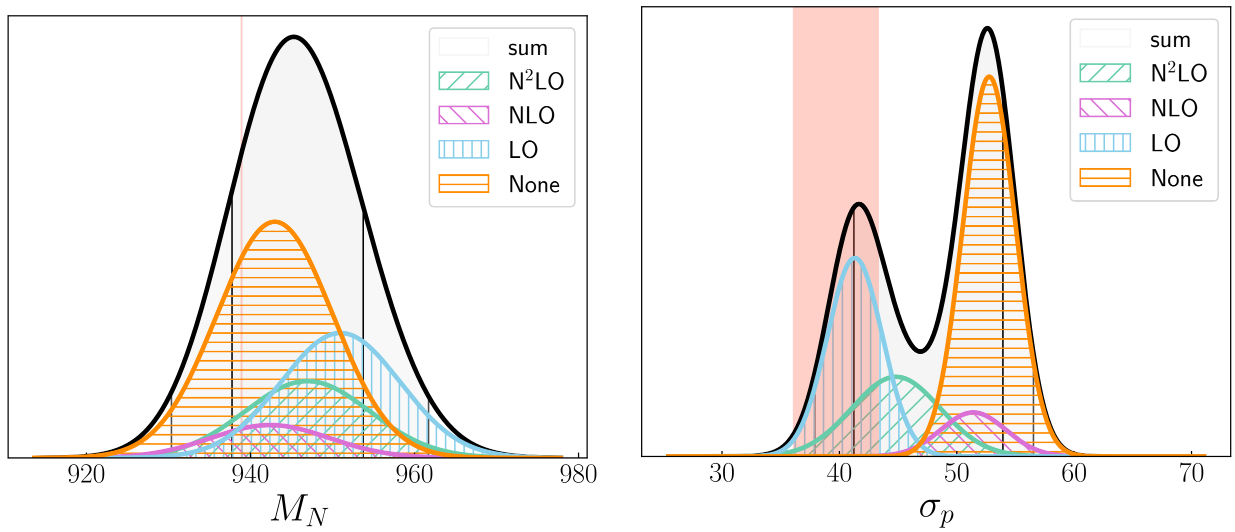

Figure 7.4: Histograms of $M_N = (M_N/\Lambda_\chi)\Lambda_\chi^{\text{phys}}$ and $\sigma_{N\pi}$. The result for M_N agrees with the PDG value (thin red band), while the histogram for $\sigma_{N\pi}$ must be interpreted more carefully. The red band on the right is the result from BMW 2020, a typical lattice determination of the sigma term which has been included for reference. We find that the distribution is multimodal, with the Taylor expansion contributing the most weight to the model average. However, we caution against giving too much credence to the Taylor fit: although we have priored our models equally here, we have *a priori* reason to believe the Taylor fit is misleading us. Specifically, we do not believe the Taylor model accurately captures the lattice spacing dependence for $\sigma_{\pi N}$, as we expect the contribution from Λ_χ to compete against the LLO contribution from M_N/Λ_χ, which is not possible if the LLO term is just a constant.

$$\sigma_{N\pi} = \frac{1}{2}\epsilon_\pi \left[1 + \epsilon_\pi^2\left(\frac{5}{2} - \frac{1}{2}\bar{\ell}_3 - 2\bar{\ell}_4\right) + \mathcal{O}\left(\epsilon_\pi^3\right)\right] \overbrace{\left[\Lambda_\chi^* \frac{\partial\left(M_N/\Lambda_\chi\right)}{\partial \epsilon_\pi} + \frac{M_N^*}{\Lambda_\chi^*}\frac{\partial \Lambda_\chi}{\partial \epsilon_\pi}\right]}^{\frac{\partial M_N}{\partial \epsilon_\pi}}$$

If we calculate each of these terms individually (including the $\epsilon_\pi/2$ prefactor), we find

$$\begin{aligned}
\frac{1}{2}\epsilon_\pi \Lambda_\chi^* \frac{\partial\left(M_N/\Lambda_\chi\right)}{\partial \epsilon_\pi} &= \frac{1}{2}\Lambda_\chi^*\left[\left(-2c_0\left(\bar{\ell}_4 - 1\right) + 2\beta_N^{(2)}\right)\epsilon_\pi^2 + \mathcal{O}\left(\epsilon_\pi^3\right)\right] \sim 10 \text{ MeV} \\
\frac{1}{2}\epsilon_\pi \frac{M_N^*}{\Lambda_\chi^*}\frac{\partial \Lambda_\chi}{\partial \epsilon_\pi} &= \frac{1}{2}M_N^*\left[2\left(\bar{\ell}_4 - 1\right)\epsilon_\pi^2 + \mathcal{O}\left(\epsilon_\pi^3\right)\right] \sim 40 \text{ MeV}
\end{aligned}$$

We make two important observations: (1) the bulk of the contribution to the sigma term comes from the fit of Λ_χ, not M_N/Λ_χ. (2) The determination of the sigma term is highly sensitive to the value of $\bar{l}_4$, as demonstrated in Fig. 7.5. A precise determination of F_π (from which we can extract $\bar{l}_4$) is therefore essential to better constrain our result for the sigma term.

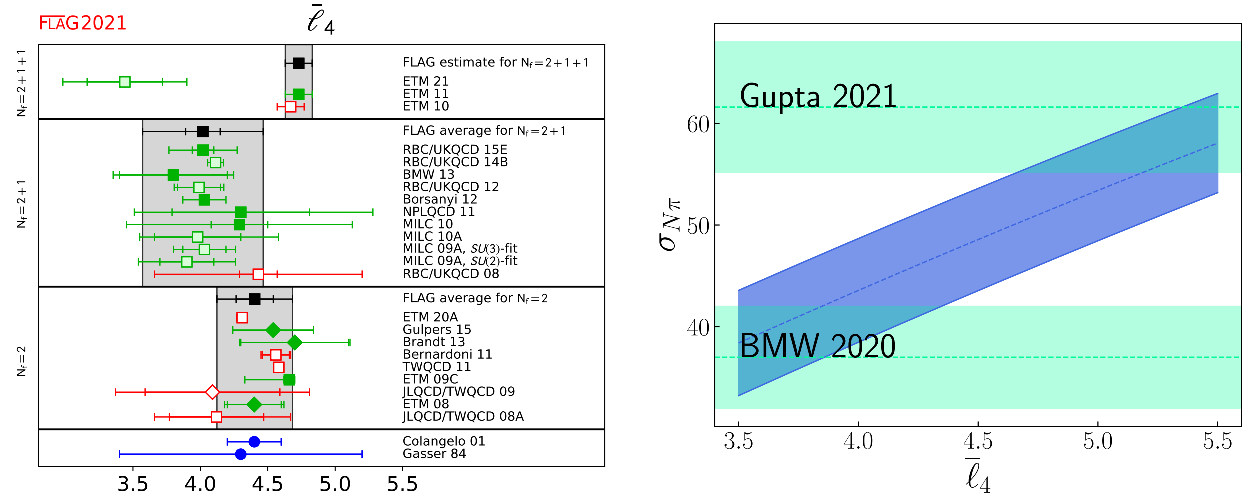

Figure 7.5: Left: FLAG average for $\bar{l}_4$, including results from RBC/UKQCD 15E [122], Gulpers [123], Brandt [124], BMW 13 [125], Borsanyi [126], NPLQCD 11 [127], MILC 10 [88], ETM 11 [128], ETM 09C [129], ETM 08 [130] (figure taken from [73]). Right: LO dependence of $\sigma_{\pi N}$ on $\bar{l}_4$ (blue band). Like $\sigma_{\pi N}$, there is a great deal of variation in measurements of $\bar{l}_4$. If $\bar{l}_4$ is on the smaller side, we get something close to a typical lattice calculation; if $\bar{l}_4$ is instead large, we get something closer to the phenomenological result. A precise fit of F_π is therefore integral to precisely determining $\sigma_{\pi N}$ using the strategy outlined in this chapter.

In future work, we plan to include a fit of m_π in our analysis so that we can determine $\bar{l}_3$. We will additionally fit M_N directly using our scale setting to be compared the technique presented here in which we instead fit M_N/Λ_χ and Λ_χ.

PROPERTIES OF THE GAMMA MATRICES AND PROJECTION OPERATORS

Gamma matrices

Recall that the gamma matrices generate a representation of the Clifford algebra $C\ell_{1,3}(\mathbb{R})$ and are defined by the anticommutative relation

$$\{\gamma^\mu, \gamma^\nu\} = 2\eta^{\mu,\nu} \, . \tag{A.1}$$

It is useful to also define the "fifth" gamma matrix,

$$\gamma^5 = i\gamma^0\gamma^1\gamma^2\gamma^3 \, , \tag{A.2}$$

which can be used to project out the different chiral components of a Dirac bispinor.

In the Weyl/chiral basis, these matrices take the form

$$\gamma^0 \overset{\text{Weyl}}{=} \begin{bmatrix} 0 & \mathbb{1} \\ \mathbb{1} & 0 \end{bmatrix} \qquad \gamma^k \overset{\text{Weyl}}{=} \begin{bmatrix} 0 & \sigma_k \\ -\sigma_k & 0 \end{bmatrix} \qquad \gamma^5 \overset{\text{Weyl}}{=} \begin{bmatrix} -\mathbb{1} & 0 \\ 0 & \mathbb{1} \end{bmatrix} \, . \tag{A.3}$$

These matrices have the following useful properties, independent of basis:

$$\left(\gamma^5\right)^\dagger = \gamma^5 \qquad \text{(Hermitian)} \tag{A.4}$$

$$\left(\gamma^5\right)^2 = \mathbb{1} \qquad \text{(Involutory)} \tag{A.5}$$

$$\left\{\gamma^5, \gamma^\mu\right\} = 0 \qquad \text{(Anticommutative with } \gamma^\mu\text{)} \tag{A.6}$$

Projection operators

Recall that we define the projection operators as

$$P_L = \frac{1}{2}\left(\mathbb{1} - \gamma^5\right) \qquad P_R = \frac{1}{2}\left(\mathbb{1} + \gamma^5\right) \, . \tag{A.7}$$

The projection operators have the following useful properties:

$$P_L + P_R = \mathbb{1} \qquad \text{(Complete)} \tag{A.8}$$

$$P_L^2 = P_L \qquad P_R^2 = P_R \qquad \text{(Idempotent)} \tag{A.9}$$

$$P_L P_R = P_R P_L = 0 \qquad \text{(Orthogonal)} \tag{A.10}$$

Combining identities from the previous section with those above, we find that

$$\overline{q}\Gamma q = \overline{q}_L \Gamma q_L + \overline{q}_R \Gamma q_R \qquad \Gamma \in \left\{\gamma^\mu, \gamma^\mu\gamma^5\right\} \tag{A.11}$$

$$\overline{q}\Gamma q = \overline{q}_L \Gamma q_R + \overline{q}_R \Gamma q_L \qquad \Gamma \in \left\{1_{2\times 2}, \gamma^5, S^{\mu\nu}\right\} \tag{A.12}$$

where $S^{\mu\nu} = \frac{i}{4}[\gamma^\mu, \gamma^\nu]$ and

$$q_L = P_L q \qquad q_R = P_R q \qquad \overline{q}_R = \overline{q} P_L \qquad \overline{q}_L = \overline{q} P_R \,. \tag{A.13}$$

LATTICE PARTICULARS & ENSEMBLE DATA

Recall from the introduction that there are numerous way to discretize QCD (a few different choices are shown in Table B.1). However, that doesn't mean all choices are equally *good*—each choice has its own set of advantages and drawbacks. For example, the action derived in Chapter 1 (known as the naive action) has a couple pesky problems: first, the fermions do not respect chiral symmetry even in the massless limit; second, for each fermion described by the action, there are 15 extra fermions in what is dubbed the fermion doubling problem. Wilson demonstrated how to remove the doublers [131], but even so the fermions did not respect chiral symmetry.

In fact, this is not from a lack of cleverness (as if anyone would have the audacity to accuse Wilson of such). The Nielsen-Ninomiya theorem [132] states that, given an even dimensional lattice gauge theory, it is impossible to build a lattice action that simultaneously (1) has no fermion doublers, (2) acts locally (i.e., only nearest neighbors can interact), and (3) respects chiral symmetry.

That said, there is a loophole here, as the Nielsen-Ninomiya theorem only applies to *even* dimensional theories. It is possible to build an odd dimensional theory that satisfies all three *desiderata*, with the fermions we're interested in living on the 4-dimensional surface of this 5-dimensional volume; this is roughly the philosophy behind domain wall fermions.

Beyond mathematical restraints, however, there are funding constraints the aspiring lattice practitioner must consider: the computational price for each fermion action is different. Moreover, since these actions are simulated on half-billion dollar high-performance computers, these computations costs have palpable financial costs, too. For reference, it is roughly an order of magnitude more expensive to simulate a domain wall fermion than a staggered fermion.

Fermion action	Doublers	Local	Chiral symmetry	Cost
Naive	Yes (16)	Yes	No	Cheap
Wilson-Clover	No	Yes	No	Cheap
Staggered	Yes (4)	No	Some	Cheap
Domain Wall	No	Yes	Yes	Expensive
Overlap	No	No	Yes	Expensive

Table B.1: A few different fermion actions for lattice QCD. We use a mixed-action, with domain wall fermions in the valence sector and staggered quarks in the sea.

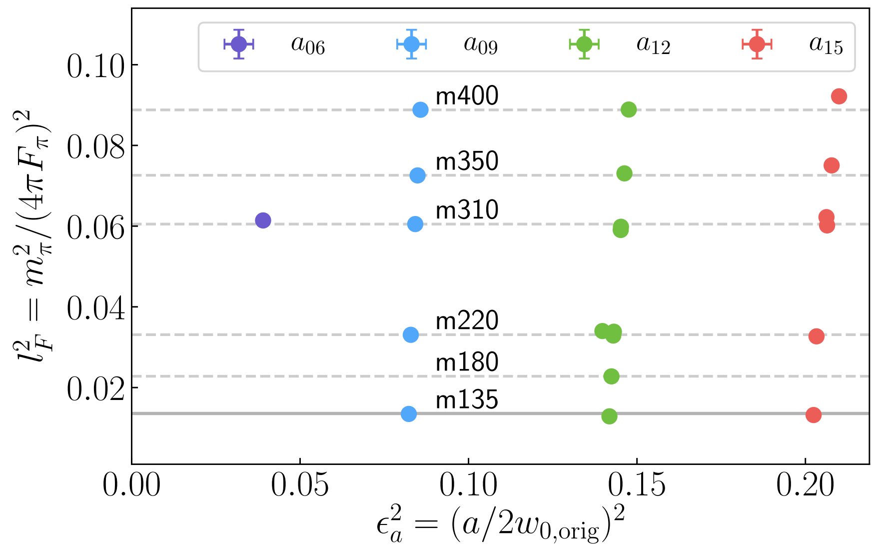

Figure B.1: Ensembles employed in these projects. The pion masses range from ~ 130 MeV to ~ 400 MeV, while the lattice spacing range from ~ 0.06 fm to ~ 0.15 fm. The strange quark masses are generally tuned near their physical point values, with a few lighter-than-physical strange quarks such that we have the option to track the slight mistuning.

Our collaboration uses a mixed action, that is, we employ a different action for the sea and valence quarks. For the sea quarks, we use staggered fermions (with MILC providing many of the staggered quark configurations [133, 134]). For the valence sector, we use domain wall fermions [77].

These projects use data from approximately 20 ensembles spanning 7 pion masses and multiple lattice spacings (see Fig. B.1).

SUMMARY OF CURVE FITTING TECHNIQUES

General considerations when extrapolating an observable to the physical point

In this thesis we have performed extrapolations of chiral observables (i.e., observables that have χPT expressions). The procedure for extrapolating a chiral observable is nearly identical for a given observable modulo the particular fit function. We summarize the procedure here.

Given an observable O with mass dimension 0, the generic extrapolation function can be written

$$O^{\text{fit}} = O^{\text{chiral}} + O^{\text{disc}} \,. \tag{C.1}$$

Here $O^{\text{chiral}} = O^{\text{chiral}}(\{m_{G_i}\})$ denotes the collection of terms that depend strictly on the pseudo-Goldstone bosons, while $O^{\text{disc}} = O^{\text{disc}}(a, L, \ldots)$ denotes the remaining terms which arise from having employed the lattice.

The O^{chiral} terms come in two varieties in this thesis: either they are derived from χPT or they are a Taylor expansion, the latter class being primarily used to test the "goodness" of the χPT fits. For example, we might have

$$\begin{aligned}
O^{\text{chiral}} =& O_0 && \left(\mathcal{O}(\epsilon^0)\right) \\
&+ \sum_{G\in\{\pi,K\}} \epsilon_G^2 \alpha_G^{(2)} && \left(\mathcal{O}(\epsilon^2)\right) \\
&+ \sum_{G\in\{\pi,K\}} \epsilon_G^4 \alpha_G^{(4)} && \left(\mathcal{O}(\epsilon^4)\right) \\
&\qquad + \epsilon_\pi^4 \beta_\pi^{(4)} \log \epsilon_\pi^2 && \\
&+ \sum_{G\in\{\pi,K\}} \epsilon_G^6 \alpha_G^{(6)} && \left(\mathcal{O}(\epsilon^6)\right) \\
&\qquad + \epsilon_\pi^6 \beta_\pi^{(6)} \log \epsilon_\pi^2 + \epsilon_\pi^6 \gamma_\pi^{(6)} \left(\log \epsilon_\pi^2\right)^2 &&
\end{aligned} \tag{C.2}$$

where $\epsilon_G = m_G/\Lambda_\chi$ and the rest are low-energy constants (LECs). When we exclude the $\log \epsilon^2$ terms from our fit, the model reduces to a Taylor expansion.

We have truncated this model at $\mathcal{O}(\epsilon^6)$, but there are in principle infinitely many more terms we could add; however, we expect that at some order the signal will be too weak to fit. The reasoning applies to the lower order terms, too. Even though the literature might provide chiral expression up to order $\mathcal{O}(\epsilon^6)$, that doesn't mean we'll necessarily be able to fit it.

In general, we take a model-agnostic approach when fitting, considering different truncations of our chiral models and averaging over the different models assuming equal weight (see the next section). Occasionally we might exclude a model if we have good *a priori* belief that it is not physical. In the case above, we might consider the models

$$\begin{array}{rl} +1: & \text{Taylor } \mathcal{O}(\epsilon^2) \\ +2: & \text{Taylor } \mathcal{O}(\epsilon^4) + \{0, \log \epsilon^2\} \\ +3: & \text{Taylor } \mathcal{O}(\epsilon^6) + \{0, \log \epsilon^2, (\log \epsilon^2)^2\} \\ \hline 6: & \text{chiral choices} \end{array} \tag{C.3}$$

In this case, we're comparing Taylor models with/without χPT-motivated logarithms. Note that even though the $(\log \epsilon^2)^2$ term is also a χPT term at $\mathcal{O}(\epsilon^6)$, the signal might nevertheless be too weak to fit, depending on the size of the LEC.

Lattice artifacts primarily stem from the size of the lattice spacings. These artifacts are accounted for by using a Taylor Ansatz, for example

$$O^{\text{disc}} \supset d_a \epsilon_a^2 + \left(d_{aa}\epsilon_a^2 + d_{al}\epsilon_\pi^2 + d_{as}\epsilon_K^2\right)\epsilon_a^2 + \cdots \tag{C.4}$$

where $\epsilon_a = a/2w_0$ is a dimensionless proxy for the lattice spacing (see Chapter 4 for the definition of w_0). The discretization errors start at $\mathcal{O}(\epsilon_a^2)$ as a consequence of the particular lattice action we employ [135].

The next obvious discretization effect comes from the lattice's finite volume. Although the real world might be infinite, the lattice certainly isn't—the typically lattice is only a few femtometers across, so it is possible for virtual particles to bump into the "edge" of the universe. Or at least it would be, were it not for the fact that our boundary conditions are periodic. Loop integrals in the effective field theory must consequently be adjusted for finite volume, as now particles can "wrap around" before interacting. Typically this means replacing a $\log$ with a $\log$ plus Bessel function.

Additionally O^{disc} might include terms that are specific to our choice of lattice action, such as radiative corrections.

Once the models have been decided on and the fits have been performed, the final step is to extrapolate to the physical point, which is defined as the continuum, infinite volume limit where observables take their physical/PDG values. As our lattice assumes the SU(2) limit, we take the isospin average of observables as needed, e.g. $m_\pi = (m_{\pi^-} + m_{\pi^0} + m_{\pi^+})/3$.

All fits are performed using the software packages `gvar` and `lsqfit` [136, 137, 138], which implement nonlinear least squares regression with (Bayesian) priors.

Model averaging

Typically when we extrapolate observables in our work, we consider many different models. Rather than choose the “best” model (which could lead to bias or underestimate our uncertainty), we instead perform a model average over the different models employed in our work.

Our averaging procedure is performed under a Bayesian framework, following the procedure described in [120, 81] and with greater detail in [139]. Suppose we are interested in estimating the posterior distribution of $Y = M_\Xi$, i.e. $P(Y|D)$. To that end, we must marginalize over the different models M_k.

$$P(Y|D) = \sum_k P(Y|M_k, D)P(M_k|D) \tag{C.5}$$

Here $P(Y|M_k, D)$ is the distribution of Y for a given model M_k and dataset D, while $P(M_k|D)$ is the posterior distribution of M_k given D. The latter can be written, in accordance to Bayes theorem, as

$$P(M_k|D) = \frac{P(D|M_k)P(M_k)}{\sum_l P(D|M_l)P(M_l)} \,. \tag{C.6}$$

We can be more explicit with what the latter is in the context of our fits. First, mind that we are *a priori* agnostic in our choice of M_k. We thus take the distribution $P(M_k)$ to be uniform over the different models. We calculate $P(D|M_l)$ by marginalizing over the parameters (LECs) in our fits:

$$P(D|M_k) = \int \prod_j \mathrm{d}\theta_j^{(k)} \, P(D|\theta_j^{(k)}, M_k)P(\theta_j^{(k)}|M_k) \,. \tag{C.7}$$

After marginalization, $P(D|M_k)$ is just a number. Specifically, it is the Bayes factor of M_k: $P(D|M_k) = \exp(\texttt{logGBF})_{M_k}$. Thus

$$P(M_k|D) = \frac{\exp(\texttt{logGBF})_{M_k}}{K \sum_l \exp(\texttt{logGBF})_{M_l}} \tag{C.8}$$

with K the number of models included in our average.

Suppose A and B are statistics computed on models $\{M_k\}$ (e.g., $A = M_\Xi$, $B = M_{\Xi^*}$, and $M_k =$ "a simultaneous fit of M_Ξ and M_{Ξ^*} to N^{2}LO in the χPT expansion"). The model average of an observable (e.g., A) is straightforward.

$$\mathrm{E}[Y] = \sum_k \mathrm{E}[Y|M_k]\, P(M_k|D) \tag{C.9}$$

The model-averaged covariance between A and B is given by

$$\begin{aligned}
\mathrm{Cov}\,[A,B] &= \langle AB \rangle - \langle A \rangle \langle B \rangle \\
&= \sum_k \langle AB \rangle_k \, p(M_k|D) - \left(\sum_k \langle A \rangle_k \, p(M_k|D) \right) \left(\sum_k \langle B \rangle_k \, p(M_k|D) \right) \\
&= \sum_k \mathrm{Cov}[A,B]_k \, p(M_k|D) + \sum_k \langle A \rangle_k \langle B \rangle_k \, p(M_k|D) \\
&\quad - \left(\sum_k \langle A \rangle_k \, p(M_k|D) \right) \left(\sum_k \langle B \rangle_k \, p(M_k|D) \right)
\end{aligned} \tag{C.10}$$

where $\langle X \rangle_k$ is the expectation value of X on M_k. Notice that when $A = B$ this expression reduces to the variance expression in the references.

Finally, we add a caveat about weights. The normalized Bayes factors $p(M_k|D)$ ("the weights") can only be compared for models sharing the same response data D. In practice, this means that we can only compute the weights for models that were fit simultaneously. In principle the covariance between two observables not fit together (e.g., M_Ω and M_Ξ) needn't be 0 since the could share the same set of explanatory data (e.g., m_π), but this covariance is comparably small and can be approximated as vanishing. We expect the bulk of the correlation to arise from shared LECs.

The empirical Bayes method

The empirical Bayes method allows us to estimate the prior distribution from the data; in that sense it is not a truly ”Bayesian” approach, as the choice of prior is not data-blind. Nevertheless, it can serve as a useful point of comparison when evaluating the reasonableness of our priors.

Typically when we think of a model for a chiral expression, we imagine this to mean the choice of fit function (e.g., $M =$ “a Taylor expansion to $\mathcal{O}(m_\pi^4)$”); however, we can extend the definition of a model to also include the prior. Let us therefore denote $M = \{\Pi, f\}$ a candidate model for performing the extrapolation of some observable, where f is the extrapolation function and Π is the set of priors for the LECs. By Bayes' theorem, the most probable Π for a given f and dataset D is

$$p(\Pi|D, f) = \frac{p(D|\Pi, f)p(\Pi|f)}{p(D|f)} \,. \tag{C.11}$$

Here we recognize $p(D|\Pi, f)$ to be the familiar likelihood function and $p(D|f)$ to be some unimportant normalization constant. The curious term is the hyperprior distribution $p(\Pi|f)$, which parameterizes the distribution of the priors. We restrict our priors to the form $\pi(c_i) = N(0, \sigma_j^2)$ for LEC c_i, where the index j denotes some blocking of the LECs. For example, one might use the chiral/discretization split

$$\Pi = \begin{cases} \pi(c_\chi) & = N(0, \sigma_1^2) \\ \pi(c_{\text{disc}}) & = N(0, \sigma_2^2) \end{cases} \,. \tag{C.12}$$

The hyperprior $p(\Pi|f)$, in this context, parameterizes the σ_j. We then vary σ_j uniformly on the interval $[\sigma_j^{\text{min}}, \sigma_j^{\text{max}}]$ (in this work, $\sigma_j^{\text{min}} = 0.01$ and $\sigma_j^{\text{max}} = 100$). As we expect the LECs to be of order 1, we do not expect the optimal values of σ_j to lie near the extrema. However, if they do, we should reflect on whether the terms are disfavored by the data ($\sigma_j \sim \sigma_j^{\text{min}}$) or the LEC is much greater than expected ($\sigma_j \sim \sigma_j^{\text{max}}$).

Because the hyperprior distribution is uniform, we see that the peak of the posterior $p(\Pi|D, f)$ occurs at the peak of the likelihood function $p(D|\Pi, f)$. Thus the empirical Bayes procedure is straightforward: we find the set of priors that maximizes the likelihood function. But there is one general caveat here. We reiterate that we have blocked the LECs together. One might instead be tempted to optimize each LEC individually; however, this would be an abuse of empirical Bayes—by varying too many parameters, the uniformity assumption can no longer be made in good faith. We emphasize that the empirical Bayes method is not a substitute for careful consideration when setting priors!

Plotting lattice data by shifting their values

In general, the fit function for some observable O depends on multiple parameters (m_π, m_K, a, etc.), so the curve we're fitting is not a line but some multidimensional surface, which would generally be intractable to plot. It is significantly easier to interpret a plot of O versus a single parameter, but this means carefully taking a slice of that surface. Fortunately, this is fairly easy: we simply fix the other parameters to their physical point values while allowing the single parameter to vary.

Of course, we're not interested in plotting solely the fit; we're also interested in plotting the data, which gives us a visual indication of goodness of fit. However, this is tricky since most data is not generated at their physical values. We therefore require some heuristic for "shifting" the lattice data from their ensemble values to the physical point values.

We accomplish this task in the following manner. Suppose we're interested in including on our plot the ensemble value O_e at a given ensemble value of a variable $\boldsymbol{w}_e$ (e.g., $\boldsymbol{w}_e = m_\pi/\Lambda_\chi$ on `a12m220`). Denote the values of the remaining explanatory variables on that ensemble by $\boldsymbol{x}_e$. Then on each ensemble, we replace O_e with O_e^{shifted}, defined by

$$O_e^{\text{shifted}} = O_e + \hat{O}(\boldsymbol{w}, \boldsymbol{x}_{\text{phys}}) - \hat{O}(\boldsymbol{w}, \boldsymbol{x}) \tag{C.13}$$

where $\hat{O}$ is the fit function parameterized by the fit's posterior.

CORRELATOR FITS

Baryons

Fit function

In section 1.2, we saw how to calculate the correlator of two observables using the Euclidean path integral.

$$\langle O_2(t)O_1(0)\rangle = \frac{1}{Z_0}\int \mathcal{D}[q,\overline{q}]\mathcal{D}[U]\, e^{-S_F[q,\overline{q},U]-S_G[U]}O_2[q_{(t)},\overline{q}_{(t)},U_{(t)}]O_1[q_{(0)},\overline{q}_{(0)},U_{(0)}] \tag{D.1}$$

This (Euclidean) path integral is sampled using Monte-Carlo to determine the two-point function on the lattice. However, there is another way one might defined the correlation function. As operators (rather than functionals), the correlation function is defined as

$$\langle O_2(t)O_1(0)\rangle = \lim_{T\to\infty}\frac{1}{Z_T}\operatorname{Tr}\left\{e^{-(T-t)\hat{H}}\hat{O}_2 e^{-t\hat{H}}\hat{O}_1\right\} \tag{D.2}$$

where $Z_T = \operatorname{Tr}\left\{e^{-T\hat{H}}\right\}$. From this definition, we see that by introducing a complete set of energy eigenstates, we can rewrite this correlation function in terms of its energy spectrum.

$$\langle O_2(t)O_1(0)\rangle = \sum_{m,n}\langle m|e^{-(T-t)\hat{H}}\hat{O}_2|n\rangle\,\langle n|e^{-t\hat{H}}\hat{O}_1|m\rangle \tag{D.3}$$

$$\approx \sum_{n}\langle 0|\hat{O}_2|n\rangle\,\langle n|\hat{O}_1|0\rangle\, e^{-tE_n} \qquad \text{as } T\to\infty \tag{D.4}$$

The above formula is quite general, but it doesn't tell us how to calculate the mass of some particular baryon. To do that, we replace $\hat{O}_1, \hat{O}_2$ with operators that create a baryon from the vacuum at $t = 0$, which is then destroyed at $t = 1$.

$$\langle O_2(t)O_1(0)\rangle \to \langle\Omega|B(t)B^{\dagger}(0)|\Omega\rangle \tag{D.5}$$

Here Ω is the (QCD) vacuum and $B^{\dagger}$ is an operator that creates an excitation with quantum numbers equal to that of the specific baryon we're interested in studying. The details here are quite messy (see Chapter 6 of [8], for example), but the important bit is that these baryon interpolators links lattice sites (sources and sinks). We can either have the baryon be created/annihilated at a single source/sink (which we call Dirac or point) or some general small region on the lattice (which we call smeared).

For technical reasons, it's computationally cheaper to generate either the sink or the source smeared. In our case, the source is always smeared, which we use to generate two copies of the ensemble, one with a smeared sink and one with a point sink. The energy spectrum for either sink is the same, but the wave function overlaps can differ. Therefore, we simultaneously fit the following two equations to determine the energy spectrum:

$$C_{PS}(t) = \sum_n Z_n^{(P)} Z_n^{(S)} e^{-tE_n} \, , \tag{D.6}$$

$$C_{SS}(t) = \sum_n |Z_n^{(S)}|^2 e^{-tE_n} \, . \tag{D.7}$$

Priors

Our fits are implemented through `lsqfit` [138], a Bayesian least squares fitter; since we are performing a Bayesian fit, we require that our *degree of belief* in the values of each of our fits parameters be characterized *a priori*. For the most part, we leave our priors much wider than expected, and therefore the prior mostly serves to guide the minimizer towards non-pathological local minima.

We use the following iterative process to set our priors for the hyperons.

1. Plot the effective mass $M_{\text{eff}}(t) = \log[C(t)/C(t+1)]$ to determine a candidate time range. For the starting time t_{start}, choose a time near the first plateau. The ending time t_{end} typically has little influence on the final result and can be chosen more freely; nevertheless, it's wise to avoid a t_{end} where the noise is too great (in principle, the fitter should weigh these noisier points less, so including a few of them in the fit is fine).

2. Perform an initial fit with a very wide prior, e.g.:

```
p['E'] = [1.0(1.0), 2.0(1.0), 3.0(1.0), ···]
p['wf_dir'] = [0.0(1.0), 0.0(1.0), 0.0(1.0), ···] × e-04
p['wf_smr'] = [0.0(1.0), 0.0(1.0), 0.0(1.0), ···] × e-04
```

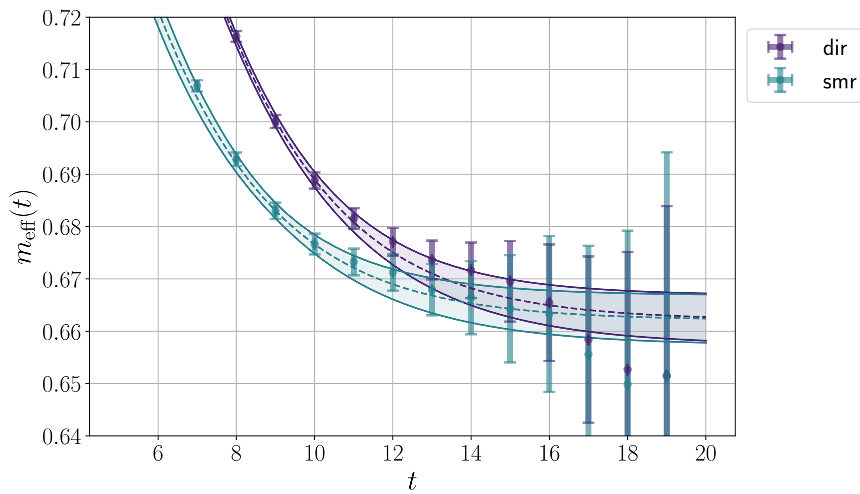

Figure D.1: Example of a correlator fit. The effective mass for a baryon asymptotes to the ground state, but the noise also grows with time.

The priors for the excited state energies, in particular, are not very good. However, the posterior will be roughly correct. Record the fit results for the ground state: $m_H \pm \sigma_{m_H}$, $A_{\text{smr}} \pm \sigma_{A_{\text{smr}}}$, $A_{\text{dir}} \pm \sigma_{A_{\text{dir}}}$.

3. Using the results of the previous fit, we can now set reasonable priors for the fit. The ground state should be roughly the same as that in our loose fit; to that end, we set the central value to be m_H from the previous fit. To prevent biasing the fit, set the width to be $\texttt{100}\sigma_{m_H}$, which in practice will cover all but the earlier and latest (nosiest) effective mass values.

   For the excited energy states, prior the next energy level to be two pions masses above the previous state with a width of one pion mass (a baryon plus two pions has the same parity and spin as the original baryon).

   For the wave function overlaps, we use the results of the previous fit. Since the Dirac wave function overlap can be negative, set the prior for the ground state to be $0 \pm 2A_{\text{smr}}$. The smeared wave function overlap must be positive, so we set the prior to $A_{\text{dir}} \pm A_{\text{dir}}$. The correlators are generated such that the excited states have smaller wave function overlaps than the ground state; therefore, it is sufficient to use the same prior for the excited states, too.

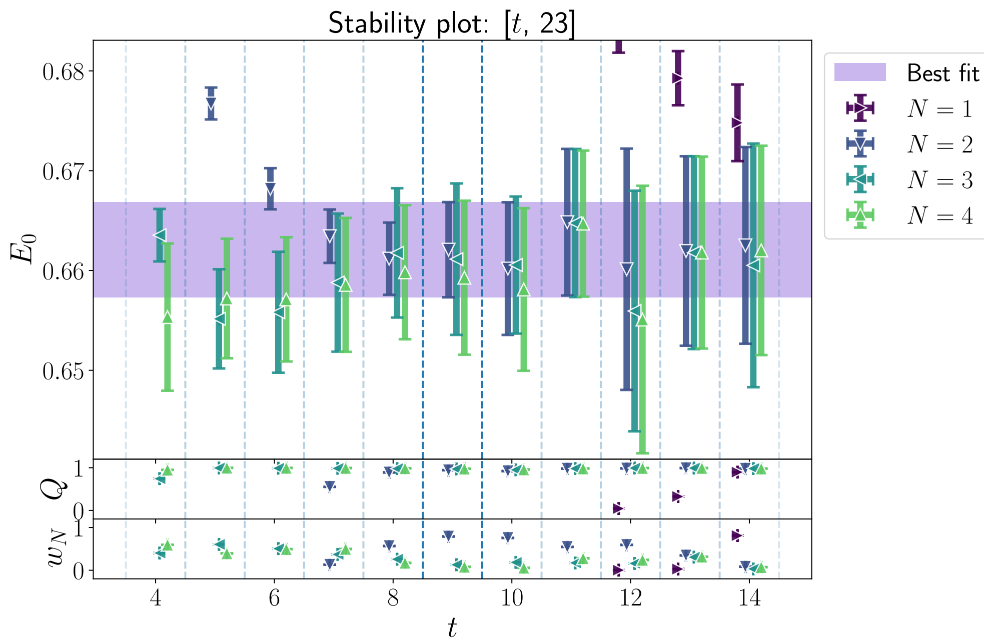

Figure D.2: Stability plot versus t_{start} and N_{states}. Here w_N denotes the relative weights of the different N_{states} fit at a fixed t, which can be used to identify when the fit is stable versus N_{states}.

This procedure will generate a prior like

$$\texttt{p['E']} = [m_H\,(100\sigma_{m_H}),\ m_H{+}2m_\pi\,(m_\pi),\ m_H{+}4m_\pi\,(m_\pi),\ \cdots]$$

$$\texttt{p['wf\_dir']} = [A_{dir}\,(A_{dir}),\ A_{dir}\,(A_{dir}),\ A_{dir}\,(A_{dir}),\ \cdots]$$

$$\texttt{p['wf\_smr']} = [0\,(2A_{smr}),\ 0\,(2A_{smr}),\ 0\,(2A_{smr}),\ \cdots]$$

(Note that $m_H + 100\sigma_{m_H} < m_H + 2m_\pi$ even after the first iteration, so the ordering of the energy spectrum is as expected.)

Fit criteria

When choosing a best candidate among fits, we rank a fit based on the following criteria:

1. **The fit should have an acceptable χ^2_ν and Q-value.** Fits with $\chi^2_\nu \gg 1$ underfit the data; fits with $\chi^2_\nu \ll 1$ overfit the data. Fits with poor Q-values either disagree strongly with the prior (in which case the choice of prior might need to be redone) or poorly match the data. Anything with $Q < 0.1$ is suspect.

2. **The fit should be stable versus time.** In practice, this means the fit should be stable versus t_{start} since the noise grows with time, resulting in the fit being mostly determined by data at earlier times. We prefer fits that are in a stability plateau, not fits that are tending upwards or downwards as shown by the stability plot.

3. **The fit should be stable versus number of states.** We prioritize fits that are nearly in exact agreement for $N_{\text{states}} = 2$ and $N_{\text{states}} = 3$ while having some agreement with the late-time $N_{\text{states}} = 1$ fit.

Mesons

The fit strategy employed for the mesons is generally taken from [140], albeit with more conservative choices for our fits. We fit the two-point correlator as a single $\cosh$ (see below), symmetrically fitting the interval $[t, T-t]$. When picking a fit, we prefer later plateaus to earlier ones, as those are the ones less likely to be contaminated by excited states; further, we choose our fit such that the majority of late-time fits fall within the error bar of the chosen fit (see stability plots below). That is, we choose as our representative fits to be the ones with errors likely noticeably larger than they could be, preferring to err on the side of overestimating our error versus underestimating it.

Because our fits are so conservative, and because the excited states are sensitive to the choice of prior (unlike the ground state), we omit stability plots of the excited states in our analysis.

Fit function

Let us briefly revisit the spectral decomposition of the correlation function.

$$\langle O_2(t) O_1(0) \rangle = \sum_{m,n} \langle m| e^{-(T-t)\hat{H}} \hat{O}_2 |n\rangle \langle n| e^{-t\hat{H}} \hat{O}_1 |m\rangle \tag{D.8}$$

Previously we simplified this sum by taking the limit $T \to \infty$. However, there is no such thing as infinity on the lattice. Like the spacial extent, we force the temporal extent to have periodic boundary conditions. For a baryon, the noise of the correlation function grows exponentially with time, so by the time the signal correlators wraps back around to the start is imperceptible. This is not the case for mesons, which have nearly constant noise, so we can no longer ignore the $\langle m| e^{-(T-t)\hat{H}} \hat{O}_2 |n\rangle$ term. This motivates the following

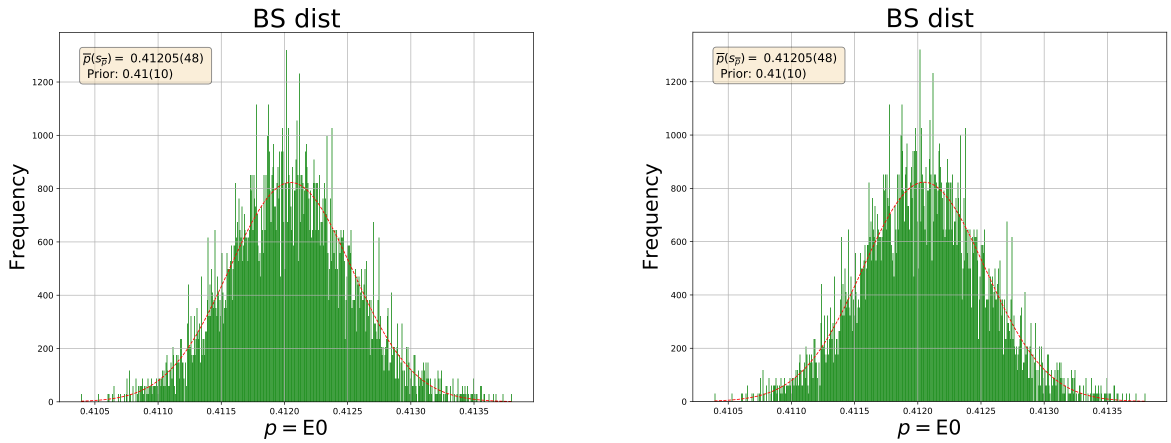

(a) Fitting $C(t) \approx A_0 \cosh\left(E_0(t - T/2)\right)$ for E_0

(b) Fitting $C(t) \approx A_0 \cosh\left(e^{\xi_0}(t - T/2)\right)$ for ξ_0

Figure D.3: Comparison of fit strategies for fitting a meson. After rerunning the fit on 5000 bootstraps resamples, the results are identical.

expression for the correlation function,

$$C(t) = \sum_n Z_n^{(PS)} Z_n^{(SS)} \left(e^{-E_n t} + e^{-E_n(T-t)}\right) . \tag{D.9}$$

Suppose we are only interested in the ground state, not the wave function overlap factors or excited states. At later times, the higher excited states will die out, leaving only the ground state to be fit. For our fit function, therefore, we fit a single state (which we've reexpressed as a hyperbolic function)

$$C(t) \approx A_0 \cosh\left(e^{\xi_0}(t - T/2)\right) \tag{D.10}$$

where we have fit $\xi_0 = \log E_0$ to ensure the ground state remains positive and we have absorbed the overlap in $A_0 = 2Z_0^{(PS)} Z_0^{(SS)} e^{-E_0 T}$. Thus we get the result for E_0 by exponentiating ξ_0.

In this fit function, E_0 is log-normally distributed; however, since the fits are employed with `lsqfit` (and the errors are propagated as `gvar` variables), by exponentiating ξ_0 we propagate the error through, thereby getting a Gaussian distribution for E_0. Refer to Fig. D.3 for a comparison of fitting E_0 directly versus fitting $\log E_0$ and exponentiating the `gvar` result.

Prior

In order to use `lsqfit`, we must first set the prior for our fit parameters, ξ_0 and A_0, which we obtain from the effective mass and effective wave function overlap, respectively. The former is constructed thus:

$$M_{\text{eff}}(t) = \text{arccosh}\left(\frac{C(t+1)+C(t-1)}{2C(t)}\right)\,, \tag{D.11}$$

while the latter is constructed like so:

$$A_{\text{eff}}(t) = \frac{C(t)}{\cosh\left(M_{\text{eff}}(t-T/2)\right)}\,. \tag{D.12}$$

When picking our priors for E_0 and A_0, we choose values that include the values of $M_{\text{eff}}(t)$ and $A_{\text{eff}}(t)$ at all but the few earliest and latest times, where contamination from higher order states is obvious. In practice, we achieve this through the following procedure, using `phi_jr_5/a15m350` as an example:

1. Pick a candidate time range for the fit by looking at the effective mass plot. Because meson statistics are so well behaved, this choice can be essentially any time range.

2. Pick very loose priors for E_0 and A_0, e.g. `p[E0] =` $1.0(1.0)$`, p[wf_dir 0] =` $0.00000(10)$

3. Record the fit result (e.g., a loose fit might yield something like $E_0 = 0.41202(77)$, $A_0 = 1.039(11)\times 10^{-11}$).

4. For E_0, keep the mean and multiply the uncertainty by 100. Use this new value for the prior. For A_0, center the mean value about 0 with an uncertainty equal to twice the mean value from the fit. Our new prior would be `p[E0] =` $0.41(10)$`, p[wf_dir 0] =` $0.0(2.1)\times 10^{-11}$).

Notice that we use E_0 when picking our prior, despite fitting $\log E_0$. As an intermediate step, we use `gvar` to convert `p[E0]` to `p[log(E0)]` when performing the fit.

These uncertainty of these priors end up being much larger than the uncertainties of any particular $M_{\text{eff}}(t)$ and $A_{\text{eff}}(t)$ as constructed from the data, so our Bayesian fit is essentially unaffected by our choice of prior; here the prior serves to assist the fitter in converging faster to the correct answer. In the $M_{\text{eff}}(t)$ and $A_{\text{eff}}(t)$ plots below (Fig. D.4), the priors are wide enough that they cover the entirety of the y-limits in the plots.

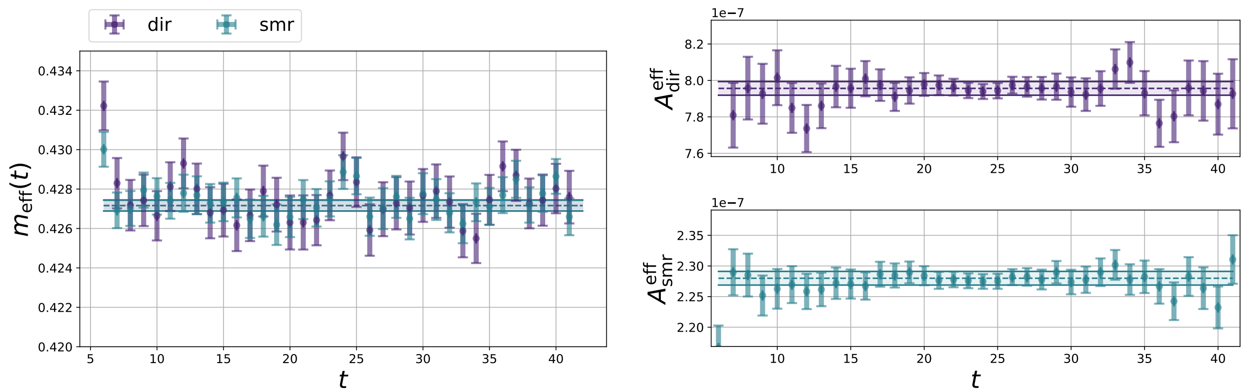

(a) Effective mass

(b) Effective wave function overlap

Figure D.4: Plots of effective quantities. Unlike for baryons, the noise is nearly constant with time.

Fit criteria

When choosing a representative fit, we evaluate the fit based on the following criteria, with importance ranked as follows:

1. **Avoid fits with $\chi^2_\nu < 0.2$.** We exclude these fits under the assumption that they are too conservative.

2. **Choose fits that agree with other fits.** Ideally the chosen fit should be wide enough such that it contains the uncertainty intervals of all but the latest and earliest symmetric fits. If there are multiple such fits, choose the one that minimally covers most fits.

3. **Prefer later plateaus.** If there is no fit that generally agrees with most of the other fits, then prefer conservative fits that agree with later plateaus.

IMPACT OF CHOICE OF Λ_χ, μ

Adapting a fixed renormalization scheme to the lattice

The appendix of [141] gives χPT expressions for the pseudoscalar decay constants, which we repeat here. The expressions are written in the form

$$F_P = F_0 \left(1 + \delta F_P + \cdots\right) \tag{E.1}$$

where F_0 is the value of F_π in the chiral limit. The NLO corrections to the decays constants are

$$\delta F_\pi = -l_\pi^0 - \frac{1}{2} l_K^0 + 4\left[\left(\epsilon_\pi^2 + 2\epsilon_K^2\right)\overline{L}_4 + 4\epsilon_\pi^2 \overline{L}_5\right] \tag{E.2}$$

$$\delta F_K = -\frac{3}{8} l_\pi^0 - \frac{3}{4} l_K^0 - \frac{3}{8} l_\eta^0 + 4\left[\left(\epsilon_\pi^2 + 2\epsilon_K^2\right)\overline{L}_4 + 4\epsilon_K^2 \overline{L}_5\right] \tag{E.3}$$

where

$$\epsilon_P = \frac{m_P}{4\pi F_\pi}\,, \qquad l_P^{P'} = \epsilon_P^2 \log\left[\left(\frac{m_P}{\mu_{P'}}\right)^2\right]\,, \qquad \overline{L}_i = (4\pi)^2 L_i\,. \tag{E.4}$$

In this case, l_P^0 corresponds to the choice $\mu = \mu_0$. We stress the following points:

1. The choice of $\Lambda_\chi = 4\pi F_\pi$ is only a proxy for the chiral scale; other choices are valid.

2. Here $\mu_0 = 4\pi F_0$ is a *fixed* renormalization scale.

For the actual lattice calculation we would prefer to avoid using a fixed renormalization scale, as a fixed renormalization scale would require scale setting. Instead, we use the lattice values of F_π and F_K as a proxy for F_0 and introduce an NNLO correction to F_K/F_π (whose value varies by ensemble) that accounts for the fact that our renormalization scale is not fixed.

To understand how we can track this correction, we begin with the NLO expression for F_K/F_π.

$$\begin{aligned}
\frac{F_K}{F_\pi} &= \frac{1 + \delta F_K + \cdots}{1 + \delta F_\pi + \cdots} \\
&\approx 1 + \delta F_K - \delta F_\pi \\
&= 1 + \frac{5}{8} l_\pi^0 - \frac{1}{4} l_K^0 - \frac{3}{8} l_\eta^0 + 4\left(\epsilon_K^2 - \epsilon_\pi^2\right)\overline{L}_5
\end{aligned} \tag{E.5}$$

Notice that the log parts can be rewritten as

$$
\begin{aligned}
l_P^0 &= \epsilon_P^2 \log\left[\left(\frac{m_P}{\mu_{P'}}\frac{\mu_{P'}}{\mu_0}\right)^2\right] \\
&= l_P^{P'} + \epsilon_P^2 \log\left[\left(\frac{\mu_{P'}}{\mu_0}\right)^2\right]
\end{aligned}
\tag{E.6}
$$

which allows us to rewrite the NLO expression for F_K/F_π as

$$
\begin{aligned}
\frac{F_K}{F_\pi} &= \left(1 + \frac{5}{8}l_\pi^{P'} - \frac{1}{4}l_K^{P'} - \frac{3}{8}l_\eta^{P'} + 4\left(\epsilon_K^2 - \epsilon_\pi^2\right)\overline{L}_5\right) - \frac{3}{4}\left(\epsilon_K^2 - \epsilon_\pi^2\right)\log\left[\left(\frac{\mu_{P'}}{\mu_0}\right)^2\right] \\
&= \frac{F_K}{F_\pi}\Big|_{\mu_0\to\mu_{P'}} - \frac{3}{4}\left(\epsilon_K^2 - \epsilon_\pi^2\right)\log\left[\left(\frac{\mu_{P'}}{\mu_0}\right)^2\right].
\end{aligned}
\tag{E.7}
$$

The last term is the renormalization scale correction (the ϵ^2 terms have been simplified using the GMOR relation (Eq. (3.74)). Available on our lattice are F_K and F_π, which we use for the sliding renormalization scale. Since $\mu_{P'}/\mu_0 = F_{P'}/F_0$, we have the following for the NNLO sliding renormalization scale corrections to the χPT expression.

$$
\begin{aligned}
-\frac{3}{4}\left(\epsilon_K^2 - \epsilon_\pi^2\right)\log\left[\left(\frac{\mu_\pi}{\mu_0}\right)^2\right] &\approx -\frac{3}{2}\left(\epsilon_K^2 - \epsilon_\pi^2\right)\delta F_\pi && = \delta^{\text{NNLO}}_{\mu=\mu_\pi} \\
-\frac{3}{4}\left(\epsilon_K^2 - \epsilon_\pi^2\right)\log\left[\left(\frac{\mu_K}{\mu_0}\right)^2\right] &\approx -\frac{3}{2}\left(\epsilon_K^2 - \epsilon_\pi^2\right)\delta F_K && = \delta^{\text{NNLO}}_{\mu=\mu_K} \\
-\frac{3}{4}\left(\epsilon_K^2 - \epsilon_\pi^2\right)\log\left[\left(\frac{\mu_K}{\mu_0}\right)\left(\frac{\mu_\pi}{\mu_0}\right)\right] &\approx -\frac{3}{4}\left(\epsilon_K^2 - \epsilon_\pi^2\right)\left(\delta F_K + \delta F_\pi\right) && = \delta^{\text{NNLO}}_{\mu^2=\mu_\pi\mu_K}
\end{aligned}
\tag{E.8}
$$

Correcting for different choices of Λ_χ

In the previous section we considered three different choices for the sliding renormalization scale by using F_K, F_π or the geometric average $\sqrt{F_K F_\pi}$. We consider the three cases instead of just a single case (say, $\mu = 4\pi F_\pi$) as this allows us to systematically evaluate the choice of μ on our fits. Similarly if we choose, for instance, $\mu = 4\pi F_K$ for our renormalization scale, it seems sensible to also set $\Lambda_\chi = 4\pi F_K$ for the chiral symmetry breaking scale. Continuing with the example, this amounts to the following modification of ϵ_P.

$$
\frac{m_P}{4\pi F_\pi} \to \frac{m_P}{4\pi F_K}
\tag{E.9}
$$

The new choice for Λ_χ introduces differences at NNLO.

$$\begin{aligned}
\frac{F_K}{F_\pi} &\approx 1 + \delta F_K - \delta F_\pi \\
&= 1 + \left[\left(\delta F_K - \delta F_\pi \right) \big|_{F_\pi^2 \to F_K^2} \right] \left(\frac{F_K}{F_\pi} \right)^2 \\
&\approx 1 + \left[\left(\delta F_K - \delta F_\pi \right) \big|_{F_\pi^2 \to F_K^2} \right] \left[1 + \left(\delta F_K - \delta F_\pi \right) \right]^2 \\
&\approx \frac{F_K}{F_\pi} \bigg|_{F_\pi^2 \to F_K^2} + 2 \left(\delta F_K - \delta F_\pi \right)^2
\end{aligned} \tag{E.10}$$

Therefore we correct for the differences by introducing a term $\delta_{\Lambda_\chi}^{\mathrm{NNLO}}$. For $F_\pi = 0$, the correction is trivially 0 (as $\Lambda_\chi = 4\pi F_\pi$ was assumed to be the cutoff). Adapting the above derivation to use the geometric average instead is straightforward. In summary,

$$\begin{aligned}
\delta_{\Lambda_\chi \to 4\pi F_\pi}^{\mathrm{NNLO}} &= 0 \\
\delta_{\Lambda_\chi \to 4\pi F_K}^{\mathrm{NNLO}} &= 2 \left(\delta F_K - \delta F_\pi \right)^2 \\
\delta_{\Lambda_\chi \to 4\pi \sqrt{F_\pi F_K}}^{\mathrm{NNLO}} &= \left(\delta F_K - \delta F_\pi \right)^2 \ .
\end{aligned} \tag{E.11}$$

REFERENCES

[1] B. C. Hall, "An elementary introduction to groups and representations," (2000), arXiv:math-ph/0005032 [math-ph] .

[2] J. Maciejko, "Representations of lorentz and poincaré groups," (2020).

[3] D. Tong, "Lectures on quantum field theory," (2007).

[4] D. J. Griffiths, *Introduction to elementary particles* (Wiley-VCH Verlag, 2014).

[5] W. Greiner, S. Schramm, and E. Stein, *Quantum chromodynamics* (Springer, 2007).

[6] J. Schwichtenberg, "Demystifying gauge symmetry," (2019), arXiv:1901.10420 [physics.hist-ph] .

[7] J. Shapiro, "Group theory in physics," (2017).

[8] C. Gattringer and C. B. Lang, *Quantum chromodynamics on the lattice*, Vol. 788 (2010) pp. 1–343.

[9] A. Deur, S. J. Brodsky, and G. F. de Teramond, Nucl. Phys. **90**, 1 (2016), arXiv:1604.08082 [hep-ph] .

[10] S. Rivat, Synthese , 1 (2020).

[11] J. D. Wells, *Effective theories in physics: From planetary orbits to elementary particle masses*, Springer Briefs in physics (Springer, Heidelberg, Germany, 2012).

[12] S. M. Carroll, *Spacetime and Geometry* (Cambridge University Press, 2019).

[13] O. Heaviside, The Electrician **31**, 281 (1893).

[14] J. Pierrus, *Solved Problems in Classical Electromagnetism: Analytical and Numerical Solutions with Comments* (Oxford University Press, USA, 2018).

[15] C. W. F. Everitt *et al.*, Phys. Rev. Lett. **106**, 221101 (2011), arXiv:1105.3456 [gr-qc] .

[16] M. Popenco, (2017), 10.1007/978-3-658-17221-3.

[17] D. B. Kaplan, "Lectures on effective field theory," (2016).

[18] A. Falkowski, "Lectures on effective field theory," (2020).

[19] C. Arzt, Phys. Lett. B **342**, 189 (1995), arXiv:hep-ph/9304230 .

[20] S. Weinberg, Eur. Phys. J. H **46**, 6 (2021), arXiv:2101.04241 [hep-th] .

[21] C. P. Burgess, *Introduction to Effective Field Theory* (Cambridge University Press, 2020).

[22] S. Weinberg, Phys. Rev. D **22**, 1694 (1980).

[23] F. R. Klinkhamer, Mod. Phys. Lett. A **28**, 1350010 (2013), arXiv:1112.2669 [hep-ph] .

[24] S. Scherer and M. R. Schindler, *A Primer for Chiral Perturbation Theory*, Vol. 830 (2012).

[25] V. Koch, Int. J. Mod. Phys. E **6**, 203 (1997), arXiv:nucl-th/9706075 .

[26] J. F. Donoghue, E. Golowich, and B. R. Holstein, *Dynamics of the standard model*, Vol. 2 (CUP, 2014).

[27] M. Golterman, in *Les Houches Summer School: Session 93: Modern perspectives in lattice QCD: Quantum field theory and high performance computing* (2009) pp. 423–515, arXiv:0912.4042 [hep-lat] .

[28] S. R. Sharpe, in *Workshop on Perspectives in Lattice QCD* (2006) arXiv:hep-lat/0607016 .

[29] G. Ecker, in *Hadron Physics 1996* (1996) pp. 125–167, arXiv:hep-ph/9608226 .

[30] D. Tong, "Gauge theory," (2018).

[31] G. Eichmann, "Qcd and hadron physics," (2020).

[32] M. Gell-Mann, (1961), 10.2172/4008239.

[33] M. Gell-Mann and M. Levy, Nuovo Cim. **16**, 705 (1960).

[34] A. Zee, *Quantum field theory in a nutshell* (2003).

[35] T. Brauner, Symmetry **2**, 609 (2010), arXiv:1001.5212 [hep-th] .

[36] J. R. Pelaez, Phys. Rept. **658**, 1 (2016), arXiv:1510.00653 [hep-ph] .

[37] S. R. Coleman, J. Wess, and B. Zumino, Phys. Rev. **177**, 2239 (1969).

[38] C. G. Callan, Jr., S. R. Coleman, J. Wess, and B. Zumino, Phys. Rev. **177**, 2247 (1969).

[39] H. Leutwyler, Lect. Notes Phys. **396**, 1 (1991).

[40] B. Finelli de Moraes, *Structure of Broken Spacetime Symmetries*, Ph.D. thesis, Utrecht U. (2020).

[41] M. Gell-Mann, R. J. Oakes, and B. Renner, Phys. Rev. **175**, 2195 (1968).

[42] E. E. Jenkins and A. V. Manohar, Phys. Lett. B **255**, 558 (1991).

[43] V. Bernard, N. Kaiser, J. Kambor, and U. G. Meissner, Nucl. Phys. B **388**, 315 (1992).

[44] G. Ecker, Lect. Notes Phys. **521**, 83 (1999), arXiv:hep-ph/9805500 .

[45] B. Kubis (2008).

[46] M. L. Goldberger and S. B. Treiman, Phys. Rev. **111**, 354 (1958).

[47] R. Sommer, PoS **LATTICE2013**, 015 (2014), arXiv:1401.3270 [hep-lat] .

[48] S. Durr *et al.*, Science **322**, 1224 (2008), arXiv:0906.3599 [hep-lat] .

[49] R. Sommer, Nucl. Phys. B **411**, 839 (1994), arXiv:hep-lat/9310022 .

[50] H. Mansour and A. Gamal, Adv. High Energy Phys. **2018**, 7269657 (2018), arXiv:1810.07693 [hep-ph] .

[51] M. Lüscher, JHEP **08**, 071 (2010), [Erratum: JHEP03,092(2014)], arXiv:1006.4518 [hep-lat] .

[52] S. Borsanyi *et al.*, JHEP **09**, 010 (2012), arXiv:1203.4469 [hep-lat] .

[53] Z. Fodor, K. Holland, J. Kuti, S. Mondal, D. Nogradi, and C. H. Wong, JHEP **09**, 018 (2014), arXiv:1406.0827 [hep-lat] .

[54] N. Miller *et al.*, Phys. Rev. D **103**, 054511 (2021), arXiv:2011.12166 [hep-lat] .

[55] O. Bar and M. Golterman, Phys. Rev. D **89**, 034505 (2014), [Erratum: Phys.Rev.D 89, 099905 (2014)], arXiv:1312.4999 [hep-lat] .

[56] B. C. Tiburzi and A. Walker-Loud, Phys. Lett. B **669**, 246 (2008), arXiv:0808.0482 [nucl-th] .

[57] H.-W. Lin *et al.* (Hadron Spectrum), Phys. Rev. D **79**, 034502 (2009), arXiv:0810.3588 [hep-lat] .

[58] J. Gasser and H. Leutwyler, Phys. Lett. B **184**, 83 (1987).

[59] G. Colangelo and C. Haefeli, Phys. Lett. B **590**, 258 (2004), arXiv:hep-lat/0403025 .

[60] E. Follana, Q. Mason, C. Davies, K. Hornbostel, G. P. Lepage, J. Shigemitsu, H. Trottier, and K. Wong (HPQCD, UKQCD), Phys. Rev. D **75**, 054502 (2007), arXiv:hep-lat/0610092 .

[61] S. Borsanyi *et al.*, (2020), arXiv:2002.12347 [hep-lat] .

[62] A. Bazavov *et al.* (MILC), Phys. Rev. **D93**, 094510 (2016), arXiv:1503.02769 [hep-lat] .

[63] R. J. Dowdall, C. T. H. Davies, G. P. Lepage, and C. McNeile, Phys. Rev. **D88**, 074504 (2013), arXiv:1303.1670 [hep-lat] .

[64] M. Bruno, T. Korzec, and S. Schaefer, Phys. Rev. D **95**, 074504 (2017), arXiv:1608.08900 [hep-lat] .

[65] V. Bornyakov *et al.*, (2015), arXiv:1508.05916 [hep-lat] .

[66] T. Blum *et al.* (RBC, UKQCD), Phys. Rev. D **93**, 074505 (2016), arXiv:1411.7017 [hep-lat] .

[67] A. Bazavov *et al.* (HotQCD), Phys. Rev. D **90**, 094503 (2014), arXiv:1407.6387 [hep-lat] .

[68] A. Deuzeman and U. Wenger, PoS **LATTICE2012**, 162 (2012).

[69] M. Bruno and R. Sommer (ALPHA), PoS **LATTICE2013**, 321 (2014), arXiv:1311.5585 [hep-lat] .

[70] M. Tanabashi *et al.* (Particle Data Group), Phys. Rev. **D98**, 030001 (2018).

[71] I. S. Towner and J. C. Hardy, Rept. Prog. Phys. **73**, 046301 (2010).

[72] P. Zyla *et al.* (Particle Data Group), PTEP **2020**, 083C01 (2020).

[73] Y. Aoki *et al.*, (2021), arXiv:2111.09849 [hep-lat] .

[74] L. Wolfenstein, Phys. Rev. Lett. **51**, 1945 (1983).

[75] W. J. Marciano, Phys. Rev. Lett. **93**, 231803 (2004), arXiv:hep-ph/0402299 [hep-ph] .

[76] S. Durr, Z. Fodor, C. Hoelbling, S. D. Katz, S. Krieg, T. Kurth, L. Lellouch, T. Lippert, A. Ramos, and K. K. Szabo, Phys. Rev. **D81**, 054507 (2010), arXiv:1001.4692 [hep-lat] .

[77] E. Berkowitz *et al.*, Phys. Rev. **D96**, 054513 (2017), arXiv:1701.07559 [hep-lat] .

[78] B. Ananthanarayan, J. Bijnens, S. Friot, and S. Ghosh, Phys. Rev. D **97**, 091502 (2018), arXiv:1711.11328 [hep-ph] .

[79] J. Gasser and H. Leutwyler, Nucl. Phys. B **250**, 465 (1985).

[80] O. Bar, G. Rupak, and N. Shoresh, Phys. Rev. D **70**, 034508 (2004), arXiv:hep-lat/0306021 .

[81] N. Miller *et al.*, Phys. Rev. D **102**, 034507 (2020), arXiv:2005.04795 [hep-lat] .

[82] J. Bijnens, Eur. Phys. J. C **75**, 27 (2015), arXiv:1412.0887 [hep-ph] .

[83] V. Cirigliano and H. Neufeld, Phys. Lett. B **700**, 7 (2011), arXiv:1102.0563 [hep-ph] .

[84] A. Bazavov *et al.*, Phys. Rev. D **98**, 074512 (2018), arXiv:1712.09262 [hep-lat] .

[85] V. G. Bornyakov, R. Horsley, Y. Nakamura, H. Perlt, D. Pleiter, P. E. L. Rakow, G. Schierholz, A. Schiller, H. Stüben, and J. M. Zanotti (QCDSF–UKQCD), Phys. Lett. B **767**, 366 (2017), arXiv:1612.04798 [hep-lat] .

[86] N. Carrasco *et al.*, Phys. Rev. D **91**, 054507 (2015), arXiv:1411.7908 [hep-lat] .

[87] T. Blum *et al.* (RBC, UKQCD), Phys. Rev. D **93**, 074505 (2016), arXiv:1411.7017 [hep-lat] .

[88] A. Bazavov *et al.* (MILC), PoS **LATTICE2010**, 074 (2010), arXiv:1012.0868 [hep-lat] .

[89] B. Blossier *et al.* (ETM), JHEP **07**, 043 (2009), arXiv:0904.0954 [hep-lat] .

[90] E. Follana, C. T. H. Davies, G. P. Lepage, and J. Shigemitsu (HPQCD, UKQCD), Phys. Rev. Lett. **100**, 062002 (2008), arXiv:0706.1726 [hep-lat] .

[91] N. Cabibbo, E. C. Swallow, and R. Winston, Phys. Rev. Lett. **92**, 251803 (2004), arXiv:hep-ph/0307214 .

[92] Y. S. Amhis *et al.* (HFLAV), Eur. Phys. J. C **81**, 226 (2021), arXiv:1909.12524 [hep-ex] .

[93] N. Miller *et al.*, in *38th International Symposium on Lattice Field Theory* (2022) arXiv:2201.01343 [hep-lat] .

[94] S. Weinberg, Phys. Rev. **112**, 1375 (1958).

[95] A. A. Alves Junior *et al.*, JHEP **05**, 048 (2019), arXiv:1808.03477 [hep-ex] .

[96] F.-J. Jiang and B. C. Tiburzi, Phys. Rev. D **80**, 077501 (2009), arXiv:0905.0857 [nucl-th] .

[97] F.-J. Jiang, B. C. Tiburzi, and A. Walker-Loud, Phys. Lett. B **695**, 329 (2011), arXiv:0911.4721 [nucl-th] .

[98] A. Walker-Loud *et al.*, Phys. Rev. D **79**, 054502 (2009), arXiv:0806.4549 [hep-lat] .

[99] K. I. Ishikawa *et al.* (PACS-CS), Phys. Rev. D **80**, 054502 (2009), arXiv:0905.0962 [hep-lat] .

[100] A. Torok, S. R. Beane, W. Detmold, T. C. Luu, K. Orginos, A. Parreno, M. J. Savage, and A. Walker-Loud, Phys. Rev. D **81**, 074506 (2010), arXiv:0907.1913 [hep-lat] .

[101] H.-W. Lin, Nucl. Phys. B Proc. Suppl. **187**, 200 (2009), arXiv:0812.0411 [hep-lat] .

[102] H.-W. Lin and K. Orginos, Phys. Rev. D **79**, 034507 (2009), arXiv:0712.1214 [hep-lat] .

[103] A. Savanur and H.-W. Lin, Phys. Rev. D **102**, 014501 (2020), arXiv:1901.00018 [hep-lat] .

[104] J. He *et al.*, (2021), arXiv:2104.05226 [hep-lat] .

[105] S. P. Martin, Adv. Ser. Direct. High Energy Phys. **18**, 1 (1998), arXiv:hep-ph/9709356 .

[106] T. Falk, A. Ferstl, and K. A. Olive, Phys. Rev. D **59**, 055009 (1999), [Erratum: Phys.Rev.D 60, 119904 (1999)], arXiv:hep-ph/9806413 .

[107] D. S. Akerib *et al.* (LUX-ZEPLIN), Phys. Rev. D **101**, 052002 (2020), arXiv:1802.06039 [astro-ph.IM] .

[108] K. Abe *et al.* (Super-Kamiokande), Phys. Rev. D **102**, 072002 (2020), arXiv:2005.05109 [hep-ex] .

[109] J. R. Ellis, K. A. Olive, and C. Savage, Phys. Rev. D **77**, 065026 (2008), arXiv:0801.3656 [hep-ph] .

[110] G. S. Bali *et al.*, Nucl. Phys. B **866**, 1 (2013), arXiv:1206.7034 [hep-lat] .

[111] Y.-B. Yang, A. Alexandru, T. Draper, J. Liang, and K.-F. Liu (xQCD), Phys. Rev. D **94**, 054503 (2016), arXiv:1511.09089 [hep-lat] .

[112] S. Durr *et al.*, Phys. Rev. D **85**, 014509 (2012), [Erratum: Phys.Rev.D 93, 039905 (2016)], arXiv:1109.4265 [hep-lat] .

[113] C. Alexandrou, V. Drach, K. Jansen, C. Kallidonis, and G. Koutsou, Phys. Rev. D **90**, 074501 (2014), arXiv:1406.4310 [hep-lat] .

[114] R. Gupta, S. Park, M. Hoferichter, E. Mereghetti, B. Yoon, and T. Bhattacharya, (2021), arXiv:2105.12095 [hep-lat] .

[115] R. P. Feynman, Phys. Rev. **56**, 340 (1939).

[116] T. D. Cohen, R. J. Furnstahl, and D. K. Griegel, Phys. Rev. C **45**, 1881 (1992).

[117] J. Gasser and H. Leutwyler, Annals Phys. **158**, 142 (1984).

[118] G. Ecker, Prog. Part. Nucl. Phys. **35**, 1 (1995), arXiv:hep-ph/9501357 .

[119] B. C. Tiburzi and A. Walker-Loud, Nucl. Phys. A **764**, 274 (2006), arXiv:hep-lat/0501018 .

[120] C. C. Chang *et al.*, Nature **558**, 91 (2018), arXiv:1805.12130 [hep-lat] .

[121] M. N. Butler, M. J. Savage, and R. P. Springer, Nucl. Phys. B **399**, 69 (1993), arXiv:hep-ph/9211247 .

[122] P. A. Boyle *et al.*, Phys. Rev. D **93**, 054502 (2016), arXiv:1511.01950 [hep-lat] .

[123] V. Gülpers, G. von Hippel, and H. Wittig, Eur. Phys. J. A **51**, 158 (2015), arXiv:1507.01749 [hep-lat] .

[124] B. B. Brandt, A. Jüttner, and H. Wittig, JHEP **11**, 034 (2013), arXiv:1306.2916 [hep-lat] .

[125] S. Dürr *et al.* (Budapest-Marseille-Wuppertal), Phys. Rev. D **90**, 114504 (2014), arXiv:1310.3626 [hep-lat] .

[126] S. Borsanyi, S. Durr, Z. Fodor, S. Krieg, A. Schafer, E. E. Scholz, and K. K. Szabo, Phys. Rev. D **88**, 014513 (2013), arXiv:1205.0788 [hep-lat] .

[127] S. R. Beane, W. Detmold, P. M. Junnarkar, T. C. Luu, K. Orginos, A. Parreno, M. J. Savage, A. Torok, and A. Walker-Loud, Phys. Rev. D **86**, 094509 (2012), arXiv:1108.1380 [hep-lat] .

[128] R. Baron *et al.* (ETM), PoS **LATTICE2010**, 123 (2010), arXiv:1101.0518 [hep-lat] .

[129] R. Baron *et al.* (ETM), JHEP **08**, 097 (2010), arXiv:0911.5061 [hep-lat] .

[130] R. Frezzotti, V. Lubicz, and S. Simula (ETM), Phys. Rev. D **79**, 074506 (2009), arXiv:0812.4042 [hep-lat] .

[131] K. G. Wilson, Phys. Rev. D **10**, 2445 (1974).

[132] H. B. Nielsen and M. Ninomiya, Phys. Lett. **105B**, 219 (1981).

[133] A. Bazavov *et al.* (MILC), Phys. Rev. D **82**, 074501 (2010), arXiv:1004.0342 [hep-lat] .

[134] A. Bazavov *et al.* (MILC), Phys. Rev. D **87**, 054505 (2013), arXiv:1212.4768 [hep-lat] .

[135] S. R. Sharpe, in *Workshop on Domain Wall Fermions at Ten Years* (2007) arXiv:0706.0218 [hep-lat] .

[136] G. P. Lepage, B. Clark, C. T. H. Davies, K. Hornbostel, P. B. Mackenzie, C. Morningstar, and H. Trottier, Nucl. Phys. B Proc. Suppl. **106**, 12 (2002), arXiv:hep-lat/0110175 .

[137] P. Lepage, "gplepage/gvar: gvar," (2022), https://github.com/gplepage/gvar.

[138] P. Lepage, "gplepage/lsqfit: lsqfit," (2022), https://github.com/gplepage/lsqfit.

[139] W. I. Jay and E. T. Neil, Phys. Rev. D **103**, 114502 (2021), arXiv:2008.01069 [stat.ME] .

[140] C. Bouchard, C. C. Chang, T. Kurth, K. Orginos, and A. Walker-Loud, Phys. Rev. **D96**, 014504 (2017), arXiv:1612.06963 [hep-lat] .

[141] G. Amoros, J. Bijnens, and P. Talavera, Nucl. Phys. B **568**, 319 (2000), arXiv:hep-ph/9907264 .